UNIVERSITY OF OKLAHOMA

GRADUATE COLLEGE

MIXED METAL CARBIDES: UNDERSTANDING THE SYNTHESIS, SURFACE PROPERTIES AND CATALYTIC ACTIVITIES

A DISSERTATION

SUBMITTED TO THE GRADUATE FACULTY

in partial fulfillment of the requirements for the

Degree of

DOCTOR OF PHILOSOPHY

By

ALI MEHDAD
Norman, Oklahoma
2015

Downloaded from SHAREOK. Persistent Handle URL: https://hdl.handle.net/11244/15497

MIXED METAL CARBIDES: UNDERSTANDING THE SYNTHESIS, SURFACE PROPERTIES AND CATALYTIC ACTIVITIES

A DISSERTATION APPROVED FOR THE
SCHOOL OF CHEMICAL, BIOLOGICAL AND MATERIALS ENGINEERING

BY

_____
Dr. Friederike C. Jentoft, Chair

_____
Dr. Rolf E. Jentoft

_____
Dr. Daniel E. Resasco

_____
Dr. Lance L. Lobban

_____
Dr. Daniel T. Glatzhofer

© Copyright by ALI MEHDAD 2015
All Rights Reserved.

Acknowledgements

Firstly, I would like to express my sincere gratitude to my advisor Dr. Friederike Jentoft and also Dr. Rolf Jentoft for their continuous support and patience. Their valuable guidance helped me to finish my PhD and to grow as a researcher.

The other members of my committee Dr. Daniel Resasco, Dr. Lance Lobban and Dr. Daniel Glatzhofer, are also acknowledged, as are other faculty members and research scientist for their comments and suggestions, namely Dr. Kenneth Nicholas, Dr. Tawan Sooknoi, Dr. Richard Mallinson and Dr. Steven Crossley. Dr. Resasco provided very valuable comments and suggestions during my presentations at Biofuels meetings and I also learned a lot in his catalysis class.

It has been a great pleasure for me to work with other graduate students and postdocs namely Dr. Zhimin Liu, Alana Denning, Kelsey Potter, Dr. Matthew Wulfers, Lauren Gilbert and Chandramouli Vaddepalli. I appreciate the opportunity to work with undergraduate students, John Grinde and Grant Loveall. During my research the interactions with members of the Biofuels group were helpful and constructive especially the interactions with Dr. Tu Pham and Dr. Dachuan Shi.

I would also like to thank my family for the support, love and encouragement they provided me through my entire life.

Table of Contents

Acknowledgements iv

List of Tables ix

List of Figures x

Abstract xviii

1. Introduction 1

1.1 General introduction and motivation 1

1.2 Literature review on carbides 1

1.2.1 Electronic structure of metal carbides 3

1.2.1.1 Electronic effects of insertion of a nonmetal (nitrogen and oxygen) into the structure of molybdenum carbide 6

1.2.1.2 Effect of carbon vacancies on the DOS of molybdenum carbide 7

1.2.2 Synthesis of metal carbides 10

1.2.3 Catalytic activities of carbides 15

1.3 Goal and strategy 17

2. Passivation Agents for Mo_2C and W_2C: Effect on Reduction and Catalytic Activity 22

2.1 Introduction 22

2.2 Experimental section 25

2.2.1 Catalyst and materials 25

2.2.2 Passivation methods 26

2.2.2.1 Passivation with CO_2 26

2.2.2.2 Passivation with water 27

2.2.2.3 Passivation with 1% O_2/Ar 27
2.2.2.4 Passivation with "stepwise oxygen" 27
2.2.3 Fresh carbides (without passivation) 28
2.2.4 Temperature-programmed reduction (TPR) 28
2.2.5 Catalytic tests 28
2.2.6 Characterization 29
2.3 Results 29
2.3.1 Characterization of samples 29
2.3.2 Passivation of carbides with air, carbon dioxide and water 31
2.3.3 Reduction of passivated samples 38
2.3.4 Catalytic activity 41
2.4 Discussion 45
2.4.1 Synthesis and passivation of carbides 45
2.4.2 Reduction of passivated carbides 49
2.4.3 Toluene hydrogenation on Mo_2C and W_2C 52
2.5 Conclusions 59
References 60
3. Synthesis, Characterization and Catalytic Activity of Single Phase Mixed Metal Carbides of Molybdenum and Tungsten 66
3.1 Introduction 66
3.2 Experimental section 69
3.2.1 Catalyst and materials 69
3.2.2 Temperature-programmed reduction (TPR) 70

3.2.3 Reaction 70
3.2.4 Characterization 71
3.3 Results 72
3.3.1 Synthesis of mixed metal carbides 72
3.3.1.1 Direct carburization of freeze-dried materials 72
3.3.1.2 Calcination and carburization of freeze-dried precursors 76
3.3.2. Characterization of samples 79
3.3.3 Reduction of samples 85
3.3.4 Catalytic activity 86
3.4 Discussion 93
3.4.1 Synthesis of samples 93
3.4.2 Passivation and reduction of samples 103
3.4.3 Toluene hydrogenation to methylcyclohexane on mixed Mo-W carbides 104
3.4.4 Reaction of toluene at 400 °C on mixed Mo-W carbides 106
3.5 Conclusions 110
4. Mixed molybdenum-niobium carbides catalyst: synthesis, characterization and catalytic activity 118
4.1 Introduction 118
4.2 Experimental section 119
4.2.1 Catalyst and materials 119
4.2.2 Temperature-programmed reduction (TPR) 121
4.2.3 Reaction 121
4.2.4 Characterization 122

4.3 Results 123
4.3.1 Synthesis of metal carbides 123
4.3.1.1 Carburization of precursors synthesized by hydrothermal synthesis 124
4.3.1.2 Carburization of calcined freeze-dried precursors 126
4.3.2 Characterization of the materials 129
4.3.3 Reduction of samples 133
4.3.4 Catalytic activity 134
4.4 Discussion 137
4.4.1 Carburization of samples 137
4.4.2 Reduction 145
4.4.3 Catalytic performance 147
4.5 Conclusions 150
5. Recommendations 155
6. Appendix A: GC calibration 157

List of Tables

Table 1.1: Number of atoms in the structure, equilibrium volumes V_{eq} , and formation energies E_{form} for different phases of molybdenum carbide. Adapted from [8]. 5

Table 1.2: Structures of molybdenum carbide prepared by using different carbon source 12

Table 2.1: Physisorption data for Mo_2C and W_2C 31

Table 2.2: Amounts of weight gain after passivation and weight loss after reduction ... 33

Table 3.1: Characterization data for samples prepared by direct carburization of freeze-dried precursors 84

Table 3.2: Activation energies for hydrogenation of toluene to methylcyclohexane on the series of Mo-W carbides. 87

Table 3.3: Product selectivity of toluene conversion on Mo-W carbide series 92

Table 4.1: Characterization data for Mo-Nb carbide samples 132

Table 4.2: Product selectivities (in %) for Mo-Nb carbides at 400 °C and 20 bar H_2 .. 136

Table 6.1: Calibration gas content 157

Table 6.2: Retention time (RT) for the gases in the calibration gas cylinder 158

Table 6.3: Peak areas for injection of calibration gases 158

Table 6.4: Toluene partial pressure at different flow rates and pressures 159

Table 6.5: Response factor (RF) for toluene (tol) and methylcyclohexane (MCH) with octane as internal standard 160

List of Figures

Figure 1.1: Crystal structure of metal carbides and metal nitrides. Reprinted from [3]. Copyright (1992), with permission from Elsevier. 3

Figure 1.2: Comparison of d-band structures of Pt (111), β-Mo_2C surfaces and Mo (110). Reprinted from [7]. Copyright (2005), with permission from Elsevier. 4

Figure 1.3: Density of states for substitution of carbon with nitrogen: (a) MoC, (b) $MoC_{0.75}N_{0.25}$ and (c) MoN. Reprinted figure with permission from [9], Copyright (1999) by American Physical Society. 6

Figure 1.4: Density of states for substitution of carbon with oxygen: (a) MoC, (b) $MoC_{0.75}O_{0.25}$ and (c) MoO. Reprinted figure with permission from [9], Copyright (1999) by American Physical Society. 7

Figure 1.5: Comparison between the DOS for stoichiometric MoC and substoichiometric $MoC_{0.75}$, (a) ɣ-MoC (top) and ɣ-$MoC_{0.75}$ (bottom) and (b) δ-MoC (top) and δ-$MoC_{0.75}$ (bottom). The Fermi level is indicated by a solid line. Reprinted figure with permission from [1], Copyright (1999) by American Physical Society. 8

Figure 1.6: Left: charge density contours for the vacancy peak at -3 eV in the δ phase. Right: the charge density contours for a stoichiometric δ phase. Reprinted figure with permission from [1], Copyright (1999) by American Physical Society. 9

Figure 1.7: Left: DOS for substitution of molybdenum with niobium: MoC. $Mo_{0.75}Nb_{0.25}C$ (mirrored).Right: DOS for substitution of molybdenum with tungsten: MoC. $Mo_{0.75}W_{0.25}C$ (mirrored). Reprinted figure with permission from [9], Copyright (1999) by American Physical Society. 9

Figure 1.8: Crystallographic phases detected during the TPR of different oxides in different hydrocarbon mixtures. Reproduced with permission from [10]. © 2008 Canadian Science Publishing.....11

Figure 1.9: Formation of cubic and hexagonal structures by carburization of MoO_3. Reprinted with permission from [20], Copyright (2004) by American Chemical Society. 13

Figure 1.10: Tetralin hydrogenation in the absence of H_2S (left), and in the presence of H_2S (right). (Reaction conditions: 0.2 g of supported catalyst, 573 K, 4 MPa; Reduction conditions: 423 K, 4 MPa). Reprinted from [31]. Copyright (2001), with permission from Elsevier. 16

Figure 1.11: Comparison of steady state HDS (left), HDN (middle) and HDO (right) of carbides and nitrides with the commercial sulfided Ni-Mo/Al_2O_3 at 643 K, 3.1 MPa. Reprinted with permission from [33], Copyright (1995) by American Chemical Society. 16

Figure 2.1: XRD data for W_2C (top) and Mo_2C (bottom).....30

Figure 2.2: Passivation of Mo_2C during the first 60 minutes. From top to bottom passivation in: 1% O_2 at 40 °C, 0.1% O_2 at 40 °C, 30% CO_2 at 100 °C, 3% water at 110 °C and Argon at 300 °C. 32

Figure 2.3: Weight gains (dashed line) and heat effects (solid line) during passivation of Mo_2C with 1% O_2 (blue) and with stepwise O_2 (red) at 40 °C.....33

Figure 2.4: Passivation of Mo_2C: in the beginning gas phase atmosphere was pure Ar then switched to 3% water in Ar at 110 °C after 68 minutes and switched to 16% O_2/Ar at 40 °C after 290 minutes. 34

Figure 2.5: TP water of Mo_2C, TG data (top) and MS data (bottom). Gas phase atmosphere was initially 100% Ar and after 68 minutes was switched to 3% water in Ar. 35

Figure 2.6: Passivation of Mo_2C: gas phase atmosphere initially was 100% Ar, after 46 minutes switched to 30% CO_2 in Ar at 100 °C and after 351 minutes switched to 16% O_2 at 40 °C. 36

Figure 2.7: TG data (top) and MS data (bottom) for $TPCO_2$ in 30%CO_2 in Ar. Gas phase atmosphere was initially 100% Ar, after 20 minutes switched to 30%CO_2/Ar. ...37

Figure 2.8: Reduction of Mo_2C in 80% H_2/Ar. The solid line represents Mo_2C passivated in 1% O_2 and the dashed line represents Mo_2C passivated in "stepwise oxygen". Water evolution is shown by the blue curve (m/z=18) and methane evolution by the green curve (m/z=15).....38

Figure 2.9: Reduction of passivated W_2C in 80% H_2/Ar. Solid line, W_2C passivated in 1% O_2 and dashed line, W_2C passivated in stepwise oxygen. Water, blue curve (m/z=18) and methane, green curve (m/z=15). 39

Figure 2.10: Reduction of passivated Mo_2C (1% O_2) with carburization mixture 10%C_2H_6/H_2. 40

Figure 2.11: TPR of Mo_2C passivated in 1% O_2. TPR was performed right after passivation (dashed line) or after 11 months (solid line). The gas phase atmosphere was 80% H_2/Ar. 41

Figure 2.12: Hydrogenation of toluene on Mo_2C at 150 °C and 20 bar H_2 pressure. Blue bars: initial activity at 150 °C, red bars: rate at 150 °C after heating to 200 and 300 °C and cooling down to 150 °C. 42

Figure 2.13: Hydrogenation of toluene on W_2C at 200 °C and 20 bar H_2 pressure. Blue bars: initial activity at 200 °C, red bars: rate at 200 °C after heating to 300 and 400 °C and cooling down to 200 °C. 43

Figure 2.14: TPR at 20 bar H_2 pressure on fresh and passivated W_2C (top) and Mo_2C (bottom). The gas phase atmosphere was 150 ml/min of H_2, and the temperature ramp was 10 K/min. 44

Figure 2.15: Hydrogenation of toluene at 150 °C and 20 bar H_2. Samples are Mo_2C in situ prepared and passivated with 1% O_2. Reduced in 1 and 20 bar H_2. Blue bar, activity at 150 °C and red bars, activity at 150 °C after heating up to 200 and 300 °C and cooling down to 150 °C. 45

Figure 2.16: Hydrogenation of toluene at 200 °C and 20 bar H_2. Samples are W_2C in situ prepared and ex situ prepared passivated with 0.1% O_2. Reduced in 1 and 20 bar H_2. Blue bars, activity at 200 °C and red bars, activity at 200 °C after heating up to 300 and 400 °C and cooling down to 200 °C. 45

Figure 3.1: Carburization of commercial MoO_3 and MoO_3 prepared from calcination of Mo-FD at 600 °C. Gas phase atmosphere was 10% C_2H_6/H_2. 73

Figure 3.2: Weight change during direct carburization of freeze-dried Mo-W series in a gas mixture of 20% CH_4 in H_2. Freeze-dried samples from top to bottom: tungsten, MoW-0.25, MoW-0.5, MoW-0.75 and molybdenum. The isothermal process is for temperature-programmed carburization of a pure tungsten precursor. 73

Figure 3.3: Water formation (top) and CO formation (bottom) during direct carburization of freeze-dried Mo-W samples in a gas mixture of 20% CH_4 in H_2. 75

Figure 3.4: Weight change during calcination of freeze-dried materials in 80% air in Ar. From top to bottom: freeze-dried tungsten, MoW-0.5 and molybdenum. 76

Figure 3.5: Water formation during calcination of freeze-dried materials in 80% air in Ar. Mo_FD (dotted line), MoW-0.5 (solid line) and W_FD (dashed line). 77

Figure 3.6: NO formation during calcination of freeze-dried materials in 80% air in Ar. Mo_FD (dotted line), MoW-0.5 (solid line) and W_FD (dashed line). 77

Figure 3.7: Weight change during carburization of calcined freeze dried materials in a 20% CH_4/H_2 mixture. From top to bottom: carburization of tungsten oxide, MoW-0.5 oxide and molybdenum oxide..... 78

Figure 3.8: MS data for water formation (top) and CO formation (bottom) during carburization of calcined freeze-dried samples in a mixture of 20% CH_4/H_2. Blue curve is for MoO_3, green curve is for MoW-0.5 oxide and red curve is for WO_3. 79

Figure 3.9: XRD data for Mo-W-C prepared from direct carburization of freeze dried precursors. From top to bottom: molybdenum carbide, MoWC-0.75, MoWC-0.5, MoWC-0.5, MoWC-0.25, tungsten carbide, Ni (ICDD: 00-004-0850) and Mo_2C (ICDD: 00-035-0787). Ni used as the internal standard. 80

Figure 3.10: XRD data for calcined freeze dried precursors from top to bottom: Mo, MoW-0.5 and W oxides. Gas mixture was 80% air in Ar..... 81

Figure 3.11: XRD data for Mo-W carbides series. From bottom to top: (a) Ni (ICDD:00-004-0850), (b) Mo_2C (ICDD:00-035-0787), (c) molybdenum carbide prepared from oxide at 720 °C, (d) W_2C prepared from oxide at 750 °C, (e) WC (ICDD: 00-051-0939), (f) tungsten carbide prepared from oxide at 900 °C, (g) WC (ICDD: 00-020-1316), (h) MoWC-0.5 prepared from oxide at 700 °C, (i) MoWC-0.5 prepared from

oxide at 800 °C, (j) W (ICDD: 00-004-0806), (k) MoWC-0.5 prepared from freeze-dried precursor at 590 °C, (l) WC (00-025-1047) and (m) WC prepared from freeze-dried precursor at 870 °C. Gas mixture was 20% CH_4 in H_2. 82

Figure 3.12: Unit cell volume vs. composition for Mo-W carbide series prepared by direct carburization of freeze-dried precursors in a 20% CH_4/H_2 mixture..... 83

Figure 3.13: MS data for temperature-programmed reduction (TPR) of passivated samples with a temperature ramp of 10 K/min. Water formation (top) and methane formation (bottom). Gas mixture was 80% H_2 in Ar. 86

Figure 3.14: Logarithm of rate vs. 1000/T for hydrogenation of toluene on Mo-W carbide series. From top to bottom: Molybdenum carbide, MoWC-0.75, MoWC-0.5, MoWC-0.25 and tungsten carbide. 87

Figure 3.15: TOF and activation energies for hydrogenation of toluene to methylcyclohexane at 250 °C and 20 bar hydrogen pressure..... 88

Figure 3.16: Rate of toluene conversion vs. time at 400 °C and 20 bar pressure for the series of Mo-W carbide samples..... 89

Figure 3.17: Product selectivity vs. conversion during toluene hydrogenation at 400 °C and 20 bar hydrogen pressure on Mo-W carbide series. 91

Figure 3.18: Toluene conversion on tungsten carbide at various temperatures and time on stream. 93

Figure 4.1: Direct carburization of HT precursors from bottom to top with Mo/Nb ratios of: pure molybdenum, 6.7, 1.96, 0.95, 0.44 and 0. Gas phase mixture 20% CH_4/70%H_2/10% Ar. 124

Figure 4.2: MS data for carburization of precursors from hydrothermal synthesis. Water formation (bottom) and CO formation (top). Gas phase mixture 20% CH_4/70%H_2/10% Ar. 125

Figure 4.3: Calcination of Nb-FD (600 °C), Mo-FD (500 °C) and Mo_6Nb_FD (600 °C) in 80% air/Ar with temperature ramp of 5 K/min. 126

Figure 4.4: Carburization of calcined precursors, from left to right: oxides of Mo_6Nb, Mo and Nb. Gas phase mixture 20% CH_4/70%H_2/10% Ar. 127

Figure 4.5: Carburization of calcined freeze-dried precursors. Gas phase mixture 20% CH_4/70%H_2/10% Ar. 128

Figure 4.6: XRD data for Mo-Nb carbide series. (a) Ni (ICDD:00-004-0850) (b) NbC (ICDD:00-038-1364) (c) Mo_2C (ICDD: 00-035-0787) (d) NbC (e) $Mo_{0.44}NbC$ (f) $Mo_{0.95}NbC$ (g) $Mo_{1.96}NbC$ (h) $Mo_{1.6}NbC$ (i) $Mo_{6.7}NbC$ (j) Mo_6NbC (k) Mo_2C 130

Figure 4.7: Lattice parameter of Mo-Nb carbides with NbC structure vs. mole fraction of niobium. Δ $MoC_{0.66}$, o (Nb/C >1), ◊ (Nb/C=1) 131

Figure 4.8: Mo/Nb precipitated during hydrothermal synthesis vs. Mo/Nb loaded in the solution 131

Figure 4.9: TPR data for mixed metal carbides. Formation of water (top) and methane (bottom) 133

Figure 4.10: Rate of toluene hydrogenation at 250 °C and 20 bar H_2 pressure for Mo-Nb carbide samples. The blue bars show initial activity and the red bars show rate of toluene conversion at 250 °C after cooling down from 400 °C. 135

Figure 4.11: Turn over frequencies (TOF) for hydrogenation of toluene at 250 °C and 20 bar H_2 pressure on a series of Mo-Nb carbides. 135

Figure 4.12: Hydrogenation of toluene on Mo-Nb carbide at 400 °C and 20 bar H_2 pressure.....137

Figure 6.1: Temperature program of the GC.....157

Figure 6.2: Peak area/%mol of the compounds vs. carbon number 160

Figure 6.3: Response factor (RF) of toluene and methylcyclohexane with octane as internal standard.....161

Abstract

Metal carbides are formed when carbon is inserted into the lattice of the metal, and metal-carbon bonds are formed. In fact, formation of the carbon-metal bonds causes a change in the electronic structure of the metal in a way that metal carbides can catalyze the reactions that usually are catalyzed by the noble metals.

The effect of variation of the amount of nonmetal (carbon or oxygen) on the catalytic activity of metal carbides was investigated. The metal carbides are pyrophoric materials, and they need to be passivated before coming in contact with the ambient. The results show that water or CO_2 cannot passivate Mo_2C at low temperatures, and at high temperatures they damage the surface of metal carbides by removal of carbidic carbon. However, oxygen can passivate metal carbides at low temperatures. Passivation in 0.1%O_2/Ar instead of 1%O_2/Ar will cause generation of more active sites during reduction. The results revealed that increasing the amount of carbidic carbon or decrease of the amount of oxygen on the (sub) surface of metal carbides results in an increasing the hydrogenation activity. Also, there is a carbon dynamics (adding or removing carbon) on the surface of metal carbide which can alter the catalytic activity of metal carbides.

Metal oxycarbides have bifunctional activity. The conversion of toluene was used to test the bifunctionality of metal (oxy) carbides. Mo_2C has strong metallic behavior and at 20 bar H_2 pressure and 400 °C, hydrogenation and hydrogenolysis products are predominant. In order to modify the metallic behavior of Mo_2C in favor of acid-catalyzed behavior, oxygen was introduced on the surface of Mo_2C to form molybdenum oxycarbide. However, oxygen can be removed at reaction conditions

required for ring contraction of six-membered rings to five-membered rings. As a remedy, Mo_2C was mixed with another metal with a higher oxophilicity such as tungsten or niobium. The results indicate that molybdenum-tungsten carbides still have strong metallic behavior with predominant hydrogenation and hydrogenolysis products. However, molybdenum-niobium oxycarbides with cubic NbC structure have lower selectivity to hydrogenolysis products and higher selectivity to ring contraction products compared to Mo-Nb (oxy) carbides with hexagonal Mo_2C structure. The results show that at 400 °C and 20 bar H_2 pressure mixed metal carbides have better stability compared to their corresponding monometallic carbides.

1. Introduction

1.1 General introduction and motivation

Catalysts are materials that increase the rate of chemical reactions by lowering the activation energies of chemical reactions. Carbides currently make up only a small group of catalysts, due to the limited number of stable carbides [1], and difficulties in their preparation.

In 1973, “noble metal like behavior” of tungsten carbide was reported [2]. Since then metal carbides have gained a great amount of attention to be used as less costly replacement of precious noble metals. They show good catalytic activity for a variety of reactions that are catalyzed by noble metals. Metal carbides have advantages over noble metals, for instance, they are resistant toward sulfur poisoning, and are refractory materials with high stability at high temperatures [3].

The chemical and physical properties of metal carbides can be tuned by substituting the cations or anions in their structures. However, there are a limited number of well defined metal carbides described in the literature, and this research is aiming to expand this class of materials.

1.2 Literature review on carbides

In general carbides can be classified by their chemical bondings into three groups: salt-like (such as methanides), covalent compounds (such as silicon carbide) and metal-like compounds which are formed by insertion of carbon into the lattice of transition metals.

Metal-like carbides are formed when the radius of the metal is 1.35 Å or larger, so the interstitial spaces will be large enough to contain the carbon. Carbides of group

IV-VI transition metals can form stable metal carbides. “Metal-like” carbides have the combined properties of three different classes of materials: they are refractory and brittle like covalent solids, have high melting points and hardness (melting point > 3300 K, hardness > 2000 kg mm^{-2}, similar to ceramics), have simple crystal structures like ionic solids, and they have electronic structures like transition metals. These qualities make them interesting materials for different applications including heterogeneous catalysis. If all the interstitial spaces are filled transition metals can form carbides with MC stoichiometry and if half of the interstitial spaces are filled they can form carbides with $MC_{0.5}$ stoichiometry [3].

The carbon insertion into the lattice of the metal will cause changes in both crystal and electronic structure of the parent metal. For instance, the metallic molybdenum has bcc structure while its carbides can have cubic or hexagonal structures. Structures of metal carbides are determined by two factors [3]:

1. Geometric factor: based on Hagg’s rule, if the nonmetal-to-metal radius ratio is less than 0.59, interstitial compounds adapt simple structures such as fcc or hcp.
2. Electronic factor: based on the Engel-Brewer theory, the structures of metals or substitutional alloys depend on *s-p* electron counts. When the *s-p* electron count increases the structure transforms in the order of bcc (Nb, Mo and W) to hcp (Tc, Ru and Os) to fcc (Rh, Pd and Pt). In the case of carbides and nitrides the *s-p* electron count will result in the following structural changes: Mo (bcc), Mo_2C (hcp) and Mo_2N (fcc).

Common crystal structure of carbides and nitrides are shown in Figure 1.1.

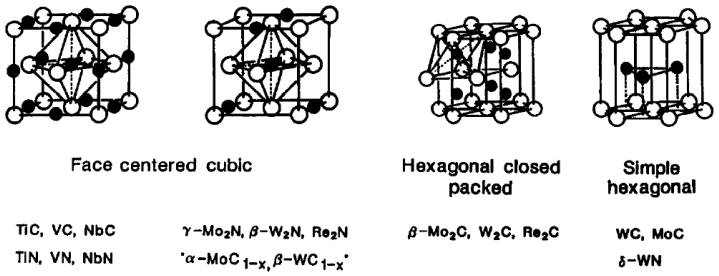

Figure 1.1: Crystal structure of metal carbides and metal nitrides. Reprinted from [3]. Copyright (1992), with permission from Elsevier.

In 1973, "Pt like" catalytic behavior of tungsten carbide was reported [2], this behavior has been attributed to a change in electronic structure of the metal through incorporation of the carbon. Below, the literatures explaining the electronic structure of metal carbides are discussed.

1.2.1 Electronic structure of metal carbides

Bonding in carbides involves the simultaneous contribution of metallic (metal-metal bonding), covalent (metal-nonmetal bonding) and ionic (charge transfer between metal and nonmetal) bonding. However, the important electronic properties are related to the amount and direction of charge transfer, which is widely believed to be from the metal to the nonmetal, and to modification of the d-band upon insertion of carbon into the lattice of the metal [4]. Upon insertion of the carbon into the lattice of the metal, the metal-metal distance increases, and based on an estimation by Heine [5] the width of the d-band is inversely proportional to the fifth power of the metal-metal distance. As a result, carbon insertion will cause a lower density of states (DOS) near the Fermi level. The higher the energy of the d-states relative to the Fermi energy ($E-E_f$), the stronger the interaction of the surface with adsorbates. The reason is, that when d-states are close

to the Fermi level, antibonding states can be shifted above the Fermi level, and become empty, and this increases the bond strength [6].

The d-band structures of platinum, metallic molybdenum and molybdenum carbide are compared in Figure 1.2 [7]. The d-band of Mo_2C is broader than that of metallic Mo, but the number of d-electrons in Mo(110) and Mo_2C(0001) are very close to each other. Therefore, by formation of the carbide the number of d-electrons does not change, which means there is no electron transfer from metal to nonmetal.

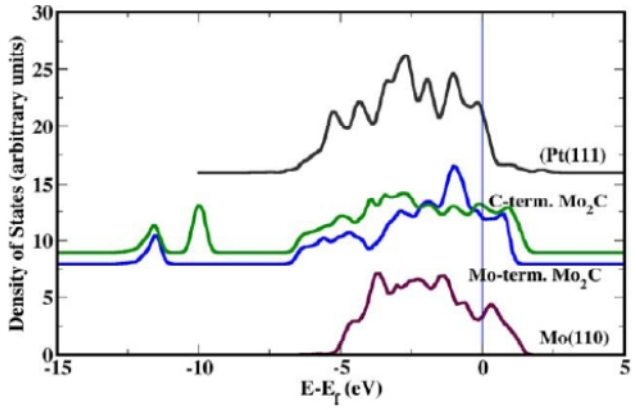

Figure 1.2: Comparison of d-band structures of Pt (111), β-Mo_2C surfaces and Mo (110). Reprinted from [7]. Copyright (2005), with permission from Elsevier.

From a structural point of view, carbides can be seen as stacking of close packed metal layers, with carbons in the interstitial positions. Metal carbides in group IV can only form cubic structures, whereas metals in group V form cubic structures at high carbon content and hexagonal structures at low carbon content. The structures of metal carbides from group VI are very different; molybdenum carbide (which is one of the most catalytically active carbides) can form up to six different structures, and their differences are due to the disorder/order transformation of the carbon atoms. There are many stable and meta-stable structures for molybdenum carbide, and the energies of

formation for their structures are very close to each other. The equilibrium volume and energy of formation for different structures of molybdenum carbide are reported in Table 1.1 [8].

Table 1.1: Number of atoms in the structure, equilibrium volumes V_{eq} , and formation energies E_{form} for different phases of molybdenum carbide. Adapted from [8].

Phase	Atoms	V_{eq} ($Å^3$)	$E_{formation}$ per atom (mRy)
MoC-η	12	20.2	9
$MoC_{0.875}$	15	19.9	4
$MoC_{0.75}$	7	19.4	5
$MoC_{0.75}$	14	19.4	-1
$MoC_{0.50}$	6	18.5	4
$MoC_{0.50}$	12	18.3	-6
$MoC_{0.25}$	5	17.3	14

1 J=$4.59x10^{17}$ Ry

It was mentioned above that by incorporation of carbon into the lattice of a metal, the metal's electronic structure will be changed. It is also interesting to see the electronic effect of substitutional impurities in molybdenum carbide. These impurities are metals such as tungsten or niobium, and nonmetals such as nitrogen or oxygen [9]. Also the effect of carbon vacancies on the DOS has been reported, because creating carbon vacancies is possible under reaction conditions that involve high temperature and high pressure of hydrogen.

1.2.1.1 Electronic effects of insertion of a nonmetal (nitrogen and oxygen) into the structure of molybdenum carbide

In Figure 1.3, the DOS of MoC is compared with those of MoN and $MoC_{0.75}N_{0.25}$. In this figure, the DOS in region I is from electrons in *s* orbitals of carbon, region II is for hybridization of *p* orbitals of carbon and *d* orbitals of molybdenum, and region III is for *d* orbitals of molybdenum. Upon insertion of nitrogen, it can be observed that energy states (*s*, *p* and hybridization of *p* and *d*) are shifted to lower energies, because nitrogen is more electronegative than carbon. Also, in region II hybridization of *p* and *d* orbitals is reduced.

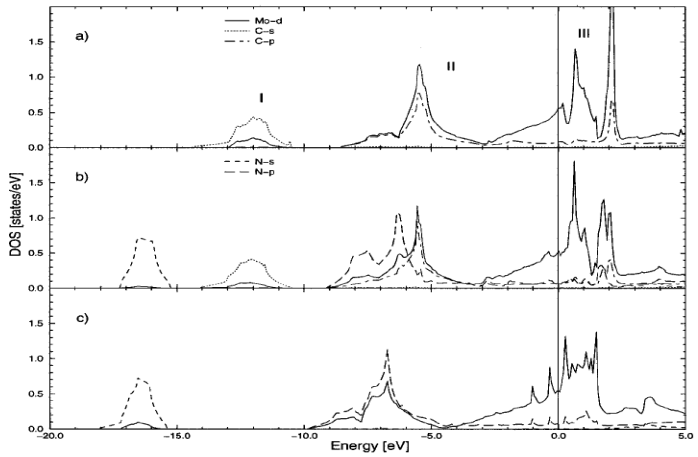

Figure 1.3: Density of states for substitution of carbon with nitrogen: (a) MoC, (b) $MoC_{0.75}N_{0.25}$ and (c) MoN. Reprinted figure with permission from [9], Copyright (1999) by American Physical Society.

In Figure 1.4, the DOS of MoC is compared with those of $MoC_{0.75}O_{0.25}$ and MoO. Here, again a downward shift in energy of *s* and *p* states can be observed from MoC to MoO. Also, *p-d* hybridization is reduced which causes *p-d* bond weakening, and this bond weakening leads to a decrease in cohesive energy compared to MoC.

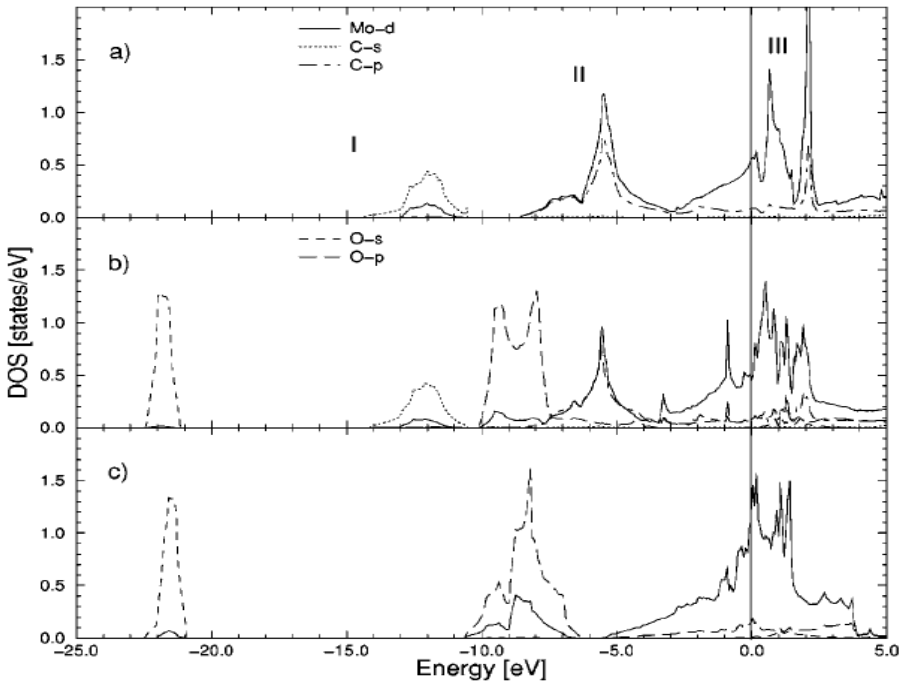

Figure 1.4: Density of states for substitution of carbon with oxygen: (a) MoC, (b) $MoC_{0.75}O_{0.25}$ and (c) MoO. Reprinted figure with permission from [9], Copyright (1999) by American Physical Society.

1.2.1.2 Effect of carbon vacancies on the DOS of molybdenum carbide

The presence of carbon vacancies in the structure of metal carbides will cause a reduction of the unit cell volume, and also a change in d-band structure. The comparison between the DOS of stoichiometric (MoC) and sub-stoichiometric (MoC_{1-X}) is shown in Figure 1.5. Figure 1.5-a is a comparison between the DOS of the hexagonal structure of MoC and that of $MoC_{0.75}$. The main difference between the stoichiometric and the substoichiometric carbide is the creation of some new peaks in region II. These peaks are called “vacancy peaks”, which are due to the unscreened Mo-Mo bonds through carbon vacancy sites. Also since there is a DOS peak at the Fermi level in $MoC_{0.75}$, this structure is less stable than MoC. But the cubic structure of $MoC_{0.75}$ in Figure 1.5-b is more stable than MoC due to the lower DOS at the Fermi level.

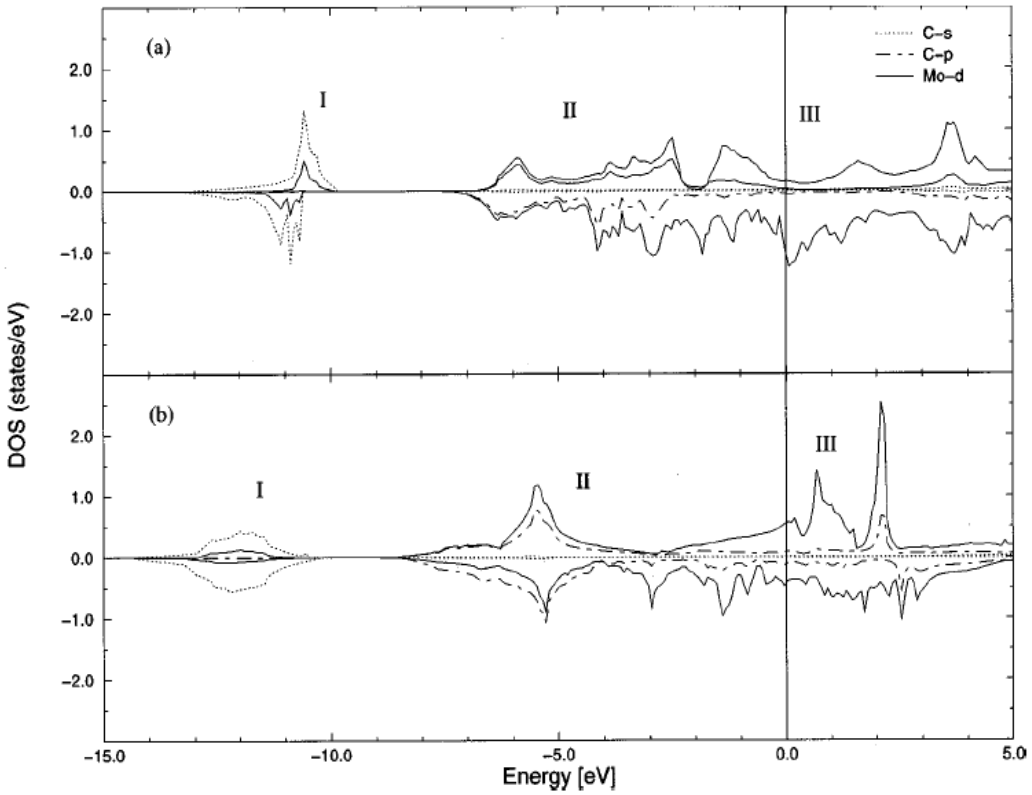

Figure 1.5: Comparison between the DOS for stoichiometric MoC and substoichiometric $MoC_{0.75}$, (a) ɣ-MoC (top) and ɣ-$MoC_{0.75}$ (bottom) and (b) δ-MoC (top) and δ-$MoC_{0.75}$ (bottom). The Fermi level is indicated by a solid line. Reprinted figure with permission from [1], Copyright (1999) by American Physical Society.

The charge density contours for the δ (cubic) phase with and without carbon vacancies are shown in Figure 1.6, the states plotted are situated on Mo atoms close to the carbon vacancy site, and the states are directed toward the next Mo atom through the carbon vacancy [1].

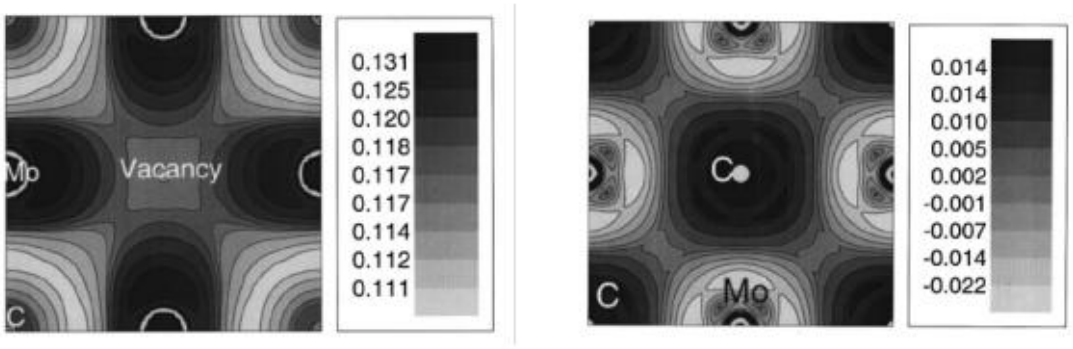

Figure 1.6: Left: charge density contours for the vacancy peak at -3 eV in the δ phase. Right: the charge density contours for a stoichiometric δ phase. Reprinted figure with permission from [1], Copyright (1999) by American Physical Society.

1.2.1.3 Effect of metal impurities on the DOS of molybdenum carbide

Since catalytic activities of molybdenum carbide mixed with another metal (M) will be discussed later; it will be important to compare the DOS of MoC with that of Mo-M-C. Density of states for substitution with tungsten and niobium are shown in Figure 1.7. It can be observed that changes in DOS are much less than in the case of the nonmetal substitution. Also, the tungsten substitution has the least effect, because molybdenum and tungsten both have the same number of valence electrons.

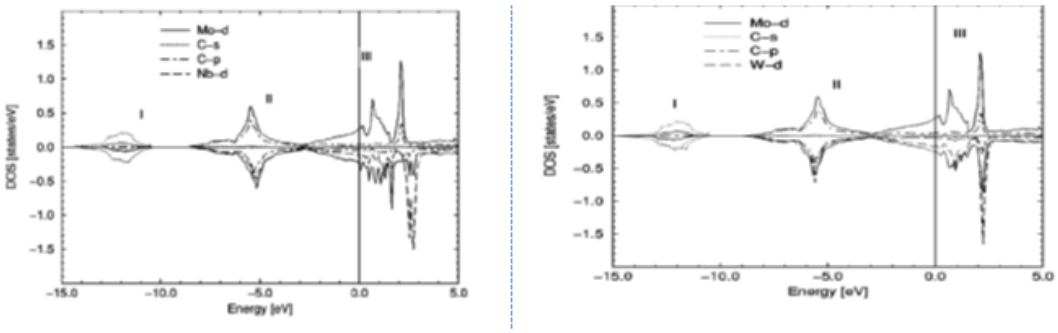

Figure 1.7: Left: DOS for substitution of molybdenum with niobium: MoC. $Mo_{0.75}Nb_{0.25}C$ (mirrored).Right: DOS for substitution of molybdenum with tungsten: MoC. $Mo_{0.75}W_{0.25}C$ (mirrored). Reprinted figure with permission from [9], Copyright (1999) by American Physical Society.

1.2.2 Synthesis of metal carbides

Structure and surface area of transition metal carbides can be tuned by the preparation method. For instance, in the case of molybdenum carbide up to six structures have been reported; among these structures the hexagonal (β-Mo_2C) is the most stable at room temperature. Other phases such as orthorhombic (1748 °C) and cubic fcc (2273 °C) have been reported to be stable at high temperatures. The fcc structure has received different names such as α-MoC_{1-x}, β-MoC_{1-x}, δ-MoC_{1-x}, α-MoC or MoC_{1-x} [10].

However, most of these phase data are from metallurgical sources (synthesis at very high temperatures). It is possible to prepare the different phases of molybdenum carbide at lower temperatures if the synthesis is conducted at a suitable temperature and the reaction time is long enough. Therefore, formation of carbides at lower temperatures is not limited by thermodynamics but a kinetic problem. Preparation at lower temperatures will lead to carbides with high surface areas. During preparation, different phases (oxide and carbides) can coexist together as shown in Figure 1.8 [10].

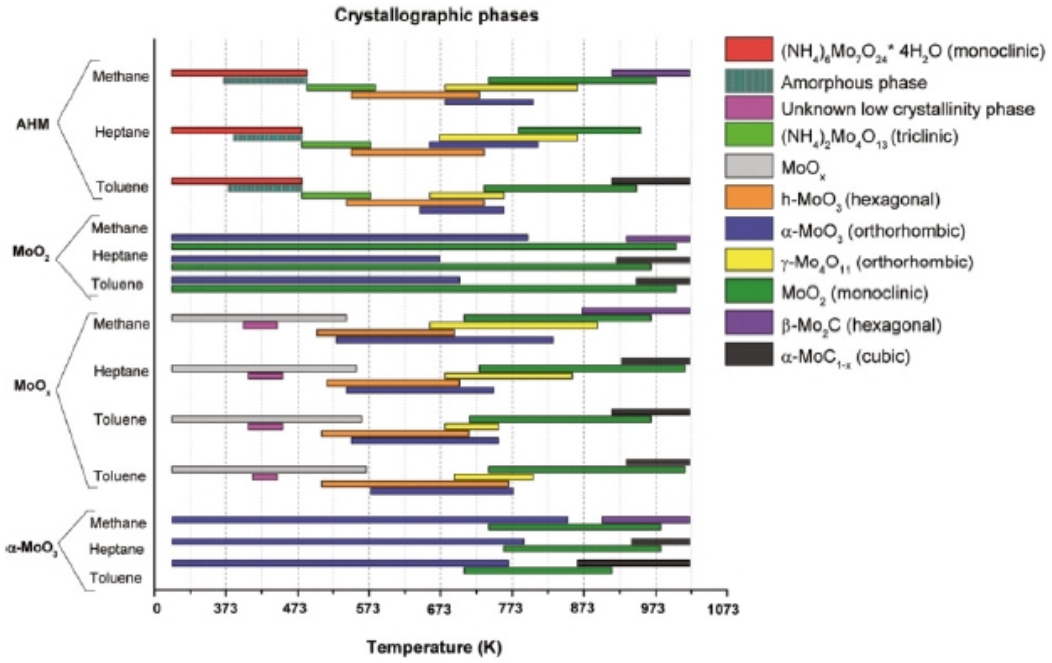

Figure 1.8: Crystallographic phases detected during the TPR of different oxides in different hydrocarbon mixtures. Reproduced with permission from [10]. © 2008 Canadian Science Publishing.

Materials with high surface area are suitable for application in catalysis. Two main methods have been reported for synthesis of high surface area carbides: temperature-programmed reaction (TPR) and the "solution method". In the TPR method, mixtures of hydrogen and a carbon source (usually a gas phase hydrocarbon) are used for carburization of the precursors which are usually oxides [10]. The role of the hydrogen is reduction and removal of deposited carbon from the surface, while the role of the hydrocarbon is both reduction and carburization. The type and the amount of hydrocarbon in the mixture are important in the determination of the final phase of the metal carbide and for the cleanness of the surface. Usually 20% methane in hydrogen is used for carburization. This composition was suggested to not thermodynamically favor coke formation [11]. Other hydrocarbons with higher molecular weight have been tried,

but the mole fraction of carbon was kept constant at 20%, for instance 10% ethane or 5% butane has been used [12].

In Table 1.2, structures of molybdenum carbide prepared with different carbon sources are reported. However, synthesis of metal carbides with ethane has been reported to prepare carbides with the highest surface area compared to the other hydrocarbons, because the carbide can be formed at a lower final temperature [12].

Table 1.2: Structures of molybdenum carbide prepared by using different carbon source

Carbon source	Molybdenum carbide phase	PDF #	Ref.
CH_4	β-Mo_2C, Hexagonal	03-065-8766	[10]
C_2H_6	Hex. & cubic	NR*	[12]
C_3H_6	η-MoC_{1-x} - cubic	NR	[13]
n-C_4H_{10}	η-MoC_{1-x} - cubic	NR	[12]
C_2H_2	MoC_{1-x}	NR	[14]
n-heptane	α-$MoC_{1-x,}$ Cubic	01-074-5548	[10]
Toluene	α-$MoC_{1-x,}$ Cubic	01-074-5548	[10]

*Not reported, in order to verify the phases different methods such as electron diffraction were used.

The other method of synthesis is called the “solution method”. In this method the carbide is formed by decomposition of a mixed salt precursor containing the metal and the carbon source. Different carbon sources have been used such as sugar [15], urea [16, 17] and hexamethylenetetramine (HMT) [18, 19]. Formation of metal carbide from decomposition of these mixed salts depends on the gas atmosphere and the final

synthesis temperature. In this method finding the right ratio between the metal and the carbon source is difficult. Since the carbon source is serving both as reducing and carburizing agent, using an excess amount of the carbon source will cause surface contamination with carbon. It is worth mentioning that with urea or HMT first nitride forms and then nitride transforms to the carbide at higher temperatures.

Making molybdenum and tungsten carbide with the cubic structure is more difficult than making the hexagonal structure. Two methods for making molybdenum and tungsten carbide with the cubic structures have been reported: one is by impregnating the oxide precursor with Pd, Pt or Ni which helps reduction to occur at lower temperatures, and the second method is first preparation of the nitride and then carburization of the nitride to the carbide. Since molybdenum and tungsten nitride both have cubic structure, carburization of the nitride will be a substitution of nitrogen with carbon without changing the structure. This process is shown in Figure 1.9 [20].

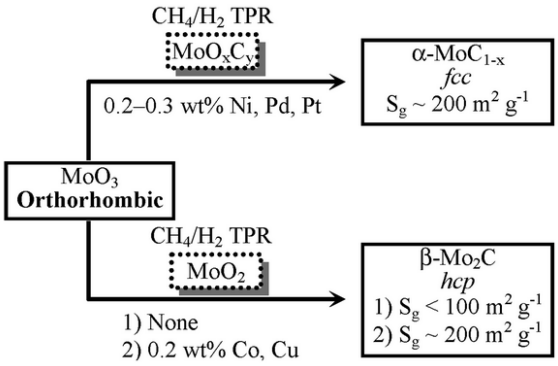

Figure 1.9: Formation of cubic and hexagonal structures by carburization of MoO_3. Reprinted with permission from [20], Copyright (2004) by American Chemical Society.

Most of the data in the carbide literature is about molybdenum carbide and after that about tungsten carbide, and not much about bimetallic carbides. The main problem

in synthesis of bimetallic carbides is synthesis of single phase mixed metal carbides. The first step in the synthesis of bimetallic carbides is the synthesis of a precursor that contains both metals. Different methods have been tried for synthesis of precursors, such as:

- Co-precipitation method: in this method a solution is made that contains both metals, and then by changing the pH of the solution, both metals precipitate at the same time [21].
- Physical mixing: this method is widely reported for synthesis of the precursor before carburization. In this method, two salts are mixed together and some ethanol will be added to the mixture to have better dispersion. They will be pressed together to remove boundaries between particles and then the mixture will be heated to high temperatures to enhance solid-solid diffusion [22].
- Hydrothermal synthesis: in this method two salts containing the metals of choice are dissolved in water, the clear solution is transferred to an autoclave and heated to form a solid under high pressure. The autoclave will be heated for several days. The resultant solid is then separated from the solution by centrifugation [23].
- Freeze drying: based on this method, two salts containing the metals are dissolved in water. Droplets of clear solution are flash frozen by dropping them into liquid nitrogen, and then freeze dried at low pressure overnight. Syntheses of Mo_3Ni_2N and V-Mo-O-N [24 ,25], $MnMoN_2$ [26], Mo-W-O-N, V-W-O-N and Mo-W-V-O-N [27], V-Cr-O-N and Mo-Cr-O-N [28] have been reported by this method.

In this research the goal in precursor synthesis is to find a versatile method for synthesis of single phase mixed metal carbide's precursors. Precursors will be carburized to form carbides.

The last step of carbide preparation is passivation. Carbides are pyrophoric, and they must be passivated before they come in contact with air for transportation or characterization. In order to avoid rapid bulk oxidation of carbides, they must be mildly passivated with low concentrations of oxygen in an inert gas. It is worth to mention that passivation has not been done consistently in the literature.

1.2.3 Catalytic activities of carbides

Early transition metal carbides have been reported as active for hydrogenation reactions such as toluene hydrogenation [29] and naphthalene hydrogenation [30]. Hydrogenation activity of supported molybdenum and tungsten carbides in the presence and absence of H_2S have been compared with the hydrogenation activity of supported Pt. Results are reported in Figure 1.10, showing that in the absence of sulfur the initial activity of WC/Al_2O_3 is similar to that of Pt/SiO_2 and is lower than that of Pt/Al_2O_3, while in the presence of H_2S, Pt/Al_2O_3 suffered deactivation but WC/Al_2O_3 showed steady activity [31]. Unlike Pt poisoned with sulfur, sulfur-poisoned Mo_2C can be regenerated [32].

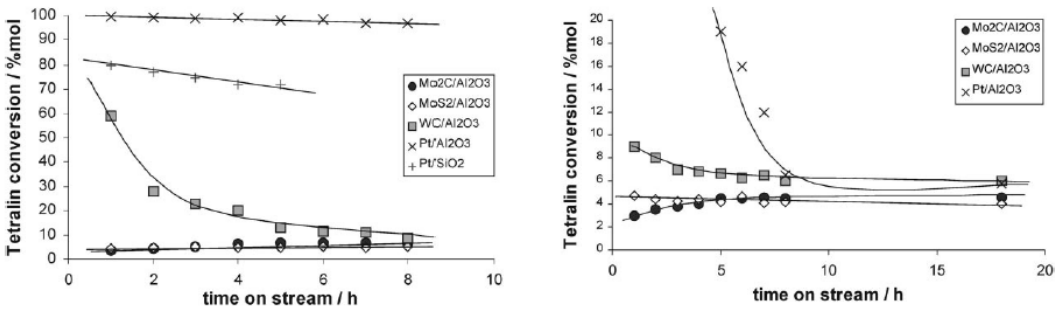

Figure 1.10: Tetralin hydrogenation in the absence of H_2S (left), and in the presence of H_2S (right). (Reaction conditions: 0.2 g of supported catalyst, 573 K, 4 MPa; Reduction conditions: 423 K, 4 MPa). Reprinted from [31]. Copyright (2001), with permission from Elsevier.

Metal carbides are also active for hydrotreating (HDS, HDN and HDO) reactions, as shown in Figure 1.11 [33]. Other reactions in which carbides have been reported to be active include ammonia decomposition [34], methane dehydroaromatization [35], partial oxidation of methane to syngas [36], water gas shift [32], and alcohol synthesis [37].

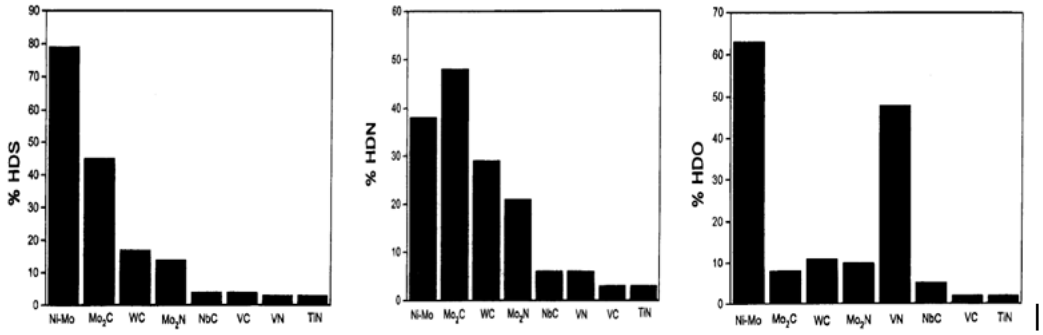

Figure 1.11: Comparison of steady state HDS (left), HDN (middle) and HDO (right) of carbides and nitrides with the commercial sulfided Ni-Mo/Al_2O_3 at 643 K, 3.1 MPa. Reprinted with permission from [33], Copyright (1995) by American Chemical Society.

Mixed metal carbides and nitrides such as Mo-Nb-C [38] and Mo-V-N [39] showed better catalytic activities toward hydrotreating reactions compared with the

corresponding monometallic carbides and nitrides. $NbMo_{1.2}OC/Al_2O_3$ is more active than commercial sulfided Ni-Mo/Al_2O_3 for HDS and HDO [40]. However, the solid solutions of mixed metal carbides with different stoichiometries have not been made to compare activities of materials with different metal ratios.

1.3 Goal and strategy

This class of materials will be expanded by preparing mixed metal carbides. The effect of adding a nonmetal or another metal into the structure of Mo_2C, on the catalytic activity of molybdenum carbide will be investigated. By preparation of well defined single phase mixed metal carbides it is possible to investigate the effect of composition on the catalytic activity. Appropriate methods for synthesis of mixed metal oxycarbides will be developed.

The thesis is structured as follows: Chapter 2 is about passivation and regeneration of Mo_2C and W_2C and the effect of varying the amount of nonmetal (carbon and oxygen) on the catalytic activities of metal carbides. Chapter 3 and 4 deal with the synthesis of mixed metal carbides of Mo-W and Mo-Nb, and their catalytic activities in comparison to that of Mo_2C.

References

[1] H. W. Hugosson, O. Eriksson, L. Nordstrom, U. Jansson, L. Fast, A. Delin, J. M. Wills, B. Johansson, Theory of phase stabilities and bonding mechanisms in stoichiometric and substoichiometric molybdenum carbide, Journal of Applied Physics, 86 (1999) 3758-3767.

[2] R. B. Levy, M. Boudart, Platinum-Like Behavior of Tungsten Carbide in Surface Catalysis, Science, 181 (1973) 547-549.

[3] S. T. Oyama, Preparation and catalytic properties of transition metal carbides and nitrides, Catalysis Today, 15 (1992) 179-200.

[4] J. G. Chen, Carbide and Nitride Overlayers on Early Transition Metal Surfaces: Preparation, Characterization, and Reactivities, Chemical Reviews, 96 (1996) 1477-1498.

[5] V. Heine, s-d Interaction in Transition Metals, Physical Review, 153 (1967) 673-682.

[6] J. K. Nørskov, T. Bligaard, J. Rossmeisl, C. H. Christensen, Towards the computational design of solid catalysts, Nature Chemistry, 1 (2009) 37-46.

[7] J. R. Kitchin, J. K. Nørskov, M. A. Barteau, J. G. Chen, Trends in the chemical properties of early transition metal carbide surfaces: A density functional study, Catalysis Today, 105 (2005) 66-73.

[8] H. K. W. Hugosson, O. Eriksson, U. Jansson, B. R. Johansson, Phase stabilities and homogeneity ranges in 4d-transition-metal carbides: A theoretical study, Physical Review B, 63 (2001) 134108.

[9] H. W. Hugosson, L. Nordström, U. Jansson, B. Johansson, O. Eriksson, Theoretical studies of substitutional impurities in molybdenum carbide, Physical Review B, 60 (1999) 15123-15130.

[10] H. J. Guzmán, W. Xu, D. Stacchiola, G. Vitale, C. E. Scott, J. A. Rodríguez, P. Pereira-Almao, In situ time-resolved X-ray diffraction study of the synthesis of Mo_2C with different carburization agents, Canadian Journal of Chemistry, 91 (2013) 573-582.

[11] J.S. Lee, S.T. Oyama, M. Boudart, Molybdenum carbide catalysts: I. Synthesis of unsupported powders, Journal of Catalysis, 106 (1987) 125-133.

[12] T. Xiao, A. P. E. York, K. S. Coleman, J. B. Claridge, J. Sloan, J. Charnock, M. L. H. Green, Effect of carburising agent on the structure of molybdenum carbides, Journal of Materials Chemistry, 11 (2001) 3094-3098.

[13] X. H. Wang, H. L. Hao, M. H. Zhang, W. Li, K. Y. Tao, Synthesis and characterization of molybdenum carbides using propane as carbon source, Journal of Solid State Chemistry, 179 (2006) 538-543.

[14] T. Xiao, H. Wang, J. Da, K.S. Coleman, M. L. H. Green, Study of the Preparation and Catalytic Performance of Molybdenum Carbide Catalysts Prepared with C_2H_2/H_2 Carburizing Mixture, Journal of Catalysis, 211 (2002) 183-191.

[15] M. Patel, J. Subrahmanyam, Synthesis of nanocrystalline molybdenum carbide (Mo_2C) by solution route, Materials Research Bulletin, 43 (2008) 2036-2041.

[16] C. Giordano, C. Erpen, W. Yao, B. Milke, M. Antonietti, Metal Nitride and Metal Carbide Nanoparticles by a Soft Urea Pathway, Chemistry of Materials, 21 (2009) 5136-5144.

[17] W. Yao, P. Makowski, C. Giordano, F. Goettmann, Synthesis of Early-Transition-Metal Carbide and Nitride Nanoparticles through the Urea Route and Their Use as Alkylation Catalysts, Chemistry – A European Journal, 15 (2009) 11999-12004.

[18] S. Chouzier, T. Czeri, M. Roy-Auberger, C. Pichon, C. Geantet, M. Vrinat, P. Afanasiev, Decomposition of molybdate-hexamethylenetetramine complex: One single source route for different catalytic materials, Journal of Solid State Chemistry, 184 (2011) 2668-2677.

[19] Z. Q. Wang, Z. B. Zhang, M. H. Zhang, The efficient synthesis of a molybdenum carbide catalystvia H_2-thermal treatment of a Mo(VI)-hexamethylenetetramine complex, Dalton Transactions, 40 (2010) 1098-1104.

[20] K. T. Jung, W. B. Kim, C. H. Rhee, J. S. Lee, Effects of Transition Metal Addition on the Solid-State Transformation of Molybdenum Trioxide to Molybdenum Carbides, Chemistry of Materials, 16 (2003) 307-314.

[21] L. Leclercq, M. Provost, H. Pastor, J. Grimblot, A. M. Hardy, L. Gengembre, G. Leclercq, Catalytic properties of transition metal carbides: I. Preparation and physical characterization of bulk mixed carbides of molybdenum and tungsten, Journal of Catalysis, 117 (1989) 371-383.

[22] C. C. Yu, S. Ramanathan, B. Dhandapani, J. G. Chen, S. T. Oyama, Bimetallic Nb-Mo Carbide Hydroprocessing Catalysts: Synthesis, Characterization, and Activity Studies, The Journal of Physical Chemistry B, 101 (1997) 512-518.

[23] T. Murayama, N. Kuramata, S. Takatama, K. Nakatani, S. Izumi, X. Yi, W. Ueda, Synthesis of porous and acidic complex metal oxide catalyst based on group 5 and 6 elements, Catalysis Today, 185 (2012) 224-229.

[24] S. Alconchel, F. Sapina, D. Beltran, A. Beltran, A new approach to the synthesis of molybdenum bimetallic nitrides and oxynitrides, Journal of Materials Chemistry, 9 (1999) 749-755.

[25] A. El-Himri, M. Cairols, S. Alconchel, F. Sapina, R. Ibanez, D. Beltran, A. Beltran, Freeze-dried precursor-based synthesis of new vanadium-molybdenum oxynitrides, Journal of Materials Chemistry, 9 (1999) 3167-3171.

[26] M. E. Himri, A. E. Himri, P. Núñez, Freeze dried precursor-based synthesis of molybdenum bimetallic nitride, Journal of Materials and Environmental Science, 2 (2011) 18-23.

[27] A. El-Himri, P. Núñez, F. Sapiña, R. Ibanez, A. Beltran, J. M. A. Martı́nez-Agudoc, Synthesis of new molybdenum-tungsten, vanadium-tungsten and vanadium-molybdenum-tungsten oxynitrides from freeze-dried precursors, Journal of Solid State Chemistry, 177 (2004) 2423-2431.

[28] A. El-Himri, F. Sapina, R. Ibanez, A. Beltran, Synthesis of new vanadium-chromium and chromium-molybdenum oxynitrides by direct ammonolysis of freeze-dried precursors, Journal of Materials Chemistry, 10 (2000) 2537-2541.

[29] M. L. Frauwallner, F. López-Linares, J. Lara-Romero, C. E. Scott, V. Ali, E. Hernández, P. Pereira-Almao, Toluene hydrogenation at low temperature using a molybdenum carbide catalyst, Applied Catalysis A: General, 394 (2011) 62-70.

[30] S. J. Ardakani, X. Liu, K. J. Smith, Hydrogenation and ring opening of naphthalene on bulk and supported Mo_2C catalysts, Applied Catalysis A: General, 324 (2007) 9-19.

[31] P. Da Costa, J. L. Lemberton, C. Potvin, J. M. Manoli, G. Perot, M. Breysse, G. Djega-Mariadassou, Tetralin hydrogenation catalyzed by Mo_2C/Al_2O_3 and WC/Al_2O_3 in the presence of H_2S, Catalysis Today, 65 (2001) 195-200.

[32] J. A. Schaidle, A. C. Lausche, L. T. Thompson, Effects of sulfur on Mo_2C and Pt/Mo_2C catalysts: Water gas shift reaction, Journal of Catalysis, 272 (2010) 235-245.

[33] S. Ramanathan, S. T. Oyama, New Catalysts for Hydroprocessing: Transition Metal Carbides and Nitrides, The Journal of Physical Chemistry, 99 (1995) 16365-16372.

[34] W. Zheng, T. P. Cotter, P. Kaghazchi, T. Jacob, B. Frank, K. Schlichte, W. Zhang, D. S. Su, F. Schüth, R. Schlögl, Experimental and Theoretical Investigation of Molybdenum Carbide and Nitride as Catalysts for Ammonia Decomposition, Journal of the American Chemical Society, 135 (2013) 3458-3464.

[35] S. Ma, X. Guo, L. Zhao, S. Scott, X. Bao, Recent progress in methane dehydroaromatization: From laboratory curiosities to promising technology, Journal of Energy Chemistry, 22 (2013) 1-20.

[36] T. C. Xiao, A. Hanif, A. P. E. York, Y. Nishizaka, M. L. H. Green, Study on the mechanism of partial oxidation of methane to synthesis gas over molybdenum carbide catalyst, Physical Chemistry Chemical Physics, 4 (2002) 4549-4554.

[37] H. C. Woo, K. Y. Park, Y. G. Kim, I. S. Nam, J. S. Chung, J. S. Lee, Mixed alcohol synthesis from carbon monoxide and dihydrogen over potassium-promoted molybdenum carbide catalysts, Applied Catalysis, 75 (1991) 267-280.

[38] C. C. Yu, S. Ramanathan, B. Dhandapani, J. G. Chen, S. T. Oyama, Bimetallic Nb-Mo Carbide Hydroprocessing Catalysts:Synthesis, Characterization, and Activity Studies, The Journal of Physical Chemistry B, 101 (1997) 512-518.

[39] C.C. Yu, S. Ramanathan, F. Sherif, S. T. Oyama, Structural, Surface, and Catalytic Properties of a New Bimetallic V-Mo Oxynitride Catalyst for Hydrodenitrogenation, The Journal of Physical Chemistry, 98 (1994) 13038-13041.

[40] V. Schwartz, S. T. Oyama, J. G. Chen, Supported Bimetallic Nb-Mo Carbide: Synthesis, Characterization, and Reactivity, The Journal of Physical Chemistry B, 104 (2000) 8800-8806.

2. Passivation Agents for Mo_2C and W_2C: Effect on Reduction and Catalytic Activity

2.1 Introduction

Since Levy and Boudart reported that tungsten carbide shows Pt-like behavior in a way that it can catalyze the oxidation of hydrogen at room temperature, the reduction of WO_3 by moist H_2 to form H_xWO_3 at room temperature, and the isomerization of 2,2 dimethylpropane to 2-methylbutane, early transitional metal carbides have gained interest as potentially less costly and sustainable replacements for precious metal catalysts [1]. It was Levy and Boudart's assertion that the surface electronic properties of tungsten were modified by the insertion of carbon into the lattice of the metal, and a more recent density functional study has shown that formation of carbon-metal bonds in transition metal carbides changes the density of states (DOS) of the metal [2], and these changes of the DOS cause different physical and catalytic properties for metal carbides compared to their parent metals [3]. Besides potentially lower cost, transition metal carbides are refractory materials that will not easily sinter, and have been reported to be resistant to sulfur poisoning [4, 5]. These qualities potentially make metal carbides promising materials for application as catalysts for a wide variety of reactions. Metal carbides have been tested for hydrogenation [5], hydrotreating [6], methane dehydroaromatization [7], partial oxidation of methane to syngas [8], ammonia decomposition [9], and water gas shift [10].

One prerequisite for the use of a material for heterogeneous catalysis is that it should have a high surface area in order to decrease material costs by optimizing contact between the carbide surface and gas or liquid phase reactants [11,12]. High

surface area transition metal carbides are usually prepared by heating a precursor material containing the metal in a reducing atmosphere that contains carbon. The transition metal in the precursor material is at an oxidation state greater than zero and the carburization is usually preceded by some reduction followed by the intercalation of carbon, usually at temperatures between 600 and 900 °C.

The fresh surfaces of carbides are reactive towards oxygen and can be pyrophoric. Ideally, pyrophoric materials would be studied without contact with air. However, it is common practice, as reported in the literature [11-13], to passivate the surfaces of transition metal carbides in order to transfer them from the synthesis reactor to the characterization equipment or the catalytic reactor. While oxidation is the most commonly used method for carbide passivation, several other passivation techniques have been discussed in the literature. The formation of a layer of carbon on the surface of the carbide has been reported to produce a surface that does not react with oxygen at room temperature. Zhao et al. found that an amorphous carbon layer on the surface of FeC particles enhanced resistance to oxidation [14]. McBreen has reported the anchoring of alkylidene layers on molybdenum carbide by reacting the carbide with cyclobutanone at sub-ambient temperatures [15,16]. The alkylidene layer is bonded to the molybdenum atoms. The surface is said to be inert because of the additional carbon depositing during alkylidene layer formation, and perhaps because of the oxygen from the ketone that also bonds with the molybdenum. Warren et al. investigated the oxidation of WC surfaces and found that a 6 Å layer of oxide formed when the WC surface was exposed to air at 25 °C, but that “when WC was exposed to water, it

resisted further oxidation" [17]. Wu et al. have investigated water and carbon dioxide as passivation agents [18].

Some reports contain reaction data that is collected from catalysts that have not been passivated [19]; however, for the majority of the literature on carbide catalysts the carbides are passivated by flowing low concentrations of oxygen in an inert diluent over the fresh carbide in the carburization reactor. It is common practice to use 0.5 or 1% oxygen as the passivation agent [11-13, 20-22]. There are two measures of the success of a passivation treatment: 1) protection of the sample from air, 2) successful desorption/re-reduction and regeneration of the active carbide surface. Wu et al. [18] have investigated the use of oxygen, water, and carbon dioxide for the passivation of molybdenum carbide supported on aluminum oxide, and reported that the carbide surface passivated in either CO_2 or water could be more fully regenerated than that passivated in oxygen. Their conclusions were based on IR spectroscopy experiments using carbon monoxide as a probe molecule to assess changes to the Mo oxidation state and the number of surface sites that could be regenerated after passivation. Shou et al. have reported the effect of passivation on the activity of a molybdenum carbide catalyst for Fischer-Tropsch synthesis and found that the passivated sample was 37% less active and reduced the alcohol production by an order of magnitude [23]. Bogatin et al. investigated NdFeB nitrides and carbides and reported they could passivate powdered carbides with CO_2 or N_2 at temperatures between 125 and 300 °C [24]. Further studies on the regeneration (reduction) of molybdenum and tungsten carbides have been reported in the literature [25, 26]. However, the results are not consistent due to the different synthesis method (different carburization gas mixture, different passivation

methods and different reduction temperatures) which lead to the presence of different amounts of carbon and oxygen on the surface.

The interaction of oxygen with the surface of metal carbides is not only important for passivation after preparation, but may also be of interest for catalytic reactions with oxygen-containing molecules such as Fischer-Tropsch synthesis, water gas shift, or biomass upgrading [27]. The presence of oxygen on the surface of metal carbides changes the product selectivities by introducing an acid functionality [28,29], changes the reforming properties [30], or acts in favor of dehydrogenation reactions [31].

The goal of this chapter is to understand the effect of compounds that have been reported as passivation agents for transition metal carbides on the fresh carbide surface. Effects of oxygen, CO_2 and water on the surface of Mo_2C [18] and oxygen on the surface of W_2C will be investigated. These two metal carbides are chosen because they are both catalytically active for various reactions and because their metal oxides have distinctly different redox properties. The regeneration of these metal carbides under different gas atmospheres will be investigated, and the effect of surface passivation and regeneration on catalytic activity using the hydrogenation of toluene as a test reaction will be studied.

2.2 Experimental section

2.2.1 Catalyst and materials

Fresh Mo_2C and W_2C were prepared by temperature-programmed reaction of MoO_3 (99.95%, Alfa Aesar) or WO_3 (99.995%, Aldrich) in a STA 4491F1 Netzsch thermogravimetric analyzer (TGA) connected to an online MS. Carburization gases

were 5 ml/min ethane (99.95%, Matheson), 35 ml/min H_2 and 10 ml/min argon (both ultra high purity from Airgas); all flow rates at STP. Synthesis methods followed reported protocol in the literature [8, 12], briefly, the oxides were heated in the carburization gas mixture from room temperature to 450 ℃ with a temperature ramp of 5 K/min, and from 450 ℃ to the final carburization temperature, with a temperature ramp of 2 K/min. The final synthesis temperatures for Mo_2C and W_2C were 650 ℃ and 700 °C, respectively. The samples were held at the final temperature for 1.5 hours until the sample weight did not change. The synthesis was carried out at atmospheric pressure.

The passivation of samples was carried out isothermally at 40 ℃ using UHP argon as diluent (Airgas). For oxygen passivation, air (zero grade, Airgas) was used at initial oxygen concentrations of 0.1 or 1 % with a total flow rate of between 50 and 400 ml/min. CO_2 (instrument grade, Airgas) and deionized water were used for passivation. Air and hydrogen were purified by flowing through a moisture trap (Agilent, MT400-2), CO_2 was purified by flowing through an oxygen trap (Z-Pure Glass Indicating Oxygen Trap), and argon was purified by flowing through a dual trap of moisture and oxygen (Z-Pure Dual Purifier). Passivation experiments using water were carried out using a saturator containing deionized water that was submerged in a 20 °C isothermal water bath giving a water partial pressure of 2.3 kPa that was then diluted in 150 ml/min Ar.

2.2.2 Passivation methods

2.2.2.1 Passivation with CO_2

The temperature was programmed to be isothermal at 35 ℃ for 20 minutes in 100% Ar followed by 20 minutes in 30% CO_2, with a total flow rate of 100 ml/min.

The temperature was increased from 35 °C to 800 °C with a temperature ramp of 5 K/min in 30% CO_2/Ar. The gas phase products were monitored by online MS. Gas phase products observed during passivation of Mo_2C were compared with gas phase products observed while applying the same temperature to an empty crucible. In another experiment, the temperature was increased to 100 °C, and held at this temperature for 3 hours in 30%CO_2/Ar, then the sample was cooled down to 40 °C and a mixture of 16% O_2/Ar was introduced into the TG.

2.2.2.2 Passivation with water

The temperature program for passivation with water was as follows: 1 hour isothermal in Ar at 110 °C, 1 hour isothermal in water/Ar (120 ml/min of Ar was bubbled through water and was introduced to the TG), and then the temperature was increased to 800 °C with a ramp of 5 K/min. In another experiment, the temperature was increased to 110 °C in Ar, and was held for one hour, and then water vapor was introduced into the TG for two hours at 110 °C. Then the TG apparatus was cooled down to 40 °C, and 16% O_2/Ar was sent to the TG.

2.2.2.3 Passivation with 1% O_2/Ar

The concentration of oxygen was 1% for 15 hours and then the concentration of oxygen was increased to 16% for one hour. The process was isothermal at 40 °C.

2.2.2.4 Passivation with “stepwise oxygen”

In this method, the concentration of oxygen in Ar was increased from 0.1% to 0.5% to 1% and to 16%. Each step was 3 hours. The process was isothermal at 40 °C.

2.2.3 Fresh carbides (without passivation)

Fresh carbides were prepared in the same reactor that was used for the catalytic reactions. The samples were synthesized in 10% ethane in hydrogen at the same flow rates and with the same temperature program as described above for sample preparation in the TG apparatus. To measure the surface area of fresh carbides, they were transferred to a glove box, while they were in the reactor, and then they were transferred to the nitrogen physisorption tube in the glove box for analysis.

2.2.4 Temperature-programmed reduction (TPR)

The TPR experiments were carried out in the TG-MS apparatus on about 12 mg of freshly passivated sample. The total flow rate was 50 ml/min of a mixture containing 80% hydrogen in argon. The temperature was increased from 40 to 700 °C with a temperature ramp of 5 K/min and was held at the final temperature for 1 hour. The gas phase products were monitored by online MS.

2.2.5 Catalytic tests

The reactor was a ¼ inch stainless steel flow reactor equipped with an Eldex liquid feed pump. The feed was 0.02 ml/min of liquid toluene (99.5%, Mallinckrodt Chemicals) and 150 ml /min STP H_2 (Ultra high purity, Airgas). The reactor total pressure was 20 bar, which was controlled by a back pressure valve. Reaction temperatures were 150, 200 and 300 °C for Mo_2C and 200, 300 and 400 °C for W_2C. The reactor was loaded with carbide or an appropriate amount of oxides to obtain a final amount of 50 mg of Mo_2C and 100 mg of W_2C. The length of the bed was increased by mixing SiC (Aldrich, 200-450 mesh) with the carbides to avoid channeling and local heating. The temperature was controlled using a thermocouple inside the reactor at the

bottom of the catalyst bed. Products were analyzed every 30 minutes using an online HP 5890 GC with a flame ionization detector (FID), equipped with a 30 m, 0.32 m GASPRO column. The reaction was carried out in the gas phase, and transfer lines to the GC were heated to 110 °C to ensure that no condensation occurred before the GC. The GC temperature program was, 5 minutes isothermal at 60 °C, then heating with 10 K/min to a final temperature of 240 °C, which was held for 4 minutes. Conversion of toluene was defined as the difference between moles of toluene in the feed and in the product divided by moles of toluene in the feed.

2.2.6 Characterization

Samples were characterized by X-ray diffraction (XRD) using a Bruker D8 instrument equipped with Cu Kα radiation. The samples were measured in reflection geometry. Diffractograms were collected with scanning steps of 0.05 in 2θ over the angular range of 20-90°. BET surface areas were measured using a Micromeritics ASAP 2010 and N_2 at 77 K. The unpassivated samples were transferred to the N_2 physisorption tube in the glove box without coming in contact with air. Pore size distributions were determined from nitrogen desorption isotherms applying the BJH method. Before measuring the surface area, the samples were degassed at 350 °C for 4 hours.

2.3 Results

2.3.1 Characterization of samples

Changes in weight were monitored by TG. For both MoO_3 and WO_3, there were two water peaks which indicate reduction by hydrogen and a CO_2 peak at the final temperature which formed with the last peak of water, indicating simultaneous

reduction and carburization. The first peak of water formed at -11.22% and -6.96% of weight loss for MoO_3 and WO_3, respectively, close to the theoretical weight loss to form MoO_2 (-11.11%) and WO_2 (-6.9%). The weight loss during conversion of the oxide precursors to the carbide products was consistent with the formation of carbides with the stoichiometry $Mo_2C_{1.16}$ and $W_2C_{1.11}$. The diffractograms of both Mo_2C and W_2C showed relatively broad peaks consistent with a highly disordered structure or very small crystallite sizes, as reported in Figure 2.1.

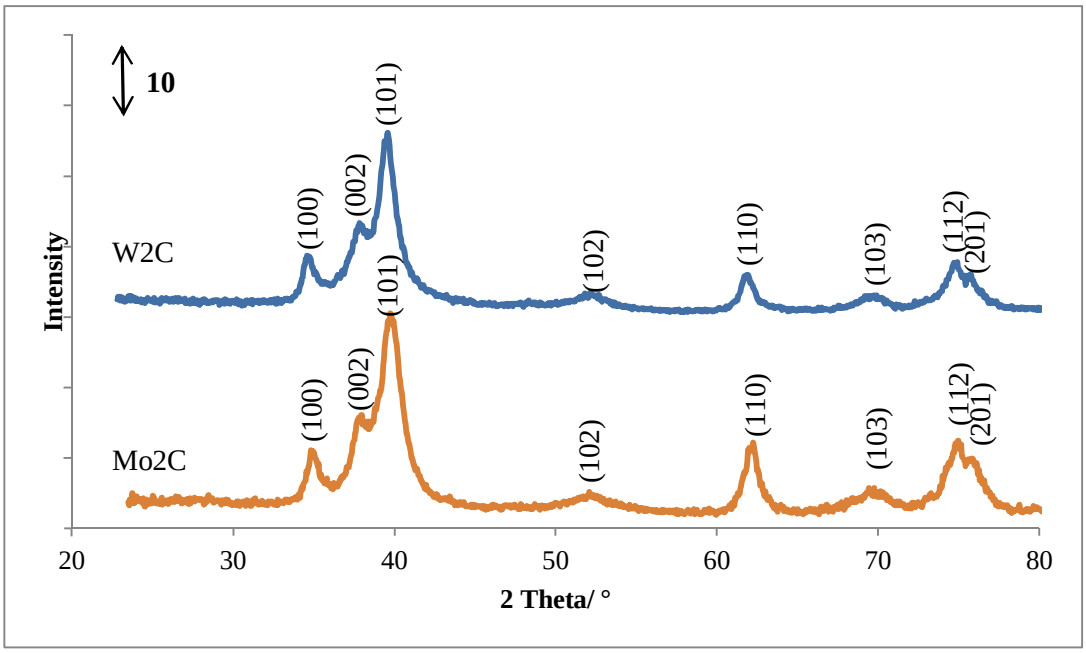

Figure 2.1: XRD data for W_2C (top) and Mo_2C (bottom)

The diffractogram of Mo_2C was consistent with the hexagonal α-Mo_2C structure (ICDD: 00-035-0787), and W_2C showed a hexagonal α-W_2C structure (ICDD: 00-035-0776).

The surface areas of the carbides were determined by the BET method and are reported in Table 2.1. The isotherms were type IV with a pore size distribution in the meso-porosity range.

Table 2.1: Physisorption data for Mo_2C and W_2C

Samples	Surface area (m^2/g)	BJH desorption pore diameter (Å)	BJH desorption pore volume (cm^3/g)
Mo_2C _1%O_2 passivated	43	36.1	0.038
W_2C _1%O_2 passivated	23	97.5	0.044
Mo_2C_fresh	58	29.2	0.047
W_2C_fresh	35	73.0	0.072

2.3.2 Passivation of carbides with air, carbon dioxide and water

Figure 2.2 shows the weight gain during the first hour of passivation in 1% oxygen at 40 °C, 0.1 % oxygen at 40 °C, 30 % CO_2 at 100 °C and 3 % H_2O at 110 °C. As a reference to gauge the background oxygen content, the weight gain in Argon flow at 300 °C is also presented in Figure 2.2.

For the case of 1 % oxygen, the weight initially increases at a rate of 0.58 % /minute and the sample gains 2 % weight within 10 minutes. For the case of 0.1 % oxygen, the weight gain is initially 0.08 %/minute and the sample gains only 0.8 % within the first 10 minutes.

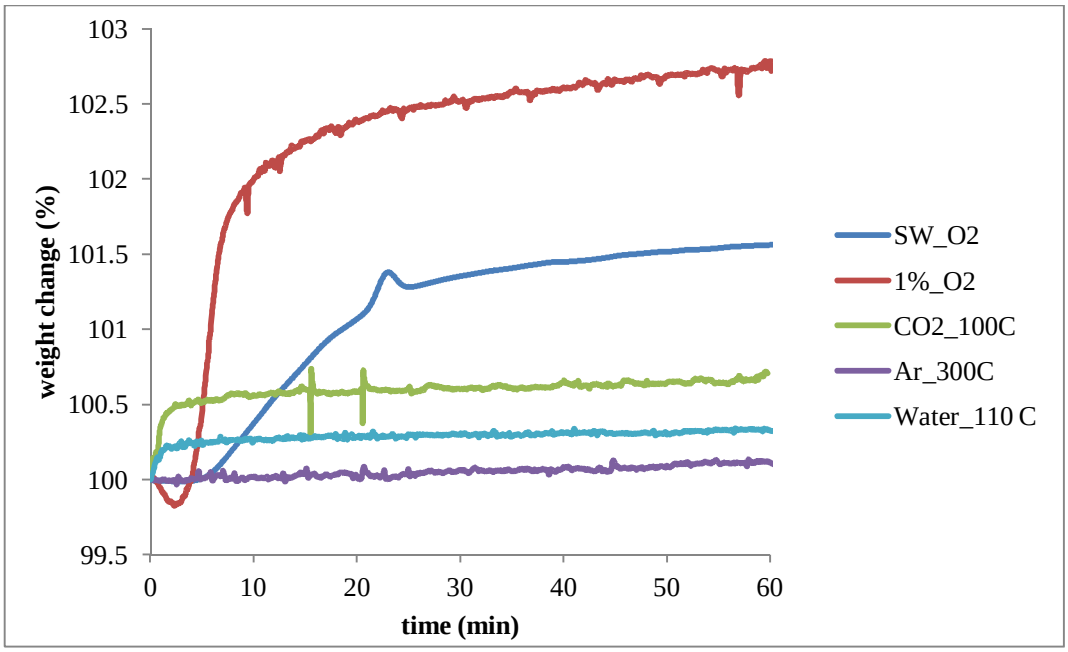

Figure 2.2: Passivation of Mo_2C during the first 60 minutes. From top to bottom passivation in: 1% O_2 at 40 °C, 0.1% O_2 at 40 °C, 30% CO_2 at 100 °C, 3% water at 110 °C and Argon at 300 °C.

Table 2.2 shows that the final weight gain (after exposure to 16% oxygen, from air, to ensure that the passivation was successful) is 3.6% for the 1.0% oxygen passivated sample vs. 3.1% weight gain for the 0.1% passivated sample. Even after exposure to 16 % oxygen for 1 hour the samples continued to gain weight at a very slow rate, as it is reported in Figure 2.3. During passivation with oxygen, the gas phase was monitored with a mass spectrometer, and there were no detectable gas phase products.

Table 2.2: Amounts of weight gain after passivation and weight loss after reduction

Sample	Final weight gain (%)	Weight loss (%) after reduction
$Mo_2C_1\%O_2$	3.58	3.51
$Mo_2C_1\%\ O_2$	-	9.7[1]
$Mo_2C_stepwise\ O_2$	3.06	2.92
$W_2C_1\%O_2$	2.78	2.71
$W_2C_stepwise\ O_2$	2.48	2.71

[1] stored in a vial for 11 months and then reduced.

Exposure of the fresh Mo_2C sample to water vapor was initially carried out at 110 °C in order to discriminate the reaction of the water with the carbide from condensation of the water. The sample gained 0.35% of the initial weight within two hours (in 3% water/Ar). However, when the water flow was stopped, the weight decreased by 0.21%, indicating that the weight gain was because of weakly adsorbed water. When the sample was subsequently exposed to 16 % oxygen at 40 °C (at 280 minutes), the weight gain was 3% as reported in Figure 2.4.

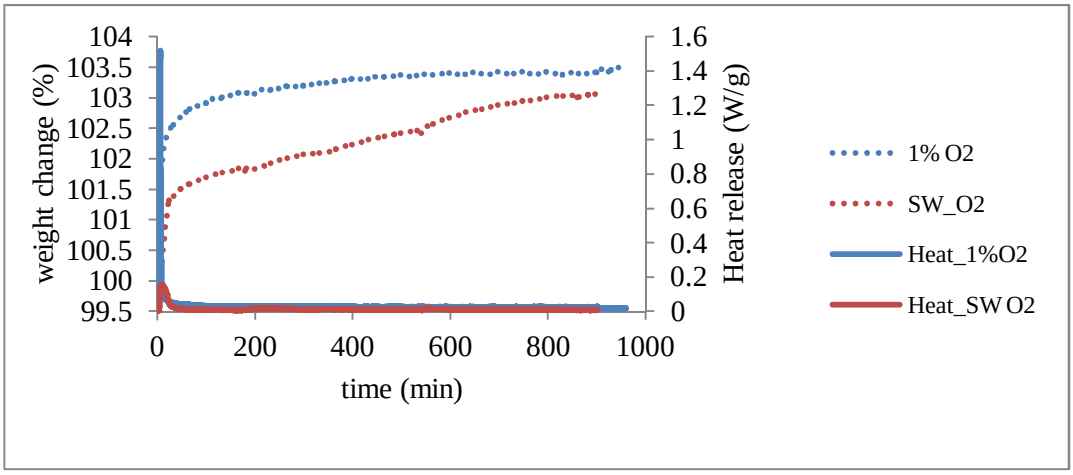

Figure 2.3: Weight gains (dashed line) and heat effects (solid line) during passivation of Mo_2C with 1% O_2 (blue) and with stepwise O_2 (red) at 40 °C.

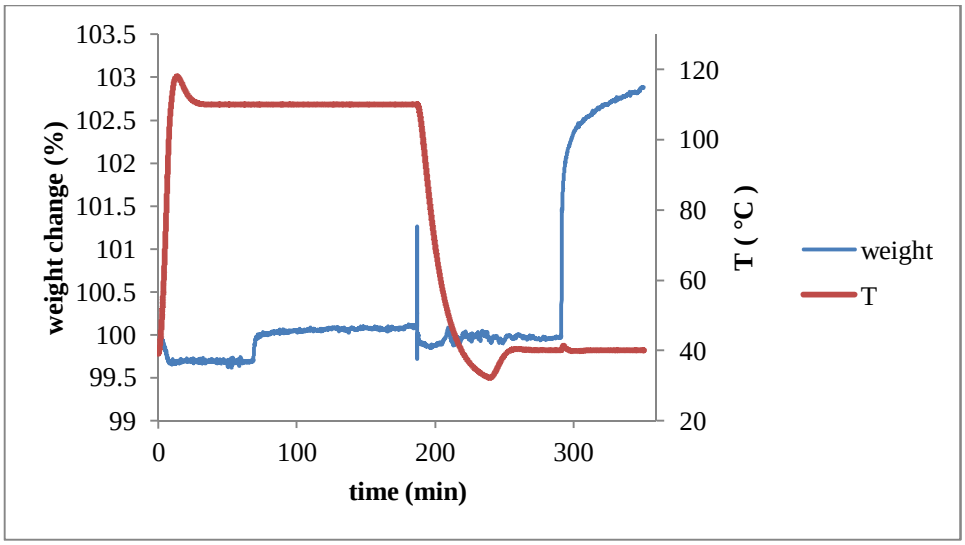

Figure 2.4: Passivation of Mo_2C: in the beginning gas phase atmosphere was pure Ar then switched to 3% water in Ar at 110 °C after 68 minutes and switched to 16% O_2/Ar at 40 °C after 290 minutes.

In order to further understand the interaction of water with the carbide surface a temperature-programmed reaction experiment was performed as shown in Figure 2.5. The weight initially decreases as some of the water is desorbed from the carbide surface, and then increases slowly as the sample is heated to 550 °C. The slow weight increase is accompanied by the desorption of carbon monoxide. At temperatures higher than 550 °C, the MS data in Figure 2.5 show the formation of hydrogen (m/z=2) and carbon monoxide (m/z = 28). The formation of CO indicates that under these conditions the oxygen in the water molecule is removing carbon from the surface of the carbide.

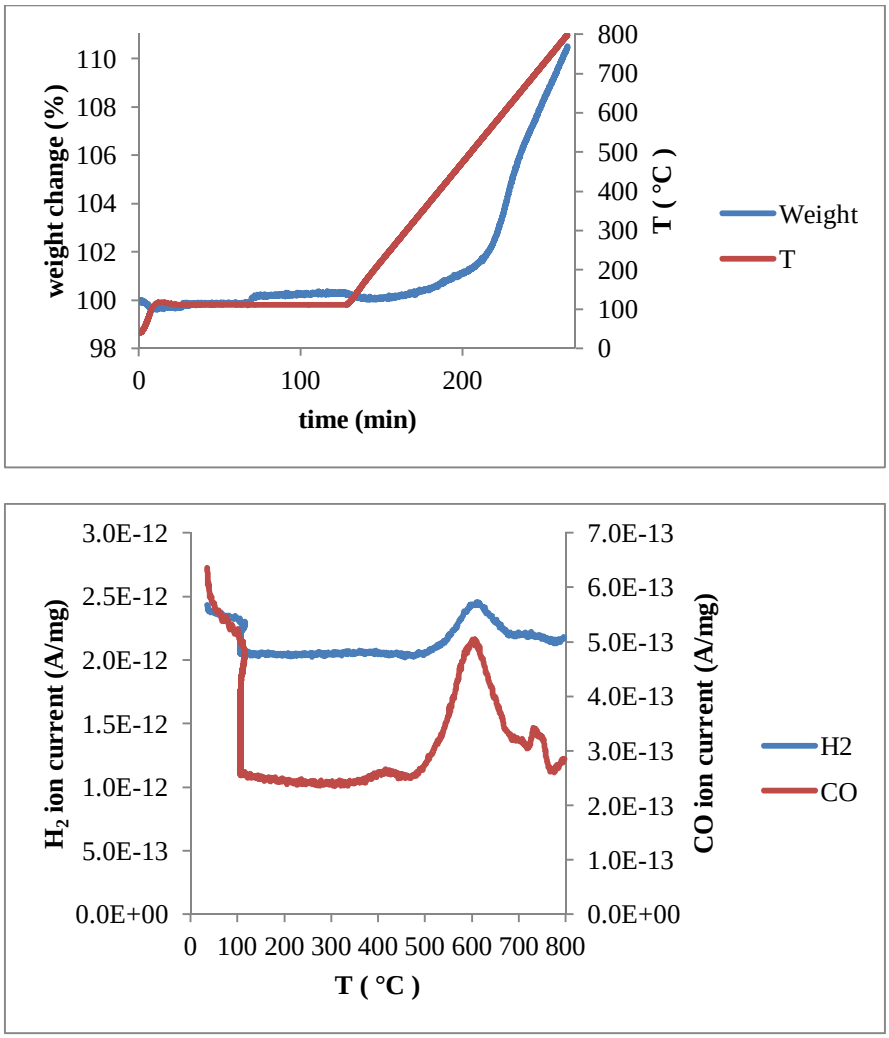

Figure 2.5: TP water of Mo_2C, TG data (top) and MS data (bottom). Gas phase atmosphere was initially 100% Ar and at after 68 minutes was switched to 3% water in Ar.

Exposure of the fresh Mo_2C sample to CO_2 was initially carried out at 100 °C for 3 hours. During this time, Mo_2C gained 0.48% weight, and within the first hour it gained 0.12% weight as is shown in Figure 2.6, with no CO gas phase products. However, when the CO_2 flow was stopped, the weight decreased by 0.12%, indicating that some of the weight gain was due to weakly adsorbed CO_2. When the sample was subsequently exposed to 16 % oxygen at 40 °C, the weight gain was 2.92% as reported in Figure 2.6.

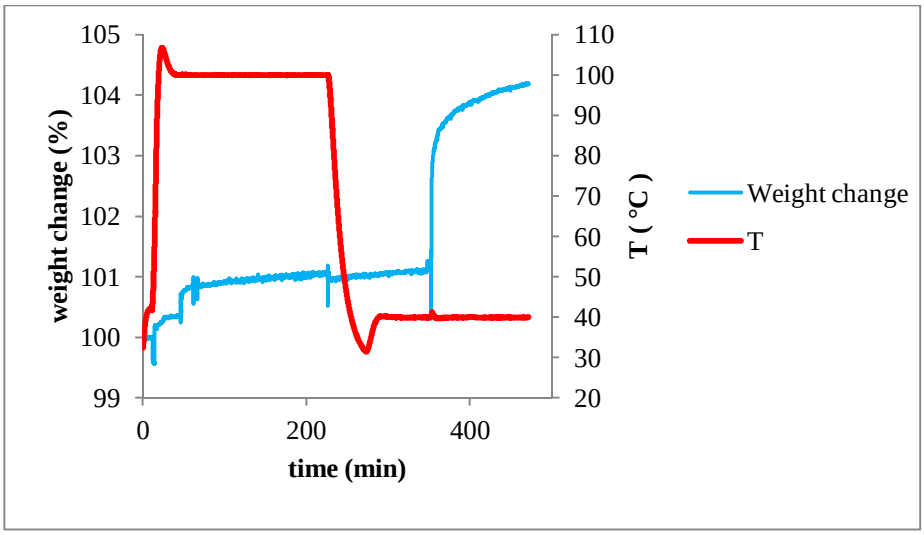

Figure 2.6: Passivation of Mo_2C: gas phase atmosphere initially was 100% Ar, after 46 minutes switched to 30% CO_2 in Ar at 100 °C and after 351 minutes switched to 16% O_2 at 40 °C.

In order to further understand the ability of CO_2 to react with the carbide a TP reaction experiment with 30% CO_2 was carried out. The TP reaction results in CO_2 are shown in Figure 2.7.

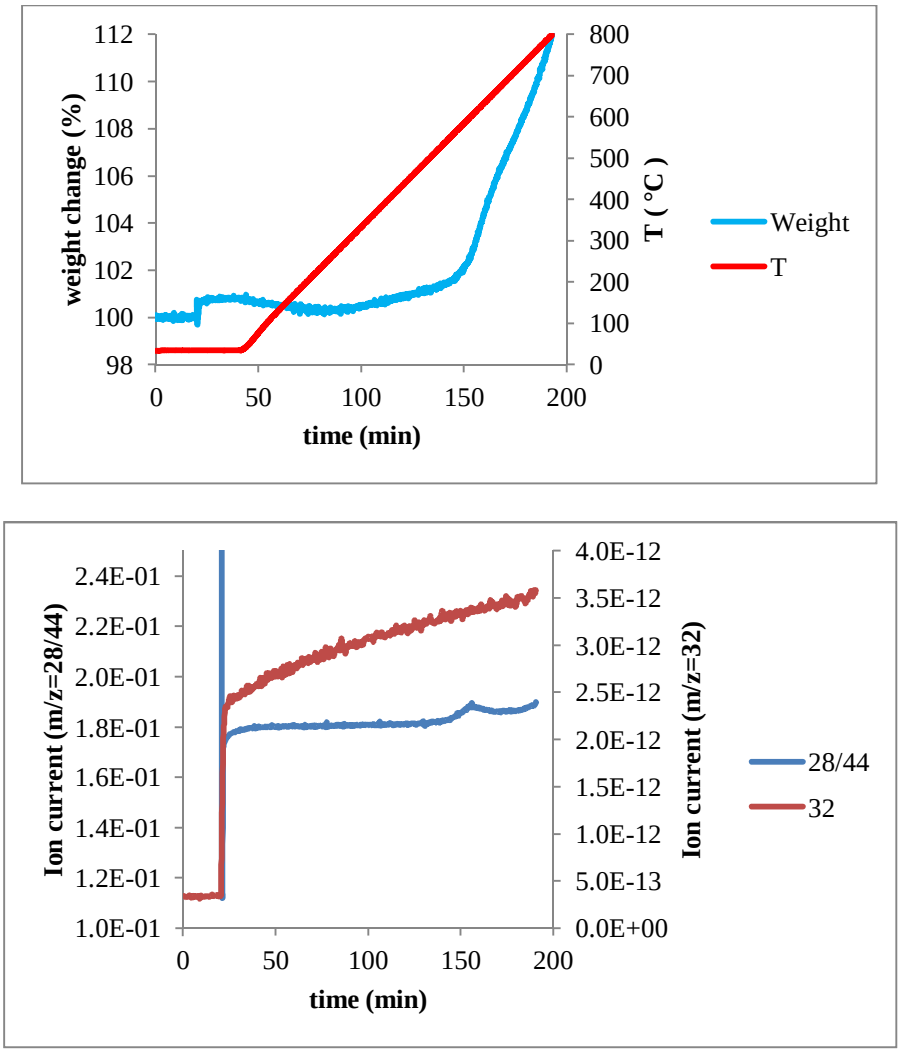

Figure 2.7: TG data (top) and MS data (bottom) for $TPCO_2$ in 30%CO_2 in Ar. Gas phase atmosphere was initially 100% Ar, after 20 minutes switched to 30%CO_2/Ar.

During the isothermal phase at 40 °C when CO_2 was present in the gas stream, there was a 0.69% weight gain that can be attributed to the adsorption of CO_2 on the carbide surface. Initially, when the sample was heated, a weight loss is observed (weight gain decrease from 0.69% to 0.34%), that is attributed to the loss of weakly adsorbed CO_2. The onset temperature for significant weight gain in 30% CO_2 is about 586 °C, and at this temperature the formation of CO (m/z = 28) is observed. The rapid

weight gain at temperatures above 580 °C is consistent with bulk oxidation of the sample.

2.3.3 Reduction of passivated samples

Temperature-programmed reduction (TPR) was used to determine an appropriate regeneration temperature. The results of TPR in hydrogen for the Mo_2C sample are shown in Figure 2.8.

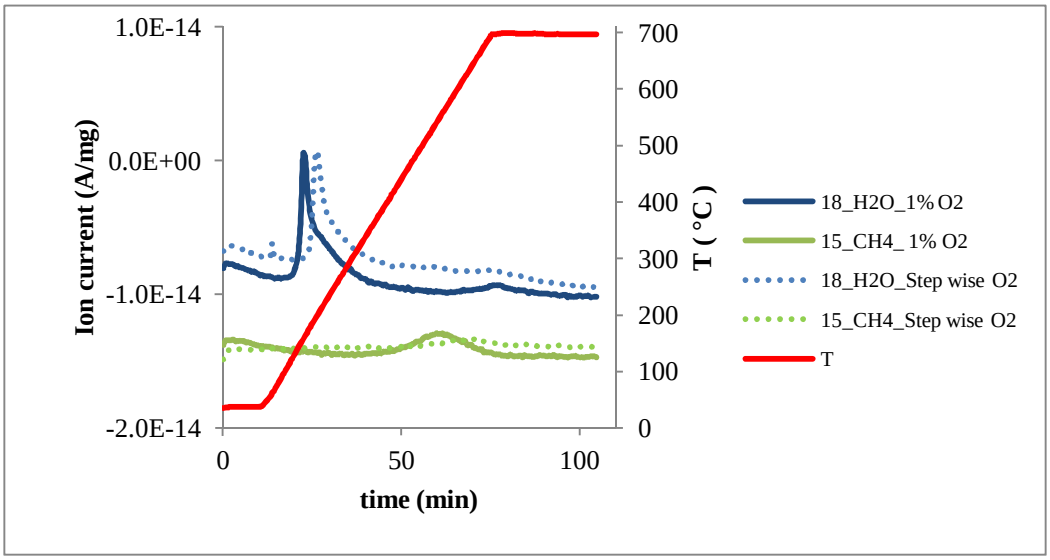

Figure 2.8: Reduction of Mo_2C in 80% H_2/Ar. The solid line represents Mo_2C passivated in 1% O_2 and the dashed line represents Mo_2C passivated in "stepwise oxygen". Water evolution is shown by the blue curve (m/z=18) and methane evolution by the green curve (m/z=15).

For the sample passivated in 1% O_2, weight loss begins at 137 °C. The MS data show the loss of water starting at 157 °C with a second much smaller peak of water evolution as the sample reaches 700 °C. The only other product detected in the MS data taken during the TPR experiments was methane (m/z= 16, 15). The sample passivated in 1% oxygen had a relatively large peak of methane formation with a maximum at about 540 °C. The sample passivated initially in 0.1% oxygen shows water evolution

beginning at about 200 °C and a relatively small evolution of methane with a maximum at about 625 °C.

The TPR results for the W_2C sample are presented in Figure 2.9.

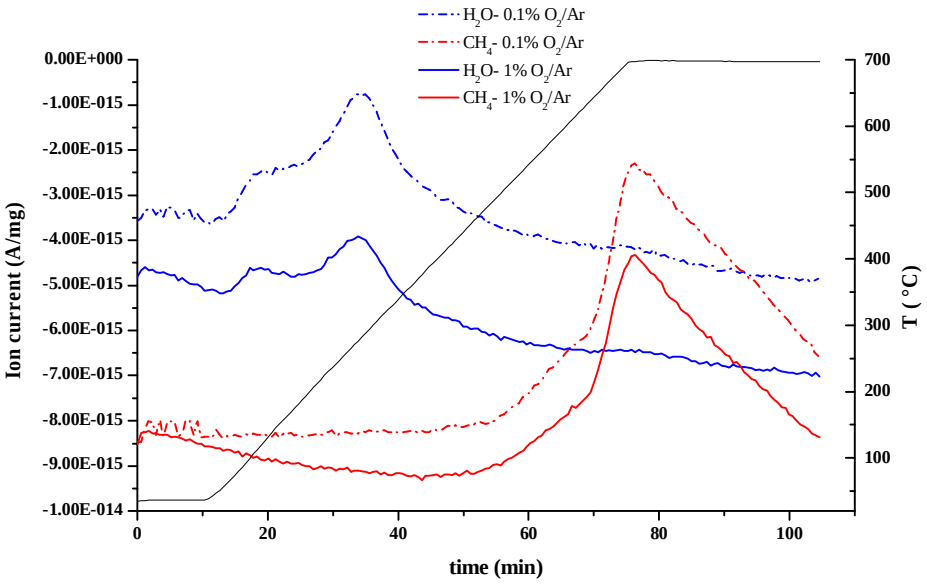

Figure 2.9: Reduction of passivated W_2C in 80% H_2/Ar. Solid line, W_2C passivated in 1% O_2 and dashed line, W_2C passivated in stepwise oxygen. Water, blue curve (m/z=18) and methane, green curve (m/z=15).

The total weight loss per gram sample is 6% for the W_2C sample and begins at 88 °C for both methods of passivation. Similar to the Mo_2C sample, the W_2C sample showed only water and methane evolution during TPR. The W_2C sample had two peaks of water evolution with maxima at 125 and 277 °C, and methane evolution started at 510 °C and increased sharply at 690 °C for both samples.

The TPR data were used to select the regeneration temperatures for both catalysts. The criteria were that the temperature should be high enough to remove the oxygen that was added during passivation, but low enough not to remove carbon (as

methane) from the surface. For the Mo_2C and W_2C samples, this temperature was 300 and 400 °C, respectively.

An additional TPR experiment was carried out with the Mo_2C sample using a combination of hydrogen and ethane (the carburization mixture), and the results are presented in Figure 2.10.

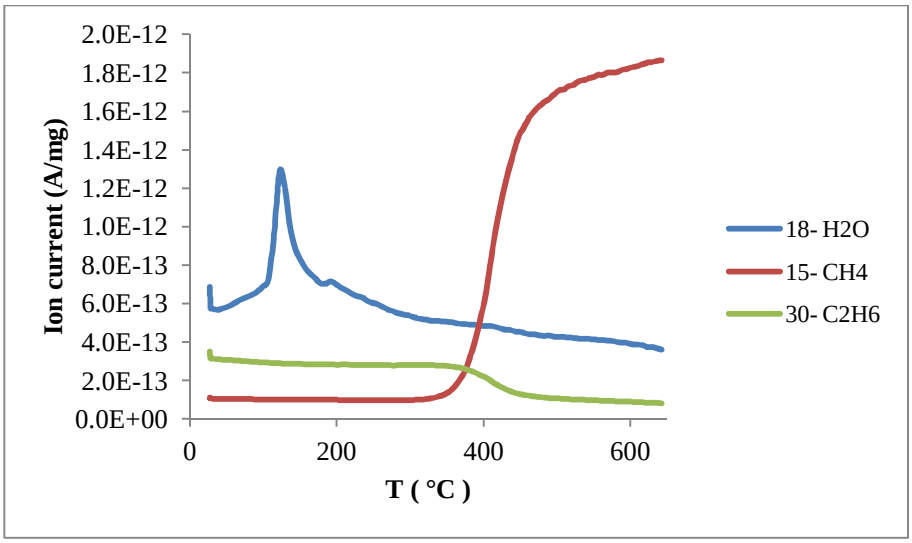

Figure 2.10: Reduction of passivated Mo_2C (1% O_2) with carburization mixture 10%C_2H_6/H_2.

Figure 2.10 shows the reduction of Mo_2C in the carburization mixture (10% C_2H_6 in hydrogen) with a temperature ramp of 5 K/min to the final carburization temperature of 650 °C. Water starts to form at 100 °C with a maximum at 122 °C. Hydrogenolysis of ethane to methane begins at 350 °C.

In order to determine if the passivation was successful, TPR was carried out on a Mo_2C sample which had been passivated in 1%O_2, and stored at room temperature in a closed vial for 11 months. Before performing the TPR experiment, TPD was done at 110 °C on the sample to remove the physisorbed water. The results showed that this sample lost 9.69% weight compared to the 4.41% weight loss during TPR of the freshly

passivated Mo_2C. Also, the weight loss associated with the removal of oxygen, indicated by formation of water in the MS data as reported in Figure 2.11, happens at higher temperature. This data reveals that reduction of the aged sample is more difficult than reduction of the freshly passivated sample, probably because of the presence of more oxygen in particular in the subsurface/bulk of Mo_2C.

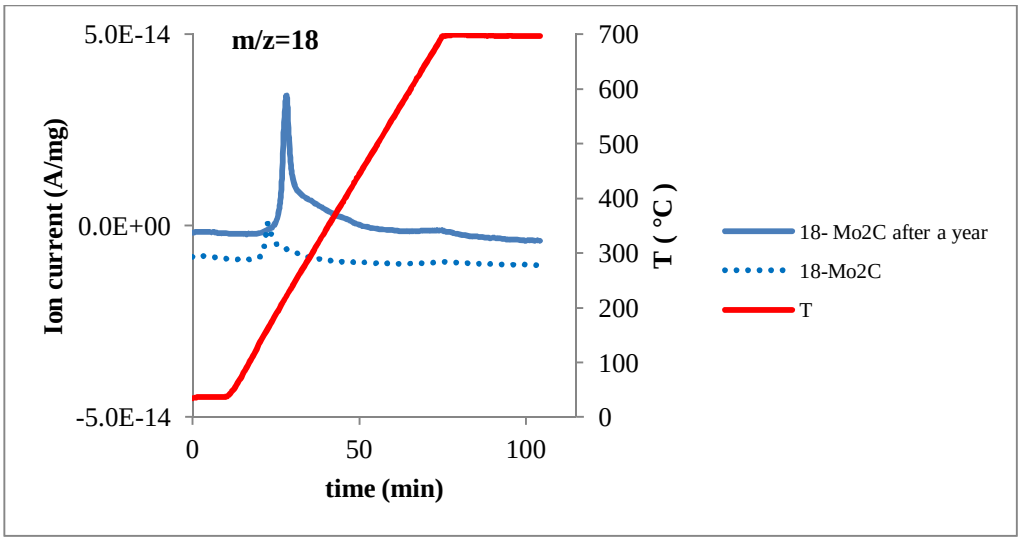

Figure 2.11: TPR of Mo_2C passivated in 1% O_2. TPR was performed right after passivation (dashed line) or after 11 months (solid line). The gas phase atmosphere was 80% H_2/Ar.

2.3.4 Catalytic activity

Hydrogenation of toluene (20 bar, H_2: toluene = 33) was used to test the catalytic activity of the carbide samples. In order to determine the effect of passivation and reduction on the catalytic activity, the activity of "fresh" samples that were not passivated or contacted with air was compared to that of passivated and reduced samples. The hydrogenation activity for the fresh (non-passivated) Mo_2C is compared with that of the 0.1% and 1% oxygen passivated Mo_2C in Figure 2.12.

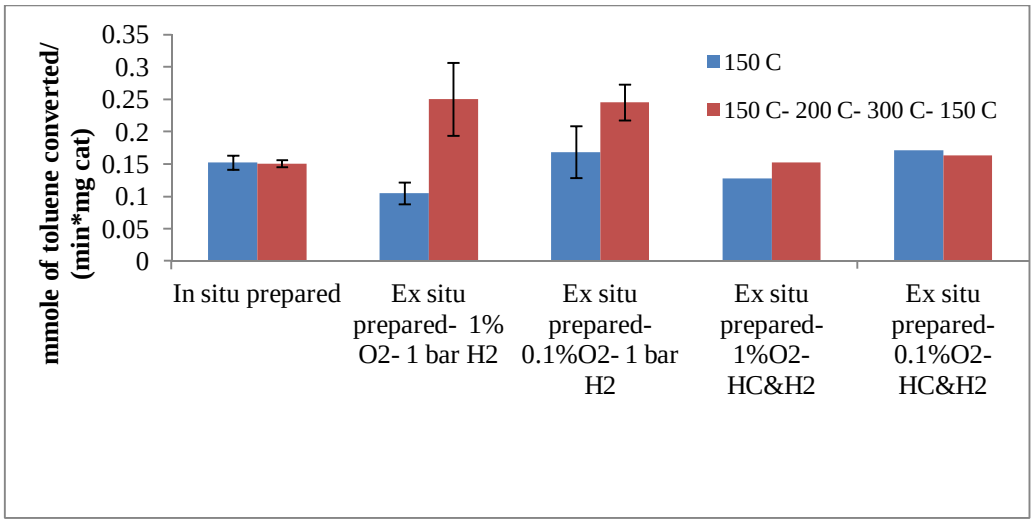

Figure 2.12: Hydrogenation of toluene on Mo_2C at 150 °C and 20 bar H_2 pressure. Blue bars: initial activity at 150 °C, red bars: rate at 150 °C after heating to 200 and 300 °C and cooling down to 150 °C.

The only product detected at 150 °C is methylcyclohexane, and the data show that the fresh sample and the 0.1% O_2 sample had the same rate of conversion, but the initial conversion at 150 °C was about 30% lower for the 1% O_2 passivated sample. The 1% O_2 passivated sample that was reduced in the synthesis gas (to 650 °C with 5 K/min, 10% ethane in hydrogen at 1 bar) showed somewhat better activity, but still lower than the fresh sample. After collecting data at 150 °C, the catalysts were tested at 200 and 300 °C and then cooled to 150 °C to determine if there was any deactivation during measurement at higher temperatures. The catalysts that were passivated and then activated in H_2 at 1 bar and 300 °C were significantly more active than the same materials directly after reduction. The Mo_2C catalysts that were reduced at 650 °C in ethane and hydrogen did not show any increase in activity after measurements at higher temperature.

Figure 2.13 shows the hydrogenation reaction results for W_2C at 200 °C. The data in blue is the initial activity at 200 °C and the data in red are for the activity at 200 °C after measurements at higher temperature (1.5 h sequentially, 200, 300 and 400 °C).

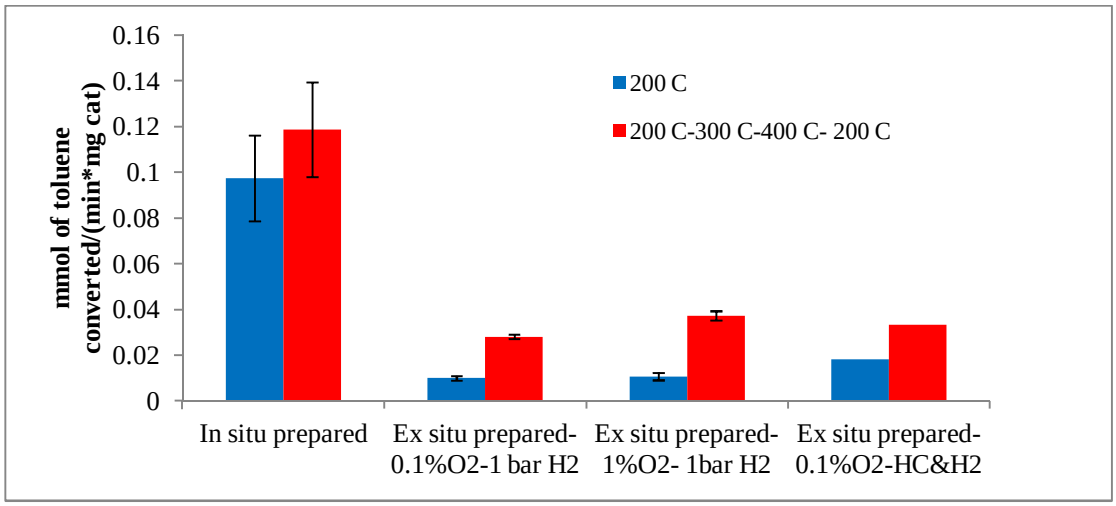

Figure 2.13: Hydrogenation of toluene on W_2C at 200 °C and 20 bar H_2 pressure. Blue bars: initial activity at 200 °C, red bars: rate at 200 °C after heating to 300 and 400 °C and cooling down to 200 °C.

Unlike the Mo_2C sample, the W_2C sample had a lower conversion rate after passivation in either 1% or 0.1% oxygen followed by regeneration in hydrogen at 400 °C. The sample that was regenerated at 700 °C in the synthesis gases showed only slightly better activity, and a similarly small increase in activity was observed after measurements at higher temperature, but still far less activity than the fresh sample.

TPR at 20 bar H_2 pressure was done on fresh and passivated Mo_2C and W_2C, and the formation of methane is reported in Figure 2.14. Results reveal that methane forms at 300 and 400 °C under 20 bar pressure for Mo_2C and W_2C, respectively.

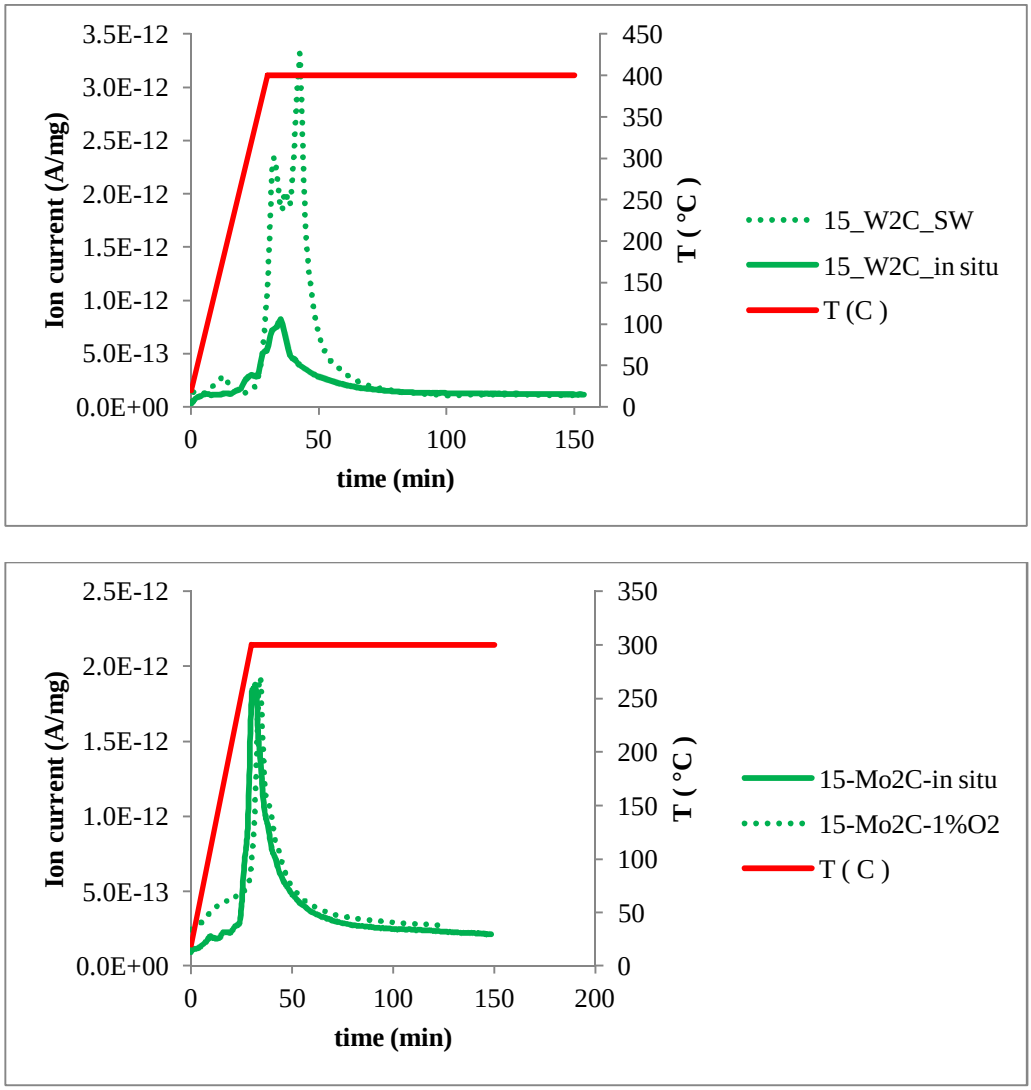

Figure 2.14: TPR at 20 bar H_2 pressure on fresh and passivated W_2C (top) and Mo_2C (bottom). The gas phase atmosphere was 150 ml/min of H_2, and the temperature ramp was 10 K/min.

The rates of reaction for hydrogenation of toluene were measured on Mo_2C and W_2C reduced at 1 and 20 bar of H_2, and were compared with those of the in situ prepared samples. Results are reported in Figures 2.15 and 2.16.

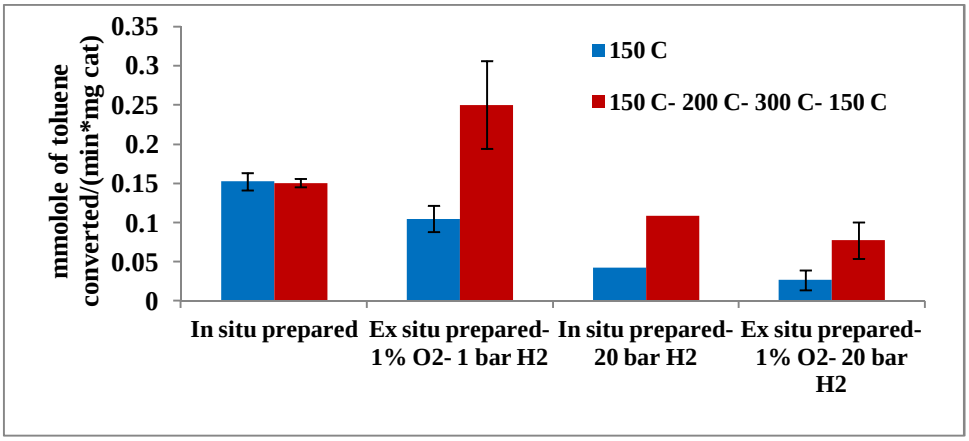

Figure 2.15: Hydrogenation of toluene at 150 °C and 20 bar H_2. Samples are Mo_2C in situ prepared and passivated with 1% O_2. Reduced in 1 and 20 bar H_2. Blue bar, activity at 150 °C and red bars, activity at 150 °C after heating up to 200 and 300 °C and cooling down to 150 °C.

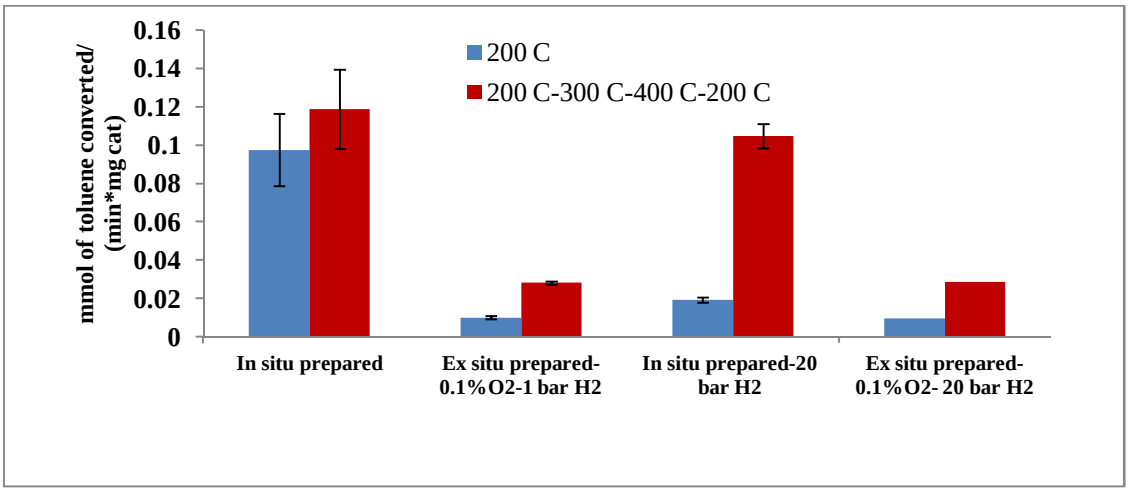

Figure 2.16: Hydrogenation of toluene at 200 °C and 20 bar H_2. Samples are W_2C in situ prepared and ex situ prepared passivated with 0.1% O_2. Reduced in 1 and 20 bar H_2. Blue bars, activity at 200 °C and red bars, activity at 200 °C after heating up to 300 and 400 °C and cooling down to 200 °C.

2.4 Discussion

2.4.1 Synthesis and passivation of carbides

XRD data show that α-Mo_2C and α-W_2C have been produced, and this bulk structure remains after passivation, Figure 2.1. The weight loss during synthesis is

28.52% or 17.83% which is consistent with the MeC_x (x>0.5) stoichiometry for molybdenum and tungsten carbides respectively. The starting materials were assumed to be MeO_3. The amounts of weight loss are lower than expected for a stoichiometry of $MeC_{0.5}$. This could be either due to a metal oxide with MeO_{3-x} stoichiometry or some trapped oxygen in the lattice of the final carbide products. The surface areas of the carbides before passivation were 58 m^2/g and 35 m^2/g for Mo_2C and W_2C, respectively. After passivation, the surface areas decreased by 26% and 34% to 43 m^2/g and 23 m^2/g for Mo_2C and W_2C, respectively, as reported in Table 2.1. These decreases in surface areas were accompanied by a decrease in pore volume. Such a loss in surface area upon passivation is consistent with the literature [22].

Different passivation agents are compared in Figure 2.2, and results indicate that only oxygen is an effective passivation agent during the isothermal process. The isothermal passivation data in Figures 2.4 and 2.6 indicate that H_2O and CO_2 are not suitable for passivation at 110 and 100 °C, respectively. This is in conflict with the reports in the literature that carbon dioxide and water can passivate Mo_2C at room temperature, and that CO_2 or N_2 can passivate mixed nitrides or carbides at increased temperature [18, 24]. The isothermal data with CO_2 at 100 °C shows weight gain, indicating a strong adsorption of CO_2 on the surface of Mo_2C, and this is consistent with reports that Mo_2C shows activity to convert CO_2 to CO at 300 °C in the presence of H_2 over bulk [32] or supported Mo_2C [33]. In order to more fully understand the interaction between water and carbon dioxide and the carbide surfaces temperature-programmed (TP) reaction experiments were performed. These experiments as shown in Figures 2.5 and 2.7 indicate that the initiation of the reaction of water with the Mo_2C surface is at

553 °C, and the reaction results in the removal of carbon from the carbide surface as CO, making water unsuitable as a passivation agent at any temperature. The TP reaction experiments with carbon dioxide show that significant weight gain and reaction with the surface of the carbide begin at about 590 °C, and at this temperature CO is produced, and presumably the carbide surface is oxidized, Figure 2.7. Dissociation of CO_2 on supported Mo_2C has also been reported in the literature as requiring temperatures higher than 550 °C [34]. The 500 to 600 °C temperature range for the reaction of either water or CO_2 is also consistent with the literature on steam reforming of methane using metal carbides [35]. It has been reported that during reforming reactions, the structure (verified by XRD) of Mo_2C was stable up to 600 °C, but at higher temperatures, bulk oxidation to MoO_2 occurred. Adding H_2 or CO thus seems to hinder oxidation by H_2O or CO_2 by providing a less oxidative atmosphere. In fact, Darujati et al. have correlated the stability of the carbide and the gas phase composition for reforming reactions using their "carburizing ratio" $[(P_{H2} + P_{CO})/(P_{H2O} + P_{CO2})]$ [36]. In the reverse water gas shift reaction, the dissociation of CO_2 is facilitated by hydrogen. DFT calculations have reported strong adsorption of CO_2 on Mo_2C (200 kJ/mole), but no reaction unless hydrogen is available on the surface [37]. It seems that both water and carbon dioxide do not react with the Mo_2C surface at room temperature. In fact, they only seem to react at close to 600 °C, when bulk oxidation of the carbide can occur. Reports of the utility of water, carbon dioxide and nitrogen for carbide passivation are most likely associated with oxygen contamination. The carbides are excellent at removing even low ppm levels of oxygen from a gas stream. Also, theoretical calculations show Mo_2C is very reactive toward oxygen [38].

Mo_2C and W_2C can be passivated with oxygen at room temperature. In recent literature, passivation with 1% oxygen at room temperature is the most common passivation method. In this work the effects of passivation in oxygen at two different oxygen partial pressures, 0.1% and 1% oxygen, have been investigated to determine if 1% oxygen is sufficiently low to not damage (over oxidize) the carbide surface. Over oxidation means oxidation to a greater extent than is needed to form a surface that is not pyrophoric in air at room temperature. The weight gains and heat effects during passivation with oxygen at 1% oxygen and at, initially, 0.1% oxygen for Mo_2C and W_2C have been reported in Figure 2.3 and Table 2.2. The majority of weight gain and associated heat evolution happened during the first thirty minutes of the passivation with both oxygen concentrations. Using the lower oxygen partial pressure decreases the initial rate of weight gain by 7.3 times in the case of Mo_2C and 6.41 times for W_2C. The rate of oxygen addition of the samples is 1.7 and 12.2 mmoles/h per catalyst mass for 0.1% and 1% O_2 in the case of Mo_2C, which means that only about 0.03 and 0.02% of the oxygen is being consumed, respectively. Because no gas phase products were observed during passivation, the change in weight can be directly related to oxygen addition. The passivated carbides adsorbed 1.72 oxygen/surface metal atom for 1% oxygen passivation and 1.5 oxygen/surface metal atom for 0.1% oxygen passivation. Although the configurations of oxygen in these passivated samples are not known, DFT calculations on β-Mo_2C have shown that the different surface planes have different reactivities toward oxygen chemisorption, and that they can adsorb different amounts of oxygen. It was reported that initially, at low oxygen coverage, oxygen prefers to adsorb on the top of Mo atoms, and for increasing coverage, oxygen atoms start to adsorb on

hollow sites between Mo atoms that are not occupied by carbon atoms [39, 40]. The amount of oxygen added to the materials in this work is consistent with 1.7 and 2.2 monolayers of oxygen for Mo_2C and W_2C, respectively.

To check if the passivation is complete (no further weight gain from adding oxygen to the carbide); at the end of the passivation with 1% O_2, the concentration of oxygen was increased to 16% for 1 hour. The rate of weight gain is not significant for both cases but there is still a slight weight increase which indicates that complete passivation needs a long time. It has been reported that oxygen is very mobile in Mo_2C and it is possible that oxygen migrates to the subsurface and even to the bulk of Mo_2C [41]. The long term stability of a passivated Mo_2C sample was tested by storing it in the laboratory for 11 months and then reducing the sample in the TG apparatus after performing TPD at 110 °C to remove the physisorbed water from the surface. The weight loss during reduction was 9.7% indicating that the passivated samples are not stable in air over extended periods of time. TPR data are reported in Figure 2.11. Reduction happens at higher temperature in the case of the sample stored for 11 months, since the oxygen diffused into the bulk and requires a higher temperature to be removed.

2.4.2 Reduction of passivated carbides

Surface regeneration was also studied. In order for the carbides to be active as catalysts, the oxide layer on the surface of the carbides must be removed. Oxygen can be removed either by TPD or TPR. During TPD, the oxygen in the carbide will react with the carbon in the structure of the carbide and leave as CO or CO_2 [41-44]. During

TPR, hydrogen reacts with oxygen and leaves as water. Since removal of oxygen by TPD damaged the carbide and requires high temperature, this is not a desirable method.

In order to find the appropriate reduction temperature, the passivated samples (without coming in contact with air) were heated in a TG-MS apparatus to 700 °C in hydrogen, results are shown in Figures 2.8 and 2.9. With both Mo_2C and W_2C, water and methane formation were observed by online MS analysis of the gas stream. In the case of Mo_2C, formation of water happens at almost the same temperature (200 °C) for both 0.1 and 1.0 % oxygen passivation. Unlike for Mo_2C passivated initially with 0.1% oxygen, for Mo_2C passivated with 1% O_2 there is a second water peak at 700 °C, and there is a methane peak at 550 °C. The high temperature water peak indicates that some oxygen is bonded more strongly to the surface of the carbide or there is oxygen from the subsurface of the Mo_2C. It has been reported in the literature that during TPR of Mo_2C, the second peak that desorbs at 300 °C is from removal of oxygen from below the surface. The second peak forms when the surface is depleted in oxygen at higher temperatures and oxygen diffuses out to the surface [26]. The evolution of methane is from removal of surface carbon, and is formed after 1% O_2 passivation and not after 0.1% passivation. This suggests that the surface of Mo_2C can be recovered more completely after the milder passivation. Presumably, the milder passivation does not disrupt the Mo – C bonds, but only adds oxygen to surface Mo atoms. From the weight gain during passivation, and the surface area of the fresh carbide, the ratio between Mo and oxygen atoms on the surface can be estimated. This is 1.7 and 2.2 oxygen atoms per Mo and W atom, respectively.

In the case of reduction of passivated W_2C, no significant difference can be seen between the reduction of W_2C passivated in 0.1 or 1 % oxygen. In both cases, there are two water peaks. The first peak is from removal of oxygen from the surface or from more highly oxidized tungsten. The second peak could be due to the removal of oxygen from less highly oxidized tungsten, or from below the surface. W_2C passivated in 0.1 or 1% oxygen gains 2.48 or 2.78% weight due to the oxidation.

The temperatures for reduction of the surface of Mo_2C and W_2C, that is, oxygen is removed but not any carbon, are 300 and 400 °C, respectively. Some papers have suggested different reduction temperatures for Mo_2C (700 °C [36] or 450 °C [32]) or W_2C (300 °C [45]). The difference in the suggested reduction temperature could be due to different synthesis methods, which may cause deposition of carbon on the surface. If there is free carbon on the surface, much higher reduction temperatures must be applied up to 600 °C [11]. It is worth to mention that the final reduction temperature could affect the amount of oxygen and carbon on the surface of metal carbides, which can change the catalytic behavior of metal carbides.

The amount of methane formation during reduction of W_2C is greater than that formed during the reduction of Mo_2C which had been passivated using 1% oxygen. This observation is potentially important for use of the carbides to catalyze reactions such as direct desulfurization (DDS), which requires the creation of vacancies on the surface of the catalyst [46, 47]. Removal of the carbon from the lattice of a carbide indicates that the carbon atoms are reactive and can participate in the reaction and leave the surface during the catalytic cycle, similar to the Mars-van Krevelen mechanism [8, 48-50].

For Mo_2C passivated with 1% O_2, complete surface reduction in hydrogen without damaging the surface is not possible as indicated by water removal after methane removal in Figure 2.8. As a remedy, the surface reduction in a mixture of hydrogen and ethane in a ratio of 1:9 during a 5 K/min ramp to the carburization temperature of 650°C was tried. The MS data are shown in Figure 2.10. Water is formed at 100 °C by removal of oxygen from the passivated surface and methane is formed at 350 °C through hydrogenolysis of ethane.

2.4.3 Toluene hydrogenation on Mo_2C and W_2C

The hydrogenation of toluene was used as a test reaction for fresh and for passivated and reactivated Mo_2C and W_2C. For Mo_2C samples, Figure 2.12 shows that the fresh Mo_2C has the highest activity while Mo_2C passivated with 1% O_2 has the lowest activity after regeneration at 300 °C. The activity of Mo_2C passivated with 0.1% oxygen and reduced with hydrogen is higher than that of Mo_2C passivated with 1% O_2. It is clear from our data that passivation damages the carbide surface even when surface oxygen is removed with no detectable carbon removal as in the case of 0.1% passivation, as IR studies prove elsewhere [51]. Reactivation of the passivated samples in the carburization gas mixture to the carburization temperature does recover all of the initial activity for the 0.1% O_2 passivated sample, but still not all of the activity for the 1% O_2 passivated sample. Oxygen could block the metal sites or form a surface oxycarbide, which would change the electronic structure and perhaps the activity of the surface. Comparison of carbide and oxycarbide electronic structure calculations in the literature indicate that the oxycarbide would exhibit less hybridization of the *d* orbitals of the metal with *p* orbitals of carbon, which leads to a lower cohesive energy and a

more inert surface. The presence of oxygen would also cause a downward shift in the energy of the *p* electrons [52].

The results reported in Figure 2.12 show that it is possible to quantitatively remove oxygen from the 0.1%O_2 passivated sample, but not from the 1% passivated sample, and this more complete oxygen removal for the 0.1% passivated sample results in a catalyst with hydrogenation rates similar to those of the fresh Mo_2C. The lower activity after regeneration for the 1% passivated sample is presumably related to the remaining oxygen that is only removed at 700 °C, which may affect the carbide electronic structure.

For the W_2C catalysts, the fresh W_2C had significantly higher hydrogenation activity than either the 0.1 or the 1% O_2 passivated sample, which both had about the same activity after regeneration. The carburization gas mixture was also used for regeneration of W_2C but there was still a significant difference between the passivated-regenerated and fresh W_2C. This shows that it is very difficult to remove the chemisorbed oxygen from the surface of W_2C.

In another experiment, during the hydrogenation of toluene at 20 bar using Mo_2C the temperature was increased to 200 and then 300 °C, and then cooled back down to 150 °C to check if any deactivation had occurred. It was a surprising observation that, not only did the catalyst not deactivate, but the used Mo_2C had a higher activity than the fresh catalyst that had not been passivated, as reported in Figure 2.12. The same increase in activity was observed for the W_2C catalyst. In the case of W_2C the initial reaction temperature was 200 °C, and then the temperature was

increased to 300 and 400 °C, and then cooled to 200 °C. As the results show in Figure 2.13, after reaction at higher temperature, the catalysts are more active at 200 °C.

For Mo_2C, the fresh carbide does not gain activity after operation at higher temperature, while the passivated and reduced samples do gain activity. Both the samples passivated with 0.1% and with 1% O_2 have similar activity after being used for hydrogenation at 20 bar at 200 and 300 °C. When the passivated Mo_2C samples are regenerated in the mixture of ethane and hydrogen, they show the same behavior as the in situ synthesized Mo_2C, namely no increase in activity after use at higher temperature. There are two explanations for this behavior. Either the gain in activity is due to removal of excess carbon at the higher reaction temperatures, or the gain in activity is related to disruption of the catalyst surface during passivation. At the end of the Mo_2C synthesis the high methane production and constant weight demonstrate that carbon is readily hydrogenated and is not likely to block the active surface. Furthermore, there is no loss of carbon detected during passivation or regeneration for Mo_2C, and therefore it is likely that passivation alters the active surface in a way that allows increased activity after reaction at higher temperature. A similar behavior has been observed for W_2C, which gains in activity when used for hydrogenation at 400 °C for two hours and subsequently is cooled to 200 °C.

To explain that activity enhancement, different scenarios can be considered:

(1) The enhancement is due to better reduction of the surface under reaction conditions compared to reduction of the surface with hydrogen at atmospheric pressure. This scenario cannot be true, because then the activity must be the same as that of the in

situ prepared sample, however, the activity is higher than that of the in situ prepared samples.

(2) The enhancement is due to surface cleaning of the carbides. It is possible that some carbon is deposited on the surface of the catalyst during the synthesis and under reaction conditions some carbon is removed, and more sites are exposed. To check this hypothesis, reduction in hydrogen for in situ prepared and 1% O_2 passivated samples at the final temperature of reaction (300 °C for Mo_2C and 400 °C for W_2C) at 20 bar pressure was performed and the gas phase products were monitored with online MS. The results are reported in Figure 2.14. For all the samples formation of methane was observed, which indicated removal of carbon from the (sub) surface of the carbides. The carbon is removed from the (sub) surface and not the bulk, because no change in structure was seen from XRD data, and this makes sense because the temperature is not high enough to change the bulk. But, is this carbon from carbidic carbon or free carbon deposited on the surface? To answer this question, the reaction was run after reduction at 20 bar; the results are shown in Figures 2.14 and 2.15. As it is shown in all cases the initial activity is lower compared to the situation of carbon not being removed, and since the activity is lower, it can be concluded that this carbon was removed from the carbidic carbon and it is not the carbon deposited on the surface. Deactivation of Mo_2C due to the removal of carbidic carbon for hydrogenation of ethylene has been reported elsewhere [41], since adsorption of hydrocarbons on the metallic surface is stronger than the adsorption on the carbidic surface [38].

(3) Acid sites could participate in hydrogenation [53]. At 20 bar pressure and high temperature, by removing carbon from the surface of the carbides Lewis acid sites are

formed which might serve as adsorption site. Toluene can adsorb on those sites and be hydrogenated by hydrogen spill over. This cannot be the case, because these Lewis sites exist when reduction was performed at 20 bar, and upon cooling, the hydrogenation activity was lower than the time when reduction happened at atmospheric pressure with no Lewis sites.

(4) When temperature is increased to 300 and 400 °C under reaction conditions, some carbons are removed from the surface of Mo_2C and W_2C, respectively. It happens because under the reaction conditions, carbon in the gas phase and carbon in the surface of the carbides are not in equilibrium. The chemical potential of carbon in the carbide is higher than the chemical potential of carbon in the gas phase (at high temperature and under reaction conditions) which leads to the transfer of carbon from the metal carbide to the gas phase. Also light gases form via cracking of toluene and hydrogenated products. These light carbonaceous compounds could fill the vacancies when the reactor is cooled down and in fact recarburize the surface. By adsorbing these carbonaceous compounds, the concentration of carbidic carbon around the metal atoms increases which changes the electronic structures of the metal. Therefore, the gain in activity can be attributed to surface reconstruction. For the reduced in situ carburized W_2C, after cooling down to 200 °C, the full activity was recovered, which indicated that all the removed carbons were replaced.

It is reported that by increasing the amount of carbidic carbon, the hydrogenation activity of Mo_2C will increase because of the change in the number and quality of active sites [54]. It was also reported that the desorption of benzene from Mo_2C that has a higher amount of carbidic carbon can happen at lower temperatures

compared to Mo_2C with a lower amount of carbidic carbon [55]. The change in the heat of adsorption can change the activation energy of reaction. As a result, the higher the carbidic carbon content, the higher the hydrogenation activity. The reason that samples passivated with initially 1% O_2, gain more activity than those initially passivated with 0.1% O_2, must be changes that happen during passivation. Using 1% O_2 compared to 0.1% O_2 releases more initial heat (Figure 2.3), which changes the surface in a way that during cooling under reaction conditions, the surface can adsorb more carbon, and becomes more active for hydrogenation. Also, carburization of the oxynitride surface during reaction conditions was reported. Oxynitride can pick up carbon during hydrogenation of propylbenzene when the temperature was increased (50 bar, 680 K) which caused carburization of the surface and when it was cooled down to 543 K, hydrogenation was increased compared to the initial rate [56].

For the temperature-programmed reduction of Mo_2C and W_2C in 20 bar hydrogen, methane formation starts at about 250 °C. For Mo_2C, the amount of methane produced/ gram catalyst is roughly the same for both the passivated sample and for the in-situ carburized sample that has not been passivated (Figure 2.14). For W_2C the size of the methane peak is roughly 5 times larger for the passivated sample than for the sample prepared in situ. The high amounts of carbon removal for the passivated W_2C are due to the role of oxygen on the surface: when oxygen is attached to the tungsten atoms and forms an oxygen-metal bond, it attracts the electrons of the metal to itself, which causes weakening of the metal-carbon bond. That is why during the reduction with hydrogen at high pressure, more carbon will leave the surface than does for the in situ carburized W_2C that does not have any metal-oxygen bond.

The selectivity on Mo_2C at 200 and 250 °C is 100% methylcyclohexane (MCH) and at higher temperatures, more light gases were produced but MCH was still the main product. Also, the conversion at 250 °C is higher than at 300 °C, this trend can be attributed to a change in the surface of the carbide at temperatures higher than 250 °C and 20 bar pressure, in which the surface will be depleted of carbidic carbon. The hydrogenation activity of metallic surfaces is generally lower than that of carbidic surfaces [57].

For W_2C, at 200 and 300 °C the selectivity toward MCH is 100% for all samples. But at 400 °C in the case of in situ prepared W_2C the selectivity to methane is 100%; however, for the oxygen-passivated W_2C samples, light gases, MCH and benzene are the products. Benzene was produced with Mo_2C in very small amounts and was not detected in products from the in situ prepared W_2C during 2 hours time on stream at 400 °C. Formation of benzene in the case of in situ prepared W_2C, when it was reduced at 400 °C and 20 bar pressure, was observed. However, the selectivity goes to mainly methane after 30 minutes of reaction, probably due to filling of vacancies (which may function as Lewis acid sites) under reaction conditions. Formation of benzene can be the result of carbon vacancies (Lewis acid) on the surface of W_2C. In order to keep theses carbon vacancies, oxygen should be on the surface of tungsten carbide. The presence of oxygen shows the difference between product selectivity of metal carbides and metal oxycarbides. Formation of benzene at high temperature is one of the differences between product selectivity of toluene conversion on Mo_2C and W_2C. Benzene formation will be discussed more in the next chapter.

One final consideration with passivation is that the physical configuration of the sample will influence the heat transfer away from the sample, and thus the oxidation rate for any particular oxygen concentration, and the oxygen concentration at which the catalyst becomes over passivated and oxygen migrates into the bulk. In this research, very small amounts of sample (ca. 40 mg) that is in fair contact with an alumina crucible of somewhat greater mass has been used. A considerable increase in the sample mass or decrease in heat removal rate would require a lower oxygen concentration, or a periodic oxygen addition with added time for cooling.

2.5 Conclusions

Different agents and methods for the passivation and regeneration of Mo_2C and W_2C have been studied. Contrary to previous reports, the results of this research found that water and carbon dioxide were not suitable for passivation of Mo_2C or W_2C. Water was found to react with the carbide surface only at 520 °C, and then it removed carbon from the surface at this temperature. Carbon dioxide also needed a high temperature of 586 °C to dissociate on the surface of carbides. At lower temperatures, neither water nor carbon dioxide adsorbed strong enough to passivate the carbide surfaces.

When passivating Mo_2C with oxygen, a mild passivation with an initial oxygen concentration of 0.1% produced a more active catalyst after reduction when compared to the more commonly reported procedure of passivation with 1% O_2. Regeneration of the sample passivated in 0.1% oxygen by reduction in one atmosphere of hydrogen at 300 °C for 2 hours was sufficient to regain the activity of an unpassivated sample. For the 1% oxygen passivated sample, the original hydrogenation activity could be recovered by treatment in the carburization gas mixture at 650 °C, the initial synthesis

temperature. Interestingly, the sample activity of the passivated sample was enhanced over that of the non passivated sample during the hydrogenation reaction at 300 °C and 20 atmospheres.

The situation for W_2C is different; regeneration of oxygen-passivated W_2C is much less effective than that of Mo_2C. Catalytic activities of regenerated material that had been passivated with either 0.1% or 1% O_2 are almost the same, and much lower than that of the in situ prepared W_2C. Even regeneration in a mixture of ethane/hydrogen at the original synthesis temperature does not cause regeneration of active sites. During reaction conditions at temperatures higher than 250 °C and 20 bar pressure the catalytic activities of carbides can change, presumably due to surface reconstruction.

Passivation in oxygen is not sufficient to protect the Mo_2C samples from further oxidation. Over 11 months at room temperature, a passivated sample will continue to react with atmospheric oxygen and will contain 2.8 times as much oxygen as the fresh sample gains during passivation. In other words, even a passivated Mo_2C sample will have a shelf life and would require further investigation for safety during bulk storage.

References

[1] R. B. Levy, M. Boudart, Platinum-Like Behavior of Tungsten Carbide in Surface Catalysis, Science, 181 (1973) 547-549.

[2] J. R. Kitchin, J. K. Nørskov, M. A. Barteau, J. G. Chen, Trends in the chemical properties of early transition metal carbide surfaces: A density functional study, Catalysis Today, 105 (2005) 66-73.

[3] J. G. Chen, Carbide and Nitride Overlayers on Early Transition Metal Surfaces: Preparation, Characterization, and Reactivities, Chemical Reviews, 96 (1996) 1477-1498.

[4] S. T. Oyama, Preparation and catalytic properties of transition metal carbides and nitrides, Catalysis Today, 15 (1992) 179-200.

[5] P. Da Costa, J. L. Lemberton, C. Potvin, J. M. Manoli, G. Perot, M. Breysse, G. Djega-Mariadassou, Tetralin hydrogenation catalyzed by Mo_2C/Al_2O_3 and WC/Al_2O_3 in the presence of H_2S, Catalysis Today, 65 (2001) 195-200.

[6] S. Ramanathan, S. T. Oyama, New Catalysts for Hydroprocessing: Transition Metal Carbides and Nitrides, The Journal of Physical Chemistry, 99 (1995) 16365-16372.

[7] S. Ma, X. Guo, L. Zhao, S. Scott, X. Bao, Recent progress in methane dehydroaromatization: From laboratory curiosities to promising technology, Journal of Energy Chemistry, 22 (2013) 1-20.

[8] T. Xiao, A. Hanif, A. P. E. York, J. Sloan, M. L. H. Green, Study on preparation of high surface area tungsten carbides and phase transition during the carburisation, Physical Chemistry Chemical Physics, 4 (2002) 3522-3529.

[9] W. Zheng, T. P. Cotter, P. Kaghazchi, T. Jacob, B. Frank, K. Schlichte, W. Zhang, D.S. Su, F. Schüth, R. Schlögl, Experimental and Theoretical Investigation of Molybdenum Carbide and Nitride as Catalysts for Ammonia Decomposition, Journal of the American Chemical Society, 135 (2013) 3458-3464.

[10] J. A. Schaidle, A. C. Lausche, L. T. Thompson, Effects of sulfur on Mo_2C and Pt/Mo_2C catalysts: Water gas shift reaction, Journal of Catalysis, 272 (2010) 235-245.

[11] J. S. Lee, S. T. Oyama, M. Boudart, Molybdenum carbide catalysts: I. Synthesis of unsupported powders, Journal of Catalysis, 106 (1987) 125-133.

[12] A. Hanif, T. Xiao, A. P. E. York, J. Sloan, M. L. H. Green, Study on the Structure and Formation Mechanism of Molybdenum Carbides, Chemistry of Materials, 14 (2002) 1009-1015.

[13] M. K. Neylon, S. Choi, H. Kwon, K. E. Curry, L. T. Thompson, Catalytic properties of early transition metal nitrides and carbides: n-butane hydrogenolysis, dehydrogenation and isomerization, Applied Catalysis A: General, 183 (1999) 253-263.

[14] X. Q. Zhao, Y. Liang, Z. Q. Hu, B. X. Liu, Oxidation characteristics and magnetic properties of iron carbide and iron ultrafine particles, Journal of Applied Physics, 80 (1996) 5857-5860.

[15] E. M. Zahidi, H. Oudghiri-Hassani, P. H. McBreen, Formation of thermally stable alkylidene layers on a catalytically active surface, Nature, 409 (2001) 1023-1026.

[16] H. Oudghiri-Hassani, E. Zahidi, M. Siaj, J. Wang, P. H. McBreen, Passivation of metal carbide surfaces: relevance to carbon nanotube–metal interconnections, Applied Surface Science, 212–213 (2003) 4-9.

[17] A. Warren, A. Nylund, I. Olefjord, Oxidation of Tungsten and Tungsten Carbide in Dry and Humid Atmospheres, International Journal of Refractory Metals and Hard Materials, 14 (1996) 345-353.

[18] W. Wu, Z. Wu, C. Liang, P. Ying, Z. Feng, C. Li, An IR study on the surface passivation of Mo_2C/Al_2O_3 catalyst with O_2, H_2O and CO_2, Physical Chemistry Chemical Physics, 6 (2004) 5603-5608.

[19] J. S. Lee, M. Boudart, Hydrodesulfurization of thiophene over unsupported molybdenum carbide, Applied Catalysis, 19 (1985) 207-210.

[20] J. M. Giraudon, L. Leclercq, G. Leclercq, A. Lofberg, A. Frennet, Organometallic route to dimolybdenum carbide via a low-temperature pyrolysis of a dimolybdenum alkyne complex, Journal of Material Science, 28 (1993) 2449-2454.

[21] T. Xiao, H. Wang, A. P. E. York, V.C. Williams, M. L. H. Green, Preparation of Nickel–Tungsten Bimetallic Carbide Catalysts, Journal of Catalysis, 209 (2002) 318-330.

[22] A. S. Rocha, A. B. Rocha, V. T. da Silva, Benzene adsorption on Mo_2C: A theoretical and experimental study, Applied Catalysis A: General, 379 (2010) 54-60.

[23] H. Shou, D. Ferrari, D. G. Barton, C. W. Jones, R. J. Davis, Influence of Passivation on the Reactivity of Unpromoted and Rb-Promoted Mo_2C Nanoparticles for CO Hydrogenation, ACS Catalysis, 2 (2012) 1408-1416.

[24] Y. Bogatin, M. Robinson, J. Ormerod, Water milling and gas passivation method for production of corrosion resistant Nd-Fe-B-N/C powder and magnets, Journal of Applied Physics, 70 (1991) 6594-6596.

[25] G. Leclercq, M. Kamal, J. F. Lamonier, L. Feigenbaum, P. Malfoy, L. Leclercq, Treatment of bulk group VI transition metal carbides with hydrogen and oxygen, Applied Catalysis A: General, 121 (1995) 169-190.

[26] K. J. Leary, J. N. Michaels, A. M. Stacy, The use of TPD and TPR to study subsurface mobility: Diffusion of oxygen in Mo_2C, Journal of Catalysis, 107 (1987) 393-406.

[27] A. L. Stottlemyer, T. G. Kelly, Q. Meng, J. G. Chen, Reactions of oxygen-containing molecules on transition metal carbides: Surface science insight into potential applications in catalysis and electrocatalysis, Surface Science Reports, 67 (2012) 201-232.

[28] E. Iglesia, F. H. Ribeiro, M. Boudart, J. E. Baumgartner, Synthesis, characterization, and catalytic properties of clean and oxygen-modified tungsten carbides, Catalysis Today, 15 (1992) 307-337.

[29] E. Iglesia, J. E. Baumgartner, F. H. Ribeiro, M. Boudart, Bifunctional reactions of alkanes on tungsten carbides modified by chemisorbed oxygen, Journal of Catalysis, 131 (1991) 523-544.

[30] M. J. Ledoux, C. P. Huu, J. Guille, H. Dunlop, Compared activities of platinum and high specific surface area Mo_2C and WC catalysts for reforming reactions: I. Catalyst activation and stabilization: Reaction of n-hexane, Journal of Catalysis, 134 (1992) 383-398.

[31] B. Frank, T. P. Cotter, M. E. Schuster, R. Schlögl, A. Trunschke, Carbon Dynamics on the Molybdenum Carbide Surface during Catalytic Propane Dehydrogenation, Chemistry – A European Journal, 19 (2013) 16938-16945.

[32] M. D. Porosoff, X. Yang, J. A. Boscoboinik, J. G. Chen, Molybdenum Carbide as Alternative Catalysts to Precious Metals for Highly Selective Reduction of CO_2 to CO, Angewandte Chemie, 126 (2014) 6823-6827.

[33] M. Nagai, K. Oshikawa, T. Kurakami, T. Miyao, S. Omi, Surface Properties of Carbided Molybdena-Alumina and Its Activity for CO_2 Hydrogenation, Journal of Catalysis, 180 (1998) 14-23.

[34] F. Solymosi, A. Oszkó, T. Bánsági, P. Tolmacsov, Adsorption and Reaction of CO_2 on Mo_2C Catalyst, The Journal of Physical Chemistry B, 106 (2002) 9613-9618.

[35] J. B. Claridge, A. P. E. York, A. J. Brungs, C. Marquez-Alvarez, J. Sloan, S. C. Tsang, M. L. H. Green, New Catalysts for the Conversion of Methane to Synthesis Gas: Molybdenum and Tungsten Carbide, Journal of Catalysis, 180 (1998) 85-100.

[36] A. R. S. Darujati, D. C. LaMont, W. J. Thomson, Oxidation stability of Mo_2C catalysts under fuel reforming conditions, Applied Catalysis A: General, 253 (2003) 397-407.

[37] H. Tominaga, M. Nagai, Density functional study of carbon dioxide hydrogenation on molybdenum carbide and metal, Applied Catalysis A: General, 282 (2005) 5-13.

[38] A. J. Medford, A. Vojvodic, F. Studt, F. Abild-Pedersen, J. K. Nørskov, Elementary steps of syngas reactions on $Mo_2C(001)$: Adsorption thermochemistry and bond dissociation, Journal of Catalysis, 290 (2012) 108-117.

[39] X. R. Shi, S. G. Wang, J. Hu, Z. Qin, J. Wang, Theoretical studies on chemisorption of oxygen on β-Mo_2C catalyst and its surface oxidation, Surface Science, 606 (2012) 1187-1194.

[40] L. Ó. János Kiss, A.P. Farkas, F. Solymosi, Surface and Subsurface Oxidation of Mo_2C/Mo(100):Low-Energy Ion-Scattering, Auger Electron, Angle-Resolved X-Ray Photoelectron, and Mass Spectroscopy Studies, The Journal of Physical Chemistry B, 109 (2005) 4638-4645.

[41] K. J. Leary, J. N. Michaels, A. M. Stacy, Carbon and oxygen atom mobility during activation of Mo_2C catalysts, Journal of Catalysis, 101 (1986) 301-313.

[42] N. Liu, S. A. Rykov, J. G. Chen, A comparative surface science study of carbide and oxycarbide: the effect of oxygen modification on the surface reactivity of C/W(111), Surface Science, 487 (2001) 107-117.

[43] T. P. St. Clair, S. T. Oyama, D. F. Cox, CO and O_2 adsorption on α-Mo_2C (0001), Surface Science, 468 (2000) 62-76.

[44] H. H. Hwu, M. B. Zellner, J. G. Chen, The chemical and electronic properties of oxygen-modified C/Mo(110): a model system for molybdenum oxycarbides, Journal of Catalysis, 229 (2005) 30-44.

[45] B. Vidick, J. Lemaitre, B. Delmon, Control of the catalytic activity of tungsten carbides: II. Physicochemical characterizations of tungsten carbides, Journal of Catalysis, 99 (1986) 428-438.

[46] R. Prins, V. H. J. De Beer, G.A. Somorjai, Structure and Function of the Catalyst and the Promoter in Co-Mo Hydrodesulfurization Catalysts, Catalysis Reviews, 31 (1989) 1-41.

[47] M. Egorova, R. Prins, Hydrodesulfurization of dibenzothiophene and 4,6-dimethyldibenzothiophene over sulfided NiMo/γ-Al_2O_3, CoMo/γ-Al_2O_3, and Mo/γ-Al_2O_3 catalysts, Journal of Catalysis, 225 (2004) 417-427.

[48] T. Namiki, S. Yamashita, H. Tominaga, M. Nagai, Dissociation of CO and H_2O during water-gas shift reaction on carburized Mo/Al_2O_3 catalyst, Applied Catalysis A: General, 398 (2011) 155-160.

[49] H. Matsumoto, C. O. Bennett, The transient method applied to the methanation and Fischer-Tropsch reactions over a fused iron catalyst, Journal of Catalysis, 53 (1978) 331-344.

[50] J. Gracia, F. Prinsloo, J. W. Niemantsverdriet, Mars-van Krevelen-like Mechanism of CO Hydrogenation on an Iron Carbide Surface, Catalysis Letters, 133 (2009) 257-261.

[51] W. Wu, Z. Wu, C. Liang, X. Chen, P. Ying, C. Li, In Situ FT-IR Spectroscopic Studies of CO Adsorption on Fresh Mo_2C/Al_2O_3 Catalyst, The Journal of Physical Chemistry B, 107 (2003) 7088-7094.

[52] H. W. Hugosson, L. Nordstrom, U. Jansson, B. Johansson, O. Eriksson, Theoretical studies of substitutional impurities in molybdenum carbide, Physical Review B, 60 (1999) 15123-15130.

[53] S. D. Lin, M.A. Vannice, Hydrogenation of Aromatic Hydrocarbons over Supported Pt Catalysts .III. Reaction Models for Metal Surfaces and Acidic Sites on Oxide Supports, Journal of Catalysis, 143 (1993) 563-572.

[54] J. S. Choi, G. Bugli, G. Djéga-Mariadassou, Influence of the Degree of Carburization on the Density of Sites and Hydrogenating Activity of Molybdenum Carbides, Journal of Catalysis, 193 (2000) 238-247.

[55] J. S. Choi, J. M. Krafft, A. Krzton, G. Djéga-Mariadassou, Study of Residual Oxygen Species over Molybdenum Carbide Prepared During In Situ DRIFTS Experiments, Catalysis Letters, 81 (2002) 175-180.

[56] G. Djéga-Mariadassou, M. Boudart, G. Bugli, C. Sayag, Modification of the surface composition of molybdenum oxynitride during hydrocarbon catalysis, Catalysis Letters, 31 (1995) 411-420.

[57] J. S. Lee, M. H. Yeom, K. Y. Park, I. S. Nam, J. S. Chung, Y. G. Kim, S. H. Moon, Preparation and benzene hydrogenation activity of supported molybdenum carbide catalysts, Journal of Catalysis, 128 (1991) 126-136.

3. Synthesis, Characterization and Catalytic Activity of Single Phase Mixed Metal Carbides of Molybdenum and Tungsten

3.1 Introduction

Alloying of early transition metals with carbon changes their catalytic behaviors such that it becomes similar in nature to that of the noble metals [1]. These materials gain attention as less costly replacement for noble metals. Preparation of monometallic carbides such as molybdenum and tungsten carbides with high surface areas makes these materials promising compounds to be used as catalysts.

The common precursors for synthesis of metal carbides are the oxide forms of the metals. Oxygen is removed and replaced with carbon in the carburization mixture (hydrocarbon/hydrogen) in a temperature-programmed reaction. The changes in physical and chemical properties of metal carbides compared to their parent metals are due to the hybridization of the *p* orbitals of carbon (nonmetal) with the *d* orbitals of the metals, which causes modification of the *d* band structure of the metal [2].

While there are many papers published about the synthesis and catalytic activities of mono metallic carbides, not many exist about bimetallic carbides, which in fact are ternary alloys of two metals with carbon. This could be due to the difficulties in making single-phase solid solutions with clean surface of this class of materials. Preparation of metal carbides with clean surface is more difficult compared to the preparation of metal nitrides with a clean surface, because of the possibility of carbon deposition on the surface of the metal carbides.

Different methods have been reported for the synthesis of precursors of (mixed) metal carbides or nitrides such as physical mixing and fusing of appropriate metal

oxides [3-7], decomposition of mixtures containing metals and different carbon sources (e.g., hexamethylenetetramine [8, 9], sugar [10] and urea [11, 12]), coprecipitation [13-16] and freeze drying methods [17-19].

In the physical mixing method, the two salts or oxides containing the appropriate metals are mixed together or dissolved in a solvent to have better dispersion and then the solvent is evaporated. The final solids are pressed and heated to a high temperature to enable solid-solid diffusion. In this method, the final product will have the same stoichiometry as the loaded metals, however the final solid is not homogenous because solid-solid diffusion is difficult and needs high temperatures. Using high temperatures will reduce the surface area of the precursors, and also some oxides such as MoO_3 sublime at temperatures higher than 650 °C.

In the decomposition method, the salts containing the metals are dissolved with the carbon source in a solvent; after removal of the solvent the solid is decomposed in inert or hydrogen atmosphere. Here, the carbon source will serve both as reducing and carburizing agent. In this method, the final product will have the same metals ratio as initially loaded. However, a homogenous mixture with a clean surface (without free carbon on the surface) is difficult to prepare. Since the carbon source should be used in excess, surface contamination with carbon possible.

In the coprecipitation method, two salts containing the metals are dissolved in water and by changing the pH, both metals precipitate at the same time. In this method, the final product will be homogenous; however, it does not necessarily have the same metals ratio as loaded in the solution. Another problem is that one salt may need base to

precipitate while the other one may need acid to precipitate, and as a result, the co-precipitation method is not a versatile method.

In the freeze drying (FD) method, two salts containing the metals are dissolved in water and droplets of solution are flash-frozen in liquid nitrogen. In this method, the final product will have the same metals ratio as loaded and is homogenous. These qualities make FD method a promising method for synthesis of precursors. After the synthesis, the precursor will be carburized to make the carbide.

Mixed metal carbides have different catalytic activities than the corresponding monometallic carbides, which can be due to geometric or electronic effects. Different mixed metal carbides have been used for various reactions, mainly for hydrotreating [7, 20], but also for other reactions such as dehydrogenation and hydrogenolysis [21].

The goal of this part of research is to prepare a series of single phase solid solutions of molybdenum and tungsten carbide. These two metal carbides are chosen because they both are catalytically active and their oxycarbides have different redox properties. For the first time to the best of our knowledge, the freeze drying method will be used for synthesis of precursors of mixed metal carbides. The freeze drying method is chosen for synthesis of the precursors because having solid solutions with exact ratios of metals is important, to investigate the effect of composition on catalytic activity. The metal composition will be varied and its effect on stability and catalytic properties of mixed Mo-W carbide will be investigated.

3.2 Experimental section

3.2.1 Catalyst and materials

Ammonium paratungstate (Alfa Aesar) and ammonium heptamolybdate (ACS reagent, 81-83% MoO_3, Sigma Aldrich) were dissolved separately in water in different molar ratios of Mo/ (Mo+W) = 0, 0.25, 0.5, 0.75 and 1, and then mixed together and stirred for 15 minutes. The total metal concentration was 0.1 M. The amounts of the different salts were adjusted to have 1 g of final product. The solution was added dropwise to the liquid nitrogen, and the obtained solid was freeze dried at a pressure of 110 µtorr in an ATR FD3.0 freeze drier.

Some freeze dried samples (pure molybdenum, pure tungsten and a mixed metal sample with Mo/ (Mo+W) = 0.5) were calcined in 80% air (zero grade, Airgas) in argon (UHP, Airgas) with a total flow rate of 50 ml/min. The temperature was increased from 40 to 600 °C with a temperature ramp of 5 K/min, and was kept at 600 °C for 30 minutes.

All carburizations were done in and monitored by a thermogravimetry analyzer (TG) connected to an online MS (Netzsch STA 449 F1 and QMS 403 C). Carburization gases were 20 ml/min of methane (UHP, Airgas), 70 ml/min H_2 and 10 ml/min argon (both ultra high purity from Airgas); all flow rates at STP. The synthesis of carbides was carried out at atmospheric pressure by heating from 40 to 450 °C at 5 K/min and from 450 to 650 °C at 2 K/min and holding at the final temperature until carburization finished. All carbides were cooled down to room temperature under flow of Ar. Mass/charge ratios 2-78 were scanned with online MS. Before exposure of the carbides to the ambient, they were passivated isothermally at 40 °C with air (zero grade, Airgas)

diluted in Ar (UHP, Airgas). The concentration of O_2 was increased from 0.1% (4 hours) to 1% (6 hours) and 16% (4 hours) in Ar, with the total flow rates between 60 and 402 ml/min.

Air and hydrogen were purified by flowing through a moisture trap (Agilent, MT400-2) and argon was purified by flowing through a dual trap of moisture and oxygen (Z-Pure Dual Purifier). In this chapter, MoW-i and MoWC-i (i=0, 0.25, 0.5, 0.75 and 1) means mixed metal precursors that were prepared by freeze drying and mixed metal carbides with the ratio of Mo/ (Mo+W) =i.

3.2.2 Temperature-programmed reduction (TPR)

The TPR experiments were carried out in the TG-MS on about 11 mg of passivated samples. The total flow rate was 100 ml/min with 80% hydrogen in argon. The temperature was held at 40 °C for 10 minutes and then increased from 40 to 700 °C with a temperature ramp of 10 K/min. The gas phase products were monitored by online MS.

3.2.3 Reaction

The reactor was a ¼ inch stainless steel flow reactor equipped with an Eldex liquid feed pump. The feed was 0.02 ml/min of liquid toluene (99.5%, Mallinckrodt Chemicals) and 150 ml /min STP H_2 (Ultra high purity, Airgas). The reactor total pressure was 20 bar, which was controlled by a back pressure valve. Samples were tested at different temperatures ranging from 193 to 275 °C and 400 °C. The reactor was loaded with different amounts of passivated carbides and the length of the bed was increased by mixing SiC (Aldrich, 200-450 mesh) with the carbides to avoid channeling and local heating. The temperature was controlled using a thermocouple inside the

reactor at the bottom of the catalyst bed. Products were analyzed every 30 minutes using an online HP 5890 GC with flame ionization detector (FID), equipped with a 30 m, 0.32 mm GASPRO column. The reaction was carried out in the gas phase, and transfer lines to the GC were heated to 110 ℃ to ensure that no condensation occurred before the GC. The GC temperature program was, 5 minutes isothermal at 60 ℃, then heating with 10 K/min to a final temperature of 240 ℃, which was held for 4 minutes.

Before running the reaction, all samples were reduced in 150 ml/min of H_2 at 350 ℃ and atmospheric pressure for 1 hour. Conversion of toluene was defined as the difference between moles of toluene in the feed and in the product divided by moles of toluene in the feed. Selectivity of compound *i* was calculated as the number of moles of compound *i* times its carbon number divided by the number of moles of products times their carbon numbers.

3.2.4 Characterization

The bulk structure of the samples was characterized by X-ray diffraction (XRD) using a Bruker D8 instrument equipped with Cu Kα radiation. The samples were measured in reflection geometry and Ni metal powder (Matheson Coleman & Bell, 200 mesh) was used for a reference. Diffractograms were collected with scanning steps of 0.05 in 2θ over the angular range of 20-90°. The cell parameters of each carbide were obtained by fitting the diffractograms using Powdercell software.

The carbon content of the samples was measured by combustion analysis in a CE-440 Elemental Analyzer. The ratios of Mo/W were determined by energy-dispersive X-ray spectroscopy (EDS) on a JEOL JSM-840A scanning electron microscope with

a Kevex X-ray analyzer and IXRF software and digital imaging capability. The operating voltage was 15 kV, and the energy range of the analysis was 0-9 keV.

BET surface areas were measured using a Micromeritics ASAP 2020 and N_2 at 77 K. Pore size distributions were determined from nitrogen desorption isotherms applying the BJH method. Before measuring the surface area the samples were degassed at 350 ℃ for four hours. The number of metal sites was measured by CO chemisorption; prior to CO chemisorption samples were reduced in H_2 at 350 ℃, then cooled down to 35 ℃ for CO chemisorption.

3.3 Results

The commercial MoO_3 and MoO_3 that was prepared from calcination of Mo-FD at 600 ℃ were carburized in a mixture of $10\%C_2H_6/H_2$ as reported in Figure 3.1. Results show that commercial MoO_3 and MoO_3 prepared from calcination of Mo-FD lost 71.45% weight compared to the theoretical value of 70.82%. MoO_3 prepared from FD precursor starts to lose weight at lower temperature and has the onset of weight loss at 498 ℃ while the commercial MoO_3 has 593 ℃ as the onset temperature for weight loss.

3.3.1 Synthesis of mixed metal carbides

Samples were prepared in the TG-MS. Both direct carburization of freeze-dried materials and carburization of calcined freeze-dried materials were tested. TG-MS was used to monitor the carburization and to find the right final carburization temperature.

3.3.1.1 Direct carburization of freeze-dried materials

The weight changes and water (m/z=18) and CO (m/z=28) formation during direct carburization of freeze-dried precursors are reported in Figures 3.2 and 3.3.

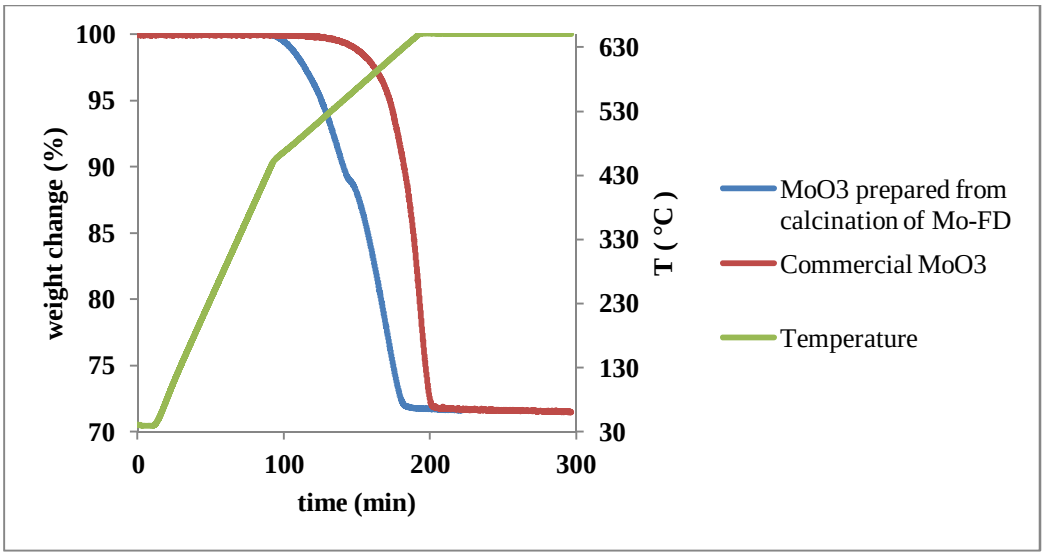

Figure 3.1: Carburization of commercial MoO_3 and MoO_3 prepared from calcination of Mo-FD at 600 °C. Gas phase atmosphere was 10% C_2H_6/H_2.

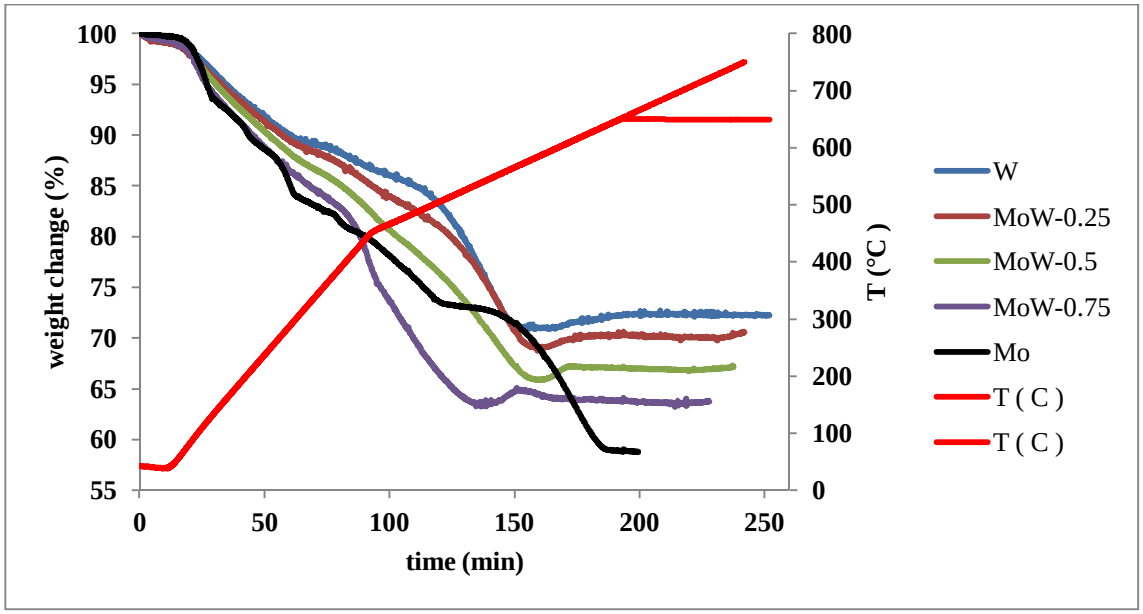

Figure 3.2: Weight change during direct carburization of freeze-dried Mo-W series in a gas mixture of 20% CH_4 in H_2. Freeze-dried samples from top to bottom: tungsten, MoW-0.25, MoW-0.5, MoW-0.75 and molybdenum. The isothermal process is for temperature-programmed carburization of a pure tungsten precursor.

The temperature was increased from 40 °C to the final temperature of carburization. Heating was stopped before carbon started to deposit on the surface. Carburization of the precursor containing only molybdenum resulted in the highest

weight loss, and carburization of the precursor containing only tungsten resulted in the lowest weight loss. The rest of the samples which are a combination of molybdenum and tungsten, have the final weight loss between the final weight loss of pure molybdenum and pure tungsten precursors.

The samples that contain tungsten first go through a continuous weight loss, and then they gain weight, which happens simultaneously with the formation of CO. The pure molybdenum sample has a continuous weight loss without any weight gain. The sample rich in molybdenum (MoW-0.75) reaches the minimum in weight before the other samples, at a temperature around 550 °C. For all mixed metal samples that contain tungsten, after reaching the minimum of weight loss and then gaining weight, the weight gain curve leveled off. However, in the case of the pure tungsten sample, a continuous weight gain was observed even after termination of CO production, which was due to the deposition of carbon on the surface. In order to avoid surface contamination, the final carburization temperature for the sample containing only tungsten did not exceed 650 °C.

MS data show that the carburization of all samples produces multiple water peaks which are an indication of reduction, and a final CO peak which forms with the last peak of water and is an indication of simultaneous reduction and carburization.

In the case of the pure molybdenum sample, the size of the CO peak is the largest compared to the rest of the samples. The samples reported in Figure 3.2 were used for XRD measurements, but for reaction or other characterization studies, all samples were prepared at a final temperature of 650 °C. The final weight losses at 650

°C were the same as the final weight losses at elevated temperatures, which were reported in Figure 3.2.

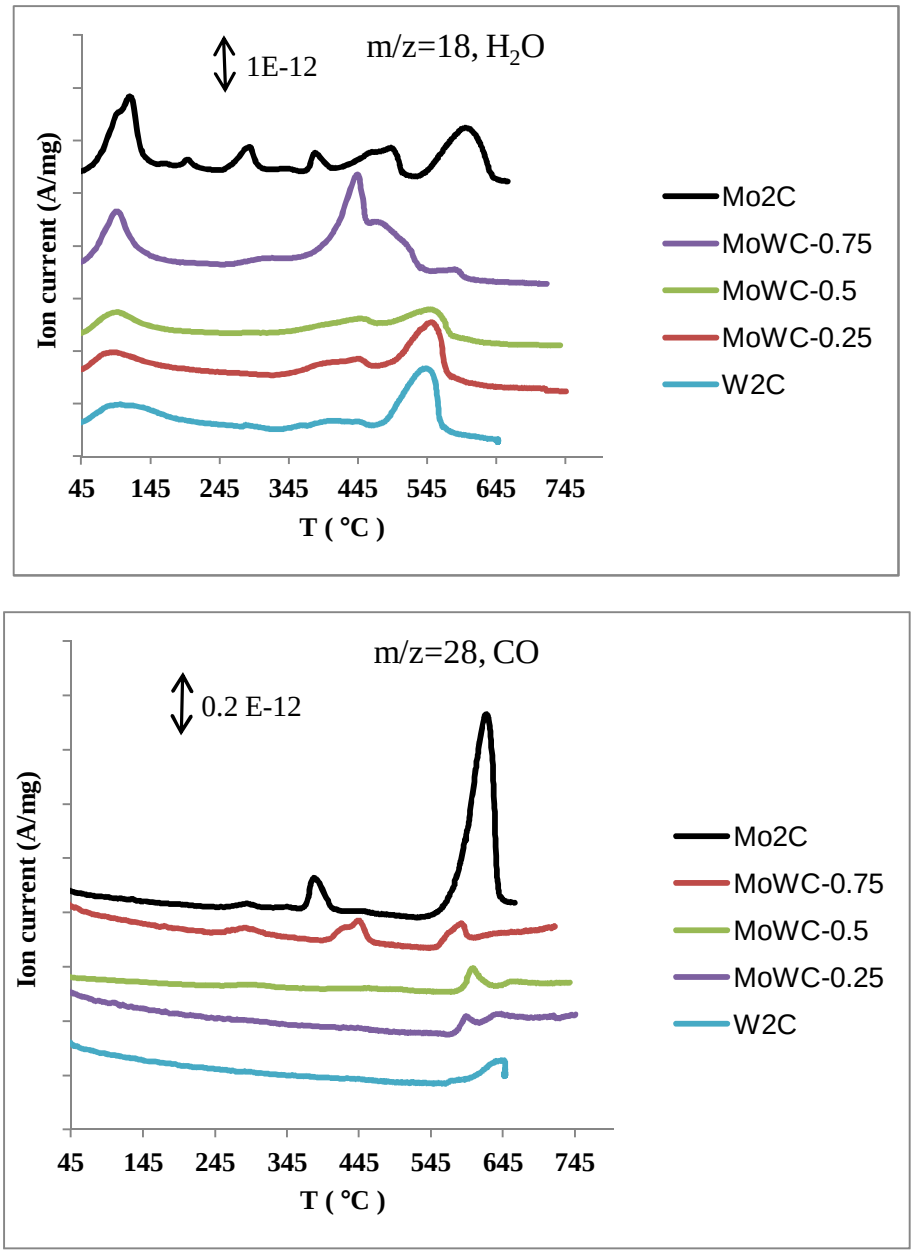

Figure 3.3: Water formation (top) and CO formation (bottom) during direct carburization of freeze-dried Mo-W samples in a gas mixture of 20% CH_4 in H_2.

.

3.3.1.2 Calcination and carburization of freeze-dried precursors

Freeze-dried precursors containing pure molybdenum, pure tungsten or a mixture of molybdenum and tungsten (MoW-0.5) were calcined in air to a final temperature of 600 °C.

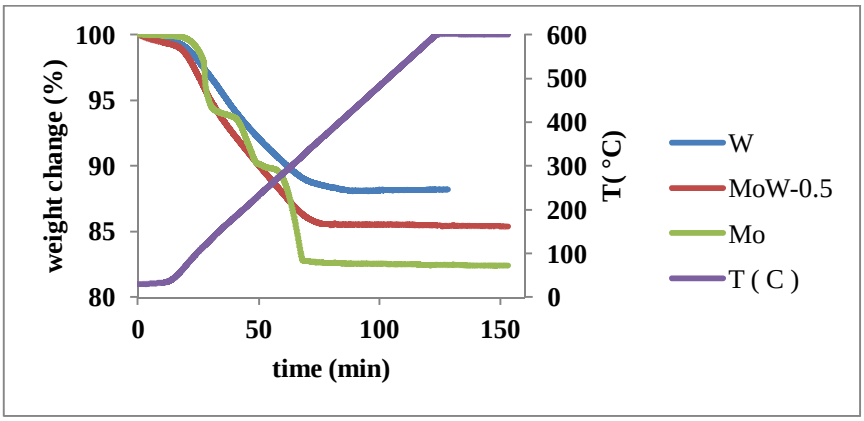

Figure 3.4: Weight change during calcination of freeze-dried materials in 80% air in Ar. From top to bottom: freeze-dried tungsten, MoW-0.5 and molybdenum.

During calcination, pure molybdenum has the highest weight loss and pure tungsten has the lowest weight loss, while the sample with the composition of MoW-0.5 exhibits a weight loss between those of pure molybdenum and pure tungsten samples as reported in Figure 3.4. Gas phase products, water (m/z=18) and NO (m/z=30), were monitored with the online MS and are reported in Figures 3.5 and 3.6, respectively. The MS data show that there are multiple water and NO peaks during calcination of the samples. The calcination of the precursor containing only tungsten needs a higher final temperature (420 °C) to reach the minimum weight, and calcination of the precursor containing only molybdenum needs the lowest final temperature compared to the other samples (350 °C). The MS data also show that the gas phase products during calcination of MoW-0.5 are similar to those observed with the pure tungsten samples; they both

have two water peaks and a broad NO peak. However, during calcination of MoW-0.5, the last water and NO peaks start to form at about 100 K lower temperature than in the case of the pure tungsten sample. Based on TG-MS data up to the final temperature of 450 °C, the weight loss curves level off and no more gas phase products form.

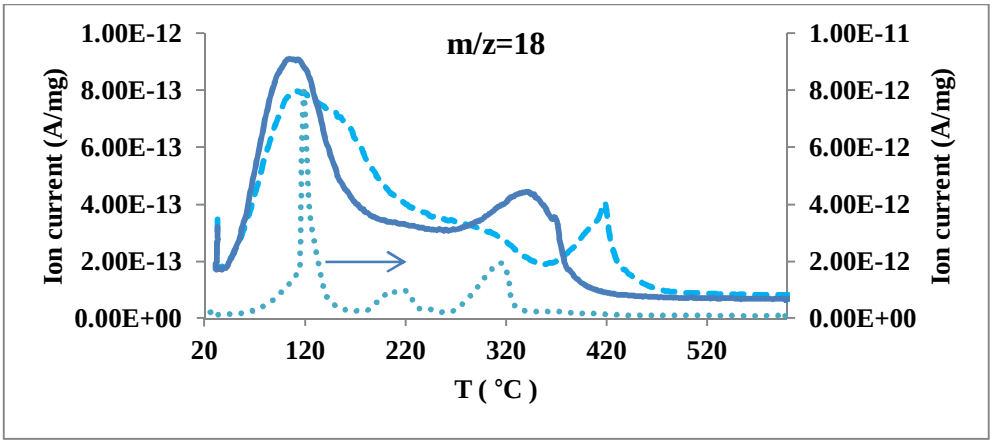

Figure 3.5: Water formation during calcination of freeze-dried materials in 80% air in Ar. Mo_FD (dotted line), MoW-0.5 (solid line) and W_FD (dashed line).

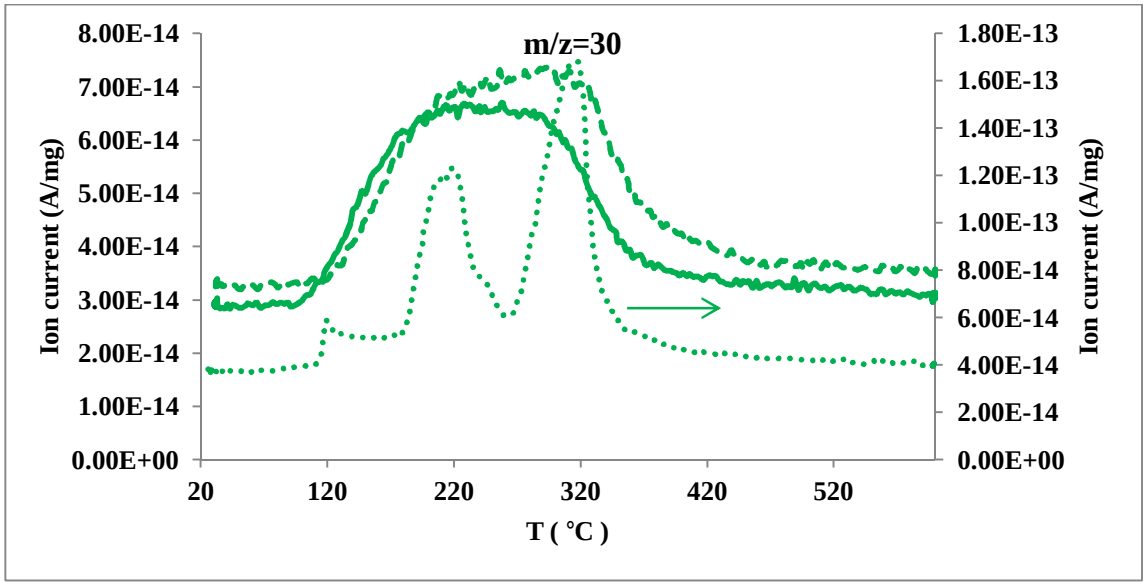

Figure 3.6: NO formation during calcination of freeze-dried materials in 80% air in Ar. Mo_FD (dotted line), MoW-0.5 (solid line) and W_FD (dashed line).

The calcined freeze-dried precursors were loaded in the TG for carburization. Weight changes and related MS data for carburization of the calcined freeze-dried materials are reported in Figures 3.7 and 3.8.

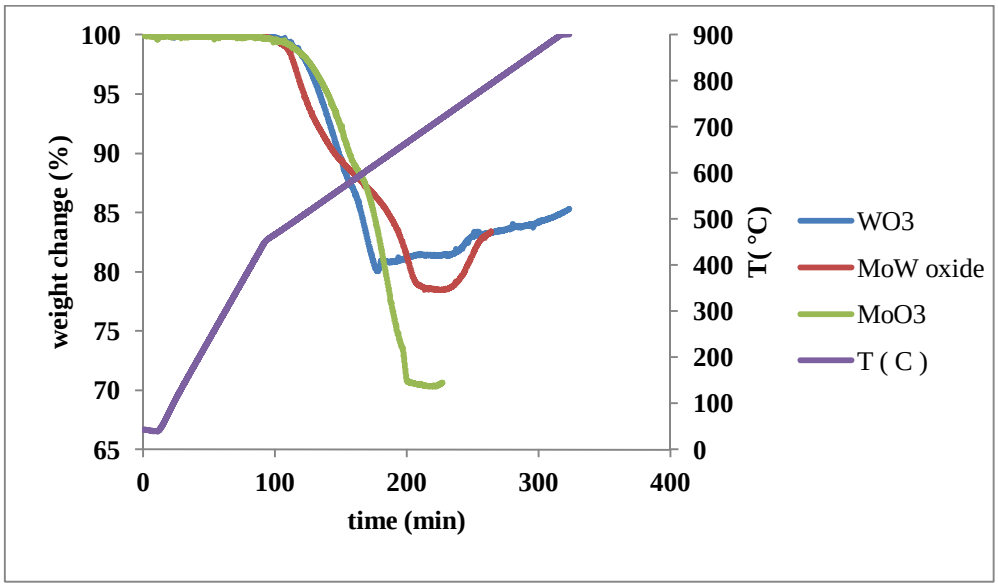

Figure 3.7: Weight change during carburization of calcined freeze dried materials in a 20% CH_4/H_2 mixture. From top to bottom: carburization of tungsten oxide, MoW-0.5 oxide and molybdenum oxide.

Here, again the sample containing only molybdenum has the highest weight loss, and the sample containing only tungsten has the lowest weight loss. Also, the sample containing only tungsten goes through a continuous weight loss before starting to gain weight. The high temperature synthesis was investigated to see if the samples go through different phases of tungsten carbide. TG-MS data show that the mixed metal oxide reduces at lower temperatures compared to the pure molybdenum oxide or pure tungsten oxide. For all three samples, two water peaks were observed which are due to the reduction, and a CO peak which forms simultaneously with the second water peak.

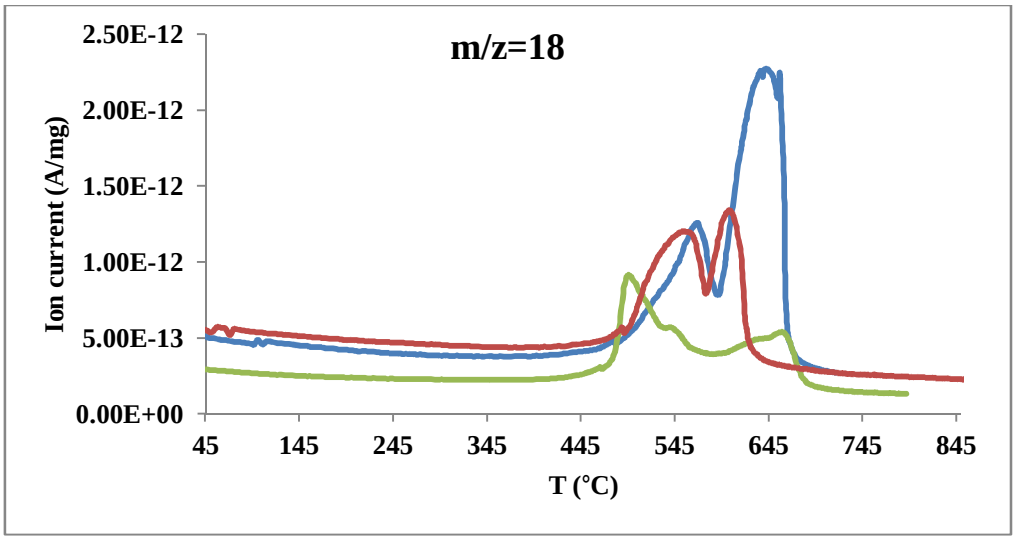

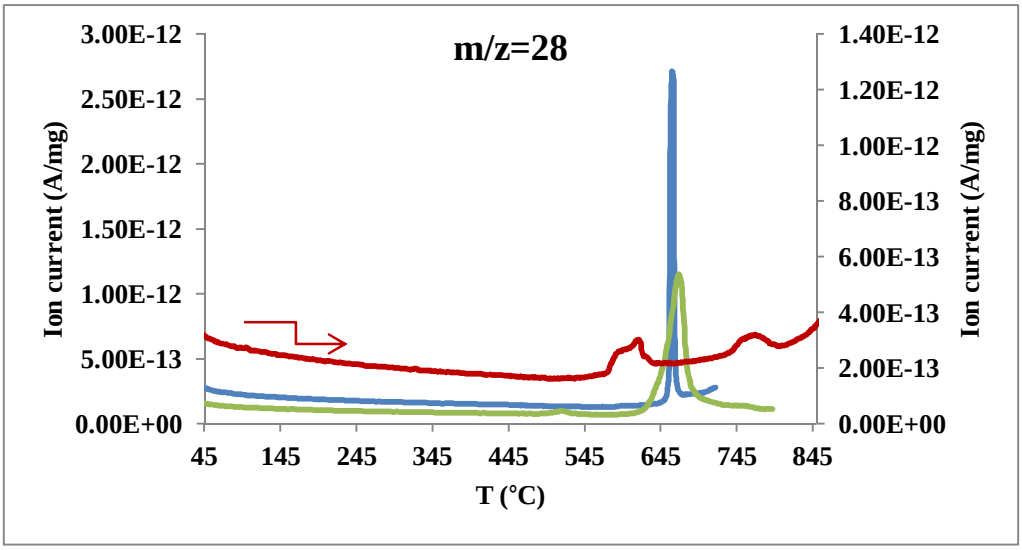

Figure 3.8: MS data for water formation (top) and CO formation (bottom) during carburization of calcined freeze-dried samples in a mixture of 20% CH_4/H_2. Blue curve is for MoO_3, green curve is for MoW-0.5 oxide and red curve is for WO_3.

3.3.2. Characterization of samples

The structures of the metal carbides were analyzed by XRD. The diffractograms of the metal carbides that were prepared by direct carburization of freeze-dried precursors are reported in Figure 3.9.

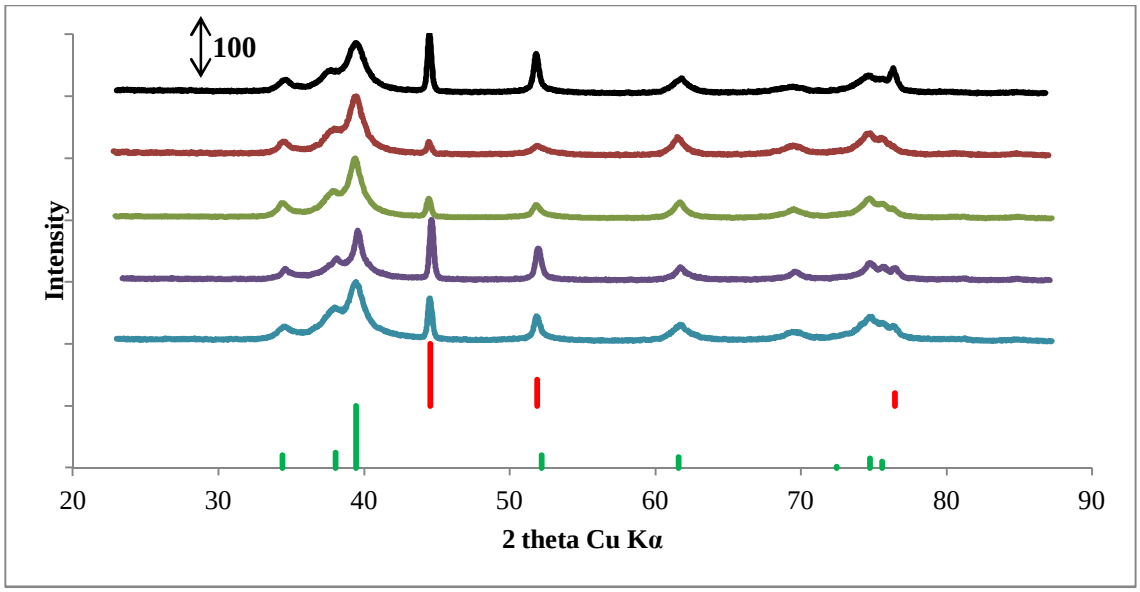

Figure 3.9: XRD data for Mo-W-C prepared from direct carburization of freeze dried precursors. From top to bottom: molybdenum carbide, MoWC-0.75, MoWC-0.5, MoWC-0.5, MoWC-0.25, tungsten carbide, Ni (ICDD: 00-004-0850) and Mo_2C (ICDD: 00-035-0787). Ni used as the internal standard.

Molybdenum carbide that was prepared by direct carburization of the FD precursor consisted of a single phase with the hexagonal structure of Mo_2C (ICDD: 00-035-0787), and carbides containing tungsten consisted of a single phase with a hexagonal structure similar to the W_2C structure (ICDD: 00-035-0776). It is important to note that these two structures are very similar to each other. Carburization of the freeze-dried tungsten-containing precursor at 870 °C resulted in a single phase with the hexagonal structure of WC (ICDD: 00-025-1047) as reported in Figure 3.11.m. The diffractograms of the samples with the hexagonal structures of Mo_2C or W_2C were fitted by using the Powdercell software and the unit cell volumes were obtained as reported in Table 3.1. The unit cell volumes are plotted versus composition in Figure 3.12.

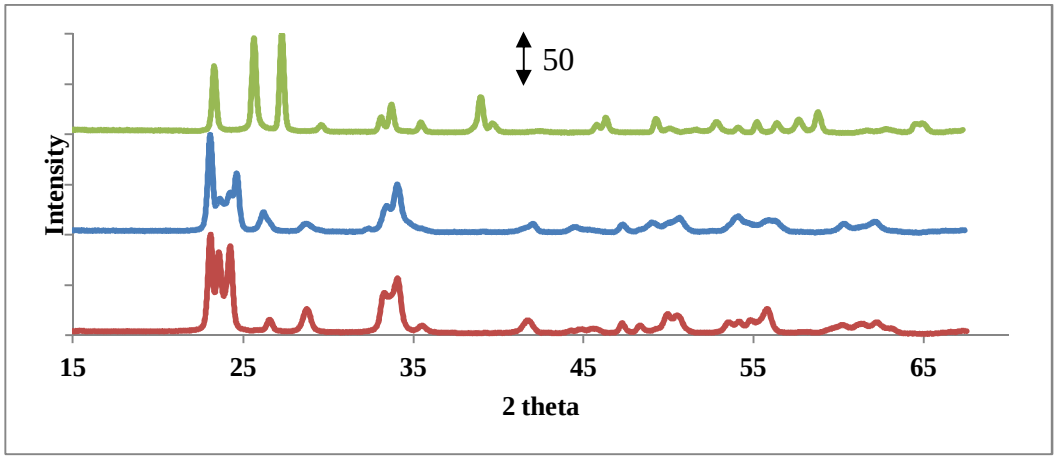

Figure 3.10: XRD data for calcined freeze-dried precursors from top to bottom: Mo, MoW-0.5 and W oxides. Gas mixture was 80% air in Ar.

XRD data for molybdenum oxide, tungsten oxide and molybdenum-tungsten oxide obtained through calcination of freeze-dried precursors are reported in Figure 3.10. The oxides have diffractograms similar to MoO_3 (ICDD: 00-005-0508) and WO_3 (ICDD: 00-043-1035). The diffractograms of MoW-0.5 oxide and tungsten oxide are similar to each other.

The diffractograms of carbides that were prepared by carburization of oxides are reported in Figure 3.11. Molybdenum carbide has the hexagonal structure the same as (ICDD: 00-035-0787) as reported in Figure 3.11.c. Tungsten carbide that was prepared at 750 °C consisted of a single phase hexagonal structure (ICDD: 00-035-0776) (Figure 3.11.d), while tungsten carbide that was prepared at 900 °C contained two hexagonal phases, W_2C (ICDD: 00-035-0776) and WC (ICDD: 00-051-0939) (Figure 3.11.f). The molybdenum-tungsten carbides that were prepared at 700 (Figure 3.11.h) and 800 °C (Figure 3.11.i) consisted of two phases similar to hexagonal W_2C (ICDD: 00-035-0776) and cubic WC (ICDD: 00-020-1316).

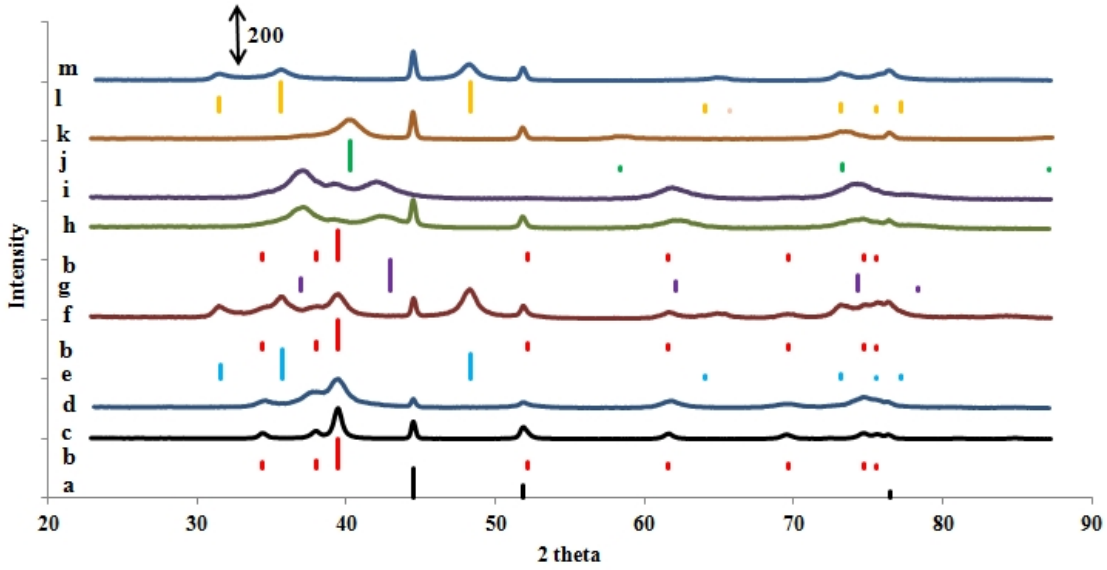

Figure 3.11: XRD data for Mo-W carbides series. From bottom to top: (a) Ni (ICDD:00-004-0850), (b) Mo_2C (ICDD:00-035-0787), (c) molybdenum carbide prepared from oxide at 720 °C, (d) W_2C prepared from oxide at 750 °C, (e) WC (ICDD: 00-051-0939), (f) tungsten carbide prepared from oxide at 900 °C, (g) WC (ICDD: 00-020-1316), (h) MoWC-0.5 prepared from oxide at 700 °C, (i) MoWC-0.5 prepared from oxide at 800 °C, (j) W (ICDD: 00-004-0806), (k) MoWC-0.5 prepared from freeze-dried precursor at 590 °C, (l) WC (00-025-1047) and (m) WC prepared from freeze-dried precursor at 870 °C. Gas mixture was 20% CH_4 in H_2.

Direct carburization of MoW-0.5 up to 590 °C produces a near-metallic phase of MoW. Its structure is similar to that of metallic tungsten (ICDD: 00-004-0806) (Figure 3.11.k).

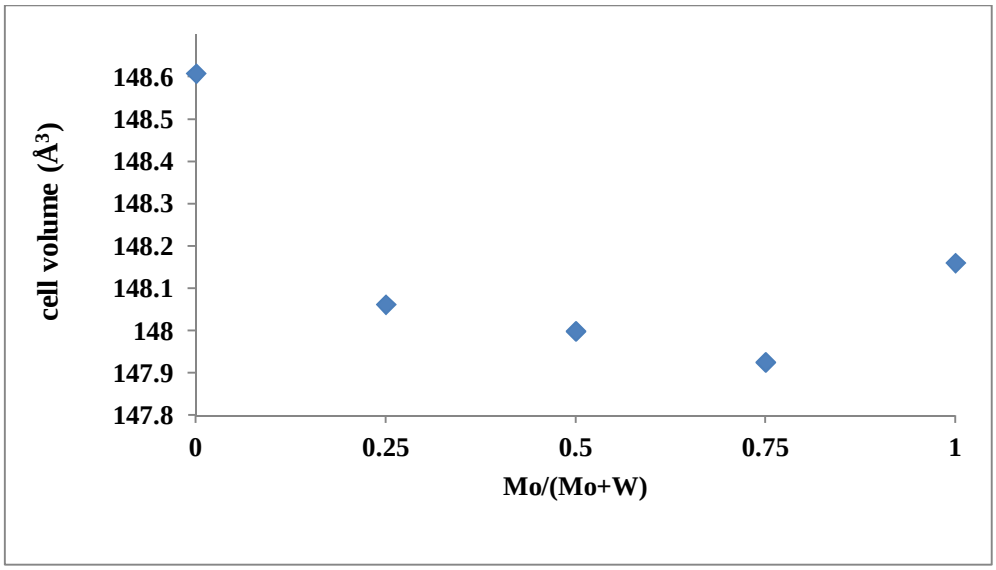

Figure 3.12: Unit cell volume vs. composition for Mo-W carbide series prepared by direct carburization of freeze-dried precursors in a 20% CH_4/H_2 mixture.

Metal ratios, carbon content, surface areas and pore size values of samples prepared by direct carburization of freeze-dried precursors are reported in Table 3.1. The pore volume, pore diameter and cell volume of monometallic carbides are higher than the mixed metal carbides. W_2C has the lowest CO uptake and by increasing the content of molybdenum the amounts of CO uptake increases. The N_2 physisorption isotherms were type IV with a pore size distribution in the meso-porosity range.

Table 3.1: Characterization data for samples prepared by direct carburization of freeze dried precursors

Sample	Mo/(Mo+W) By EDS	Carbon content (%Wt)	Weight gain during passivation (%Wt)	Surface area (m^2/g)	Cell volume ($Å^3$)	BJH Desorption average pore diameter (Å)	BJH desorption pore volume (cm^3/g)	CO uptake (µmol/g)	Site density ($µmol/m^2$)
Mo_2C	1.00	5.69±0.18	1.76	19.1	128.31	84.0	0.041	26.58	1.39
MoWC-0.75	0.79	4.51±0.20	2.38	21.8	128.10	67.4	0.028	24.74	1.13
MoWC-0.5	0.54±0.03	3.93±0.13	2.55	16	128.17	53.2	0.015	20.93	1.31
MoWC-0.25	0.26±0.06	3.20±0.06	2.26	13.8	128.22	54.6	0.023	21.39	1.55
W_2C	0.00	3.07±0.17	1.08	20.5	128.69	72.9	0.046	15.20	0.74

3.3.3 Reduction of samples

In order to find a suitable reduction temperature for reduction of passivated samples, temperature programmed-reduction (TPR) in 80% H_2 /Ar and atmospheric pressure was applied. The TPR results are shown in Figure 3.13. The main gas phase products were water (m/z=18) and methane (m/z=15). For all samples, water starts to form in the range of 100 to 350 °C. The water forms in a single broad peak or two peaks, one at lower temperature around 100 °C, and the other one at higher temperature around 300 °C. Methane starts to form at 400 °C. The lowest temperature for evolution of methane was observed for MoWC-0.5 and the highest temperature for tungsten carbide.

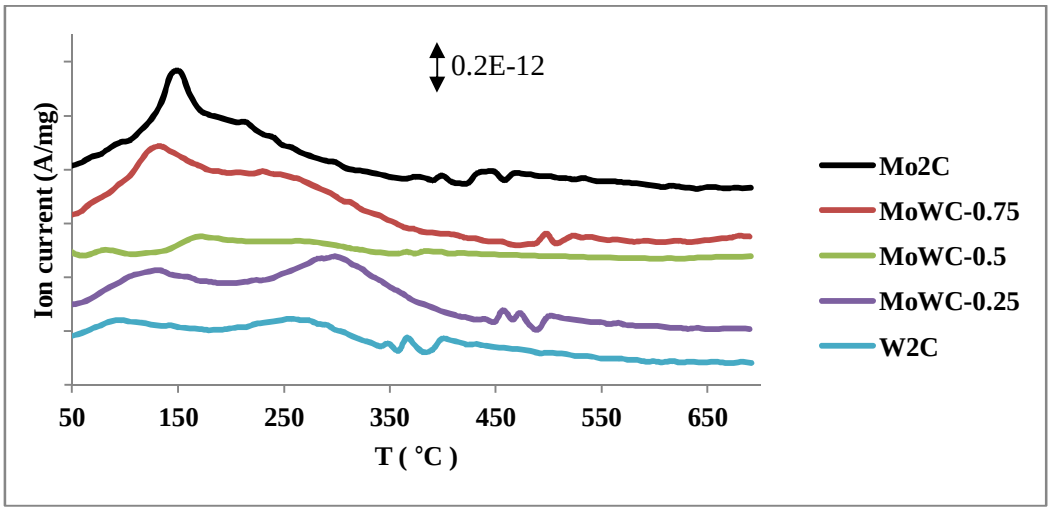

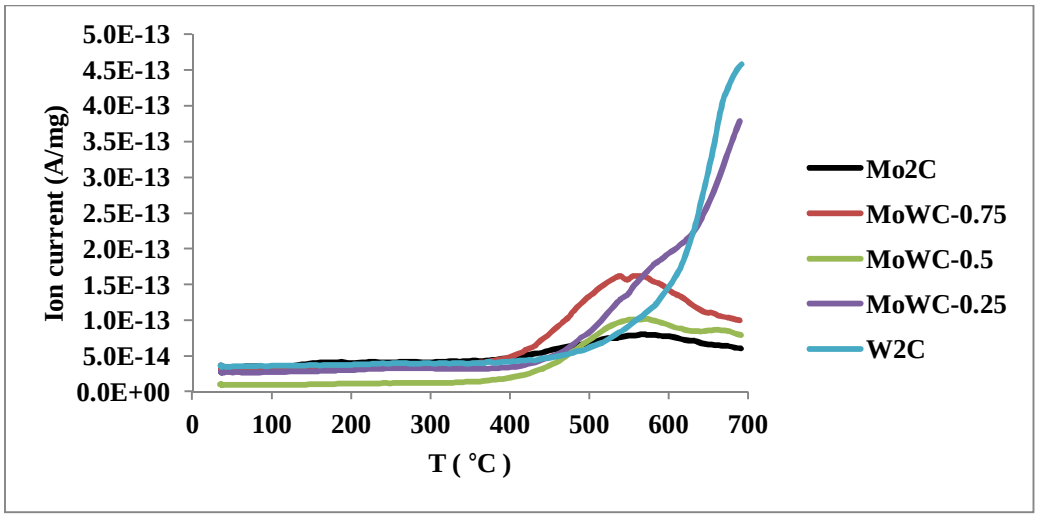

Figure 3.13: MS data for temperature-programmed reduction (TPR) of passivated samples with a temperature ramp of 10 K/min. Water formation (top) and methane formation (bottom). Gas mixture was 80% H_2 in Ar.

Molybdenum carbide has the smallest methane peak with the maximum around 550 °C. In general, the behavior of mixed metal carbides regarding methane formation is something between pure molybdenum and pure tungsten carbide. MoWC-0.5 forms two methane peaks, with maxima at 550 and 650 °C. The maxima for methane formation for MoWC-0.75 and tungsten carbide are at 550 and 700 °C respectively. MoWC-0.25 has a shoulder around 600 °C and a maximum around 700 °C.

Based on the TPR data, all samples were reduced at 350 °C before running the reaction; at this temperature, oxygen is removed from the surface without damaging the carbidic surface.

3.3.4 Catalytic activity

Hydrogenation of toluene was used to test the catalytic activities of the samples at different temperatures ranging from 193 to 275 °C and 400 °C. The only product below 300 °C for all samples is methylcyclohexane (MCH). In Figure 3.14, the

logarithm of the rate versus 1000/T is plotted to determine the activation energies for hydrogenation of toluene to MCH.

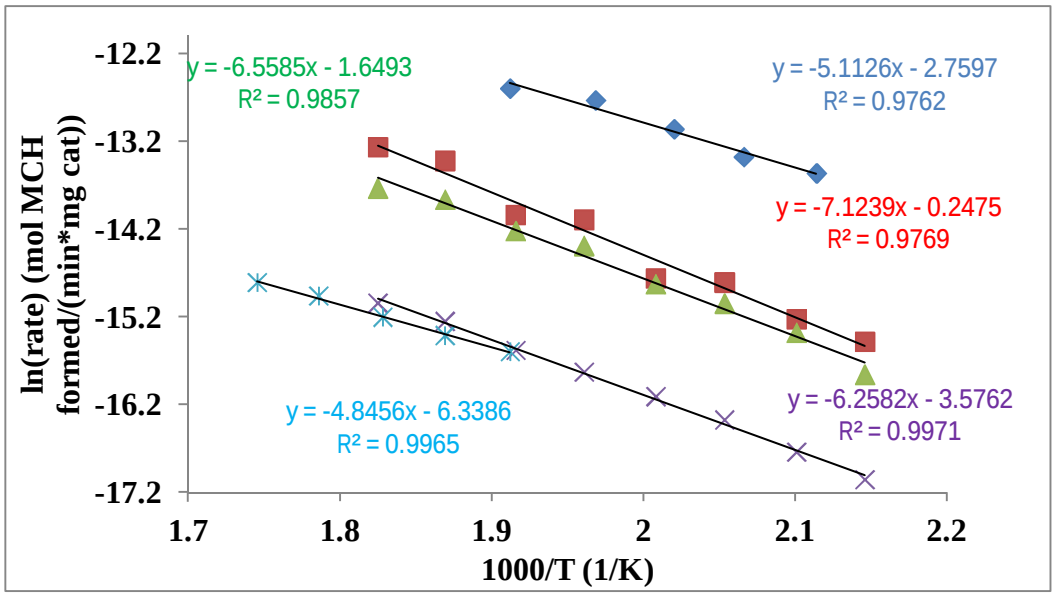

Figure 3.14: Logarithm of rate vs. 1000/T for hydrogenation of toluene on Mo-W carbide series. From top to bottom: Molybdenum carbide, MoWC-0.75, MoWC-0.5, MoWC-0.25 and tungsten carbide.

In Table 3.2, activation energies for hydrogenation of toluene to MCH on the Mo-W carbide series are reported. The values are in the range of 40 to 60 kJ/mol.

Table 3.2: Activation energies for hydrogenation of toluene to methylcyclohexane on the series of Mo-W carbides.

Sample	Slope (K)	E (kJ/mol)
Mo_2C	5.1	42.5
MoWC-0.75	7.1	59.2
MoWC-0.5	6.6	54.5
MoWC-0.25	6.3±0.1	52.0±0.9
W_2C	4.8±0.3	40.3±2.4

Turnover frequencies (TOF) for hydrogenation of toluene on the different samples at 250 °C are reported in Figure 3.15. Results show that molybdenum carbide has the highest hydrogenation activity while samples rich in tungsten have the lowest hydrogenation activities.

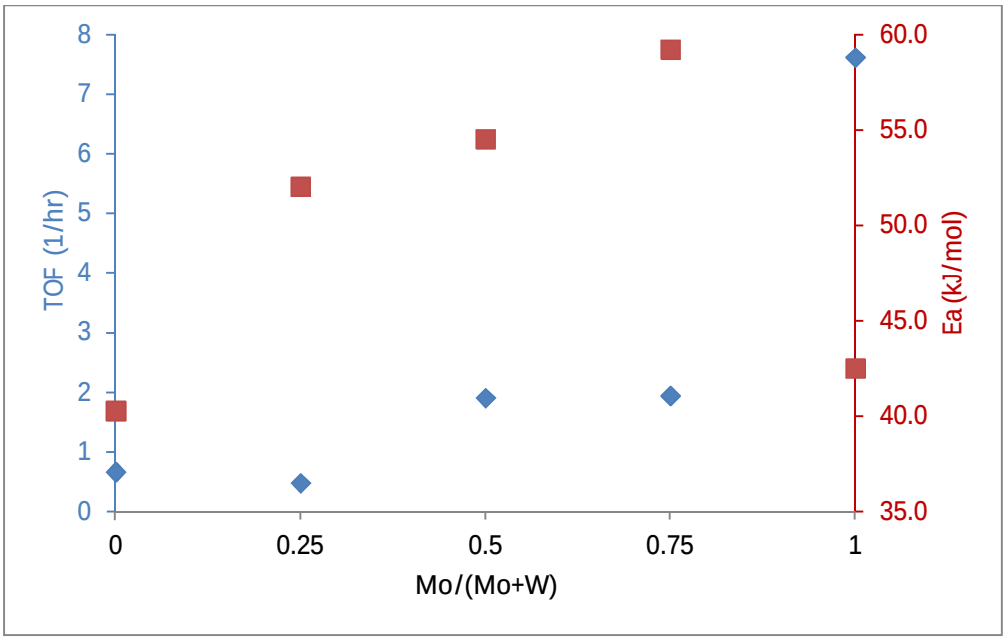

Figure 3.15: TOF and activation energies for hydrogenation of toluene to methylcyclohexane at 250 °C and 20 bar hydrogen pressure.

The stability of samples was tested at 400 °C and 20 bar pressure of H_2 over 24 hours time on stream. Results are reported in Figure 3.16.

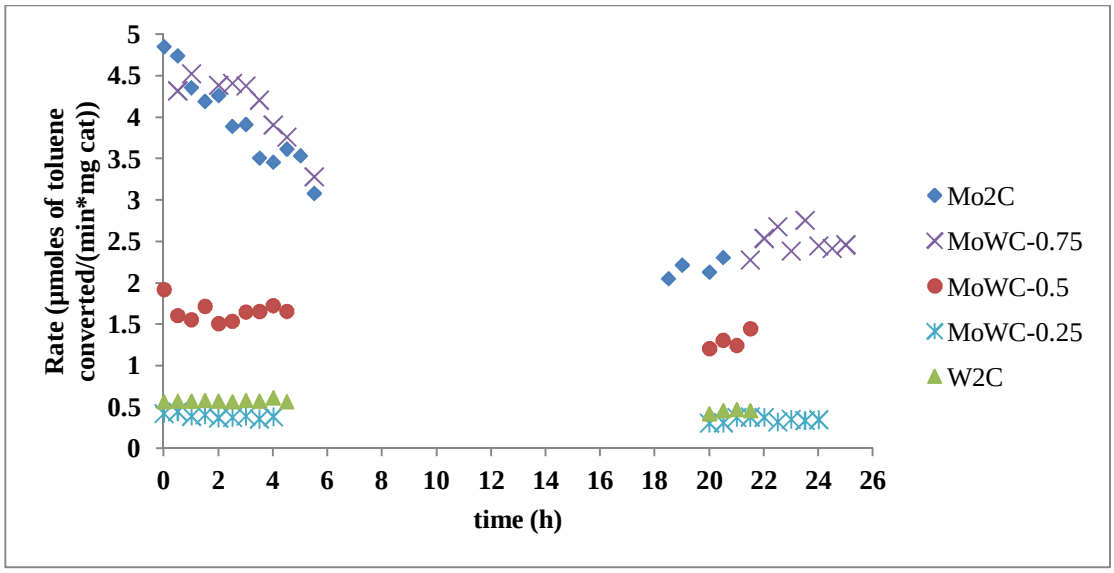

Figure 3.16: Rate of toluene conversion vs. time at 400 °C and 20 bar pressure for the series of Mo-W carbide samples.

Over this time on stream, the samples showed different deactivation rates. Molybdenum carbide had the highest activity loss of 53%, while MoWC-0.25 had the lowest activity loss of 17%. At 400 °C, products include C_1 to C_6, MCH, ethylcyclopentane (ECP), benzene and xylene. In Figure 3.17, the product selectivities versus conversion over 24 hours time on stream are reported.

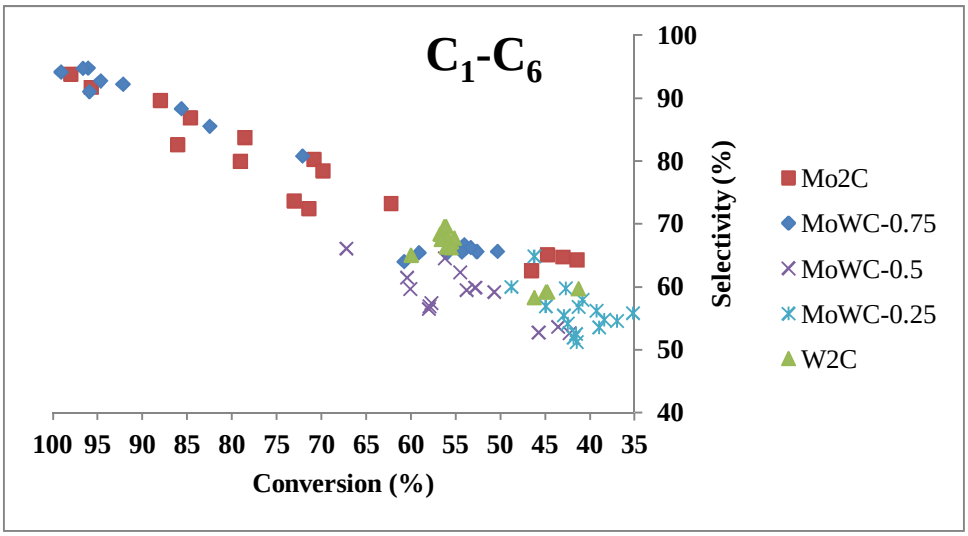

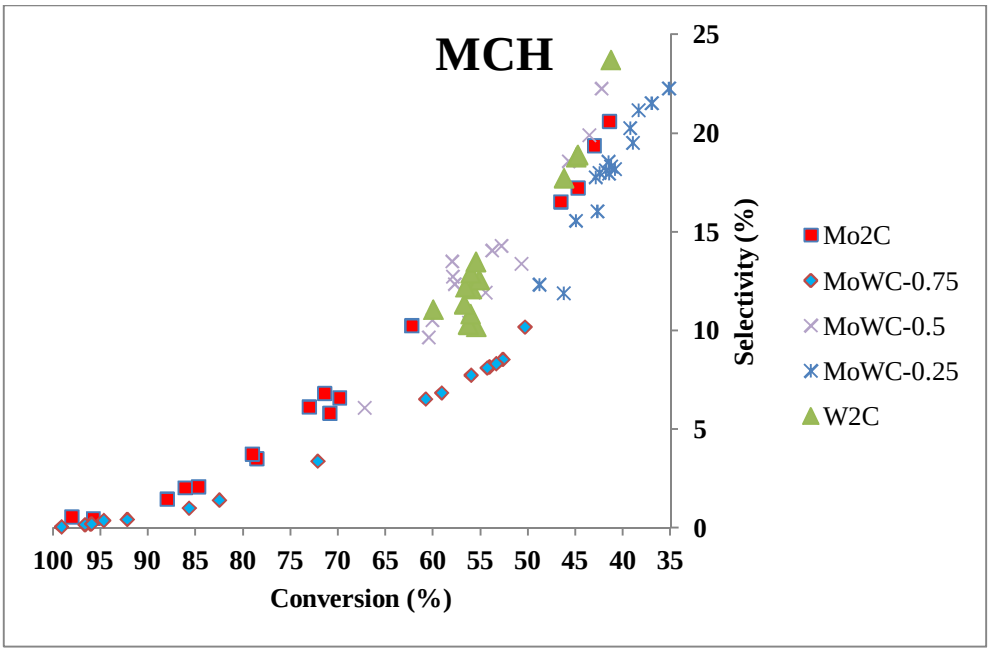
MCH
25
20
15
10
5
0
Selectivity (%)
100 95 90 85 80 75 70 65 60 55 50 45 40 35
Conversion (%)
Mo2C
MoWC-0.75
MoWC-0.5
MoWC-0.25
W2C

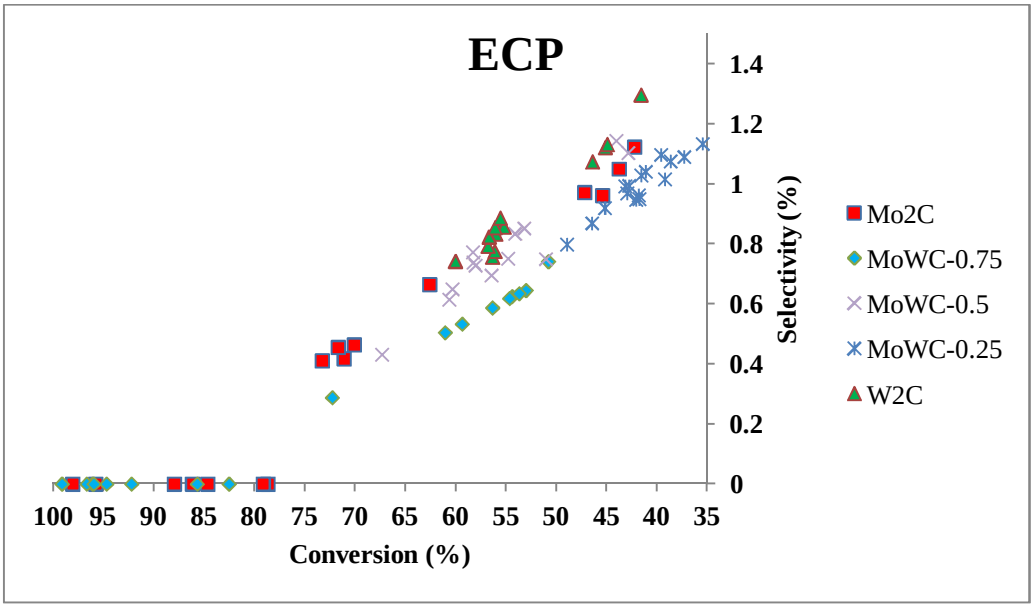
ECP
1.4
1.2
1
0.8
0.6
0.4
0.2
0
Selectivity (%)
100 95 90 85 80 75 70 65 60 55 50 45 40 35
Conversion (%)
Mo2C
MoWC-0.75
MoWC-0.5
MoWC-0.25
W2C

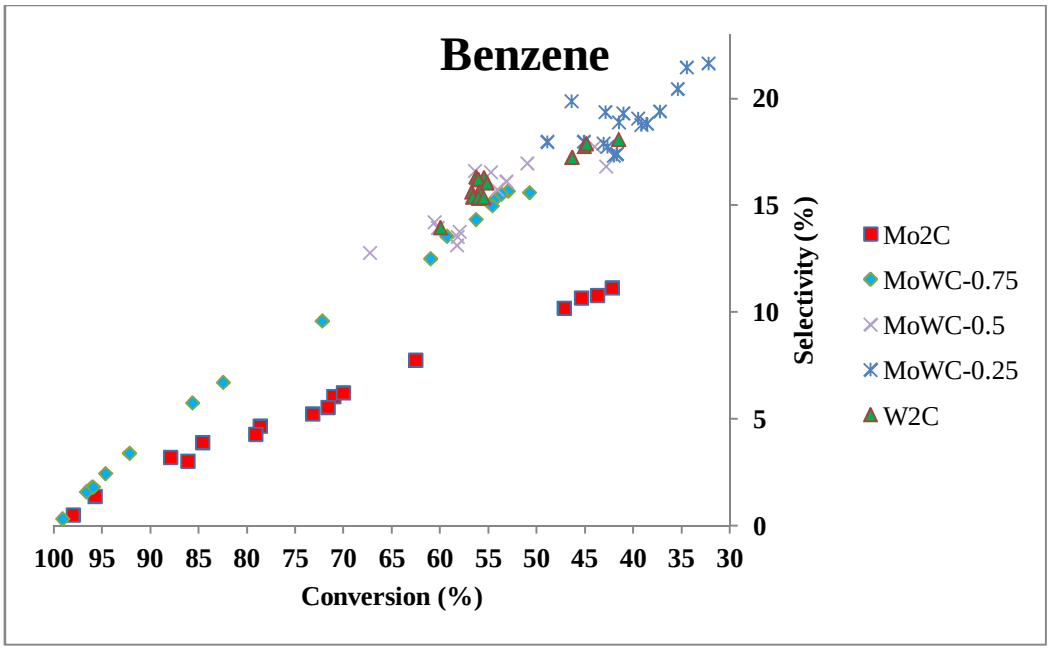

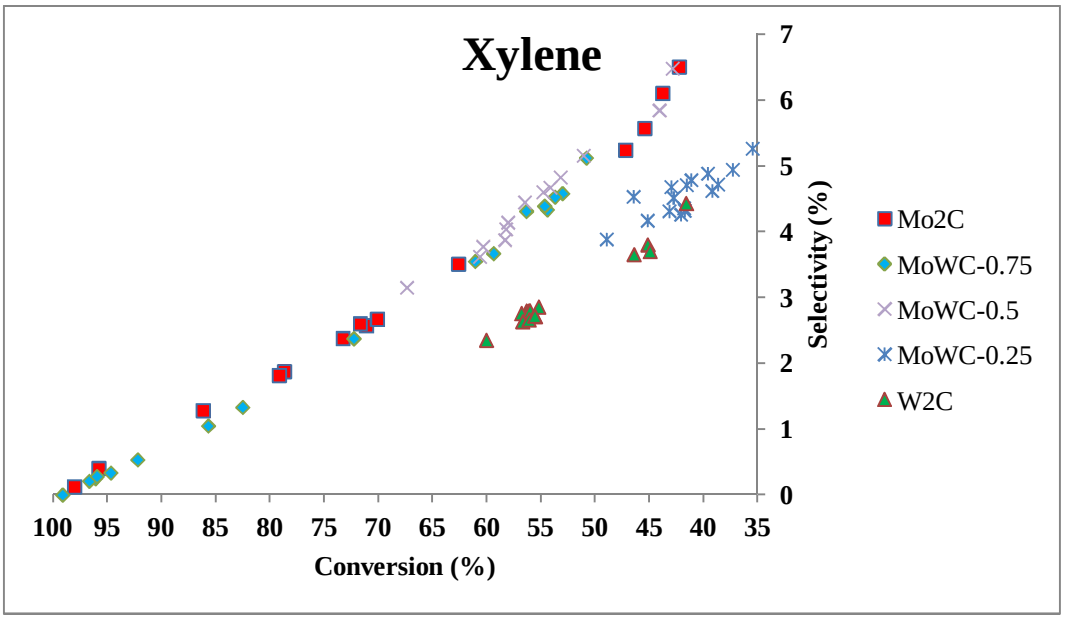

Figure 3.17: Product selectivity vs. conversion during toluene hydrogenation at 400 °C and 20 bar hydrogen pressure on Mo-W carbide series.

Table 3.3: Product selectivity of toluene conversion on Mo-W carbide series

Sample	Conv. (%)	C_1-C_6	Methyl cyclohexane	Benzene	Ethyl cyclopentane	Xylene
Mo_2C	45	64	18	11	1	6
$Mo_{1.5}W_{0.5}C$	54	70	9	16	1	5
MoWC	44	55	21	18	1	4
$Mo_{0.5}W_{1.5}C$	42	56	20	19	1	5
W_2C	45	58	19	18	1	4
MoWC	16	35	40	16	2	8

The product selectivities of toluene conversion on the Mo-W carbide series at the final conversions are compared in Table 3.3.

Also, the activity enhancement of tungsten carbide after use at 400 ℃ and subsequent cooling to the initial reaction temperature of 250 ℃ was tested and is reported in Figure 3.18. In this experiment, the temperature was increased from 250 to 400 ℃ and kept there for 20 hours, after that the catalyst was cooled down to 250 ℃ and kept at that temperature for another 20 hours, and again it was heated up to 400 ℃ and was cooled down to 250 ℃. Rates of toluene hydrogenation were measured during these times. Upon cooling down to 250 ℃, a rate enhancement was observed compared to the situation before heating up to 400 ℃. Over 20 hours time on stream at 400 ℃, deactivation by 15% was observed, but the rate at 250 ℃ is still higher than it was at the time before heating up to 400 ℃. When the samples were again heated to 400 ℃, the rate was the same as at the end of the first period at 400 ℃.

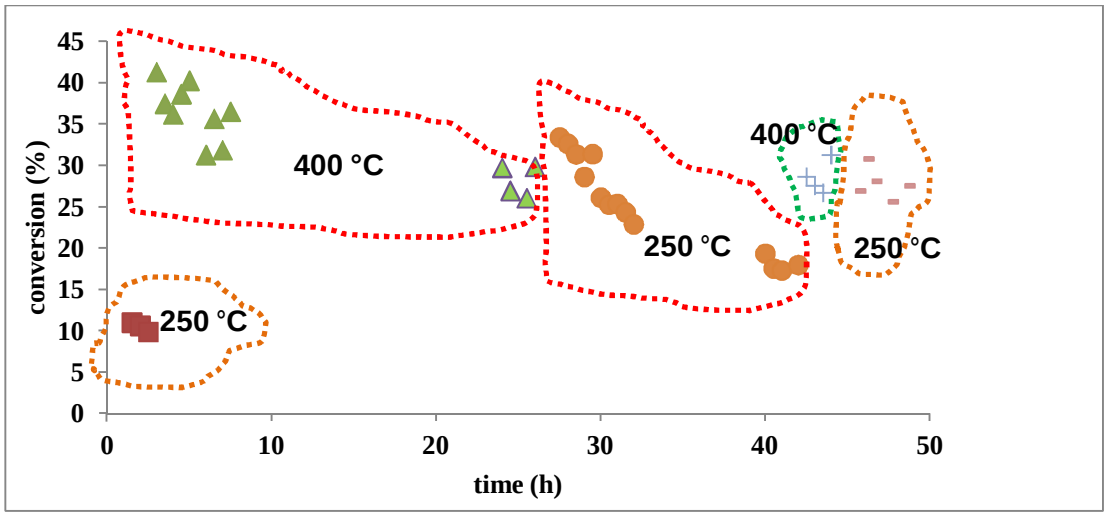

Figure 3.18: Toluene conversion on tungsten carbide at various temperatures and time on stream.

3.4 Discussion

3.4.1 Synthesis of samples

Mixed metal precursors containing molybdenum and tungsten with different molar ratios were prepared by a freeze-drying method. Using freeze-drying for synthesis of mixed metal precursors is simple, fast and the yield is around 95%. Loose powders prepared by this method are very fine, and since carburization of a solid in a gas mixture occurs by diffusion mass transfer between the solid and the gas phase, the smaller the particles, the easier the mass transfer. As a result, the final carburization temperature can potentially be lower for small particles, as it is shown in Figure 3.1.

Carburizations of all samples were done in the TG with a temperature program as it is shown in Figure 3.2. The temperature program for the carburization was not optimized, and the same program was used as for the carburization of oxide precursors in the synthesis of monometallic carbides [22]. During carburization, monitoring of two gas phase products is important: water and CO. Water forms from the reduction of the

precursors and CO forms when carbon migrates into the lattice, reacts with the lattice oxygen and replaces the oxygen to form the carbide. MS data show that during carburization of freeze-dried precursors, CO starts to form at higher temperatures simultaneously with the formation of the last water peak. Formation of water and CO at the same time is an indication of simultaneous reduction and carburization. Formation of CO during carburization indicates that the hydrocarbon source serves both as the reducing agent and the carburizing agent. When CO formation is over, carburization can be stopped.

TG data showed that for all samples except the sample that contains only tungsten, even at elevated temperatures (Figure 3.2), carbon did not deposit on the surface. However, in the case of sample containing only tungsten, there was a continuous weight gain with increasing temperature. In order to have a clean surface of tungsten carbide, the carburization was terminated when formation of CO stopped to avoid carbon deposition on the surface. Deposition of carbon on the surface during carburization of W_FD indicates that at high temperatures the rate of carbon deposition on the surface (methane dehydrogenation) is higher than the rate of free carbon hydrogenation.

The weight loss behavior and MS data for carburization of the sample containing only molybdenum are different from the rest of samples. It shows continuous weight loss until the weight loss levels off and the water and CO peaks reach to their base lines. For the samples that contain tungsten, the last water peak forms when there is a dip in the TG weight change curve. Based on weight loss values for the tungsten-containing samples and assuming that the final freeze-dried precursor have the same

stoichiometry as loaded salts, they have a stoichiometry of $WO_{0.23}$, $Mo_{0.5}W_{1.5}O_{0.48}$ and $MoWO_{0.52}$ when they reached their minimum weight. For the sample rich in molybdenum ($Mo_{1.5}W_{0.5}$) the stoichiometry at the minimum weight cannot be reported only by the TG data; because before reaching the minimum weight, sample was reduced both by hydrogen and methane (both water and CO were formed). This means that the product at the minimum weight could be oxycarbide and not oxide.

After that dip, there were weight gains for all tungsten-containing samples that happened simultaneously with the formation of CO. There were 1.22, 1.3, 1.27 and 0.33% weight gain for the samples containing only tungsten, $Mo_{0.5}W_{1.5}$, MoW and $Mo_{1.5}W_{0.5}$, respectively. The final weight changes from carburization of the freeze-dried precursors to the carbides were 27.76, 29.73, 32.84, 36.21 and 41.19% which are close to the theoretical values of 27.27, 30.03, 33.32, 37.31 and 42.26% for the samples containing only tungsten, $Mo_{0.5}W_{1.5}$, MoW, $Mo_{1.5}W_{0.5}$ and only molybdenum, respectively.

The size of the CO peak for carburization of the sample containing only molybdenum is eight and fourteen times larger than the size of the CO peaks during carburization of the sample containing only tungsten and both molybdenum and tungsten, respectively (Figure 3.3). Since methane serves both as reducing and carburizing agent, the size of the last water peak versus the size of the CO peak can be used as an indication of how much of oxygen is removed by hydrogen and how much is removed by methane. For all tungsten-containing precursors, the CO peak is smaller than the water peak. This indicates that hydrogen removes most of the oxygen, before carbon can diffuse into the lattice. As a result, it is possible that the tungsten-containing

materials go through near-metallic phase (as suggested by the stoichiometry of materials at their minimum weight), and then this near-metallic phase is carburized to the carbidic phase. To verify this hypothesis, carburization of MoW-0.5 was stopped at 590 °C (when it reached to minimum weight and before starting to gain weight) and the structure was tested by XRD as it is reported in Figure 3.11.k. At this temperature the stoichiometry of the sample obtained by TG data is $MoWO_{0.52}$.The XRD results show that when samples go through the minimum weight, they are going through the near metallic phase. The diffractograms are similar to the metallic tungsten and are broad, probably due to the presence of oxygen in the lattice of the metal. That is why the size of the CO peak for these samples is small, because there are small amounts of oxygen left to be removed by carbon. This also could be the reason that the final carbides do not have high surface areas (Table 3.1), since tungsten-containing samples go through near-metallic phase and at high temperatures sintering happens. Also, diffusion of carbon into the sintered materials is difficult; this can potentially cause tungsten-containing materials to be carbon deficient.

Formation of near metallic phases of tungsten-containing samples at this low temperature is interesting. Reduction is a diffusion phenomenon, in which metal-oxygen bonds break, and the reduction products diffuse out. As a result, if the precursor has small particles or if it is porous, diffusion would be easier and reduction can happen at lower temperatures. If reduction happens only by hydrogen, the reduction product is only water. In this case, the partial pressure of water on the surface of the solid is very important, because if water is not removed fast enough it can re-oxidize the surface. Since the freeze-dried particles are very small, the gas phase reduction products (water)

can diffuse out very fast, which causes reduction to happen at lower temperatures and also since the partial pressure of water on the surface of samples is low it is thermodynamically possible that the samples go through the near-metallic phase [23].

However in the case of carburization in a hydrogen/hydrocarbon mixture, hydrogen is a reducing agent both at low and high temperatures and methane is a reducing agent only at high temperature. The mechanism of reduction by hydrogen is different from the mechanism of reduction by methane, because hydrogen can diffuse into the lattice of metal oxides easier than the hydrocarbon, and also formation of water can hinder the reduction by hydrogen while formation of CO cannot affect reduction by methane. It is the same argument as is used to describe sulfidation in a mixture of H_2S/H_2. For carburization, first a metallic surface should form and then this metallic surface will be carburized. After formation of the metallic surface there is a competition between carburization of the metallic surface and diffusion of the metal into the bulk [24]. Operating conditions determine the result of this competition. In freeze-dried samples, diffusion of the metal into the bulk is faster.

During carburization of the MoW-0.75 precursor, it reaches its minimum weight at about 100 K lower than the other samples. This weight loss happens with the formation of a broad water peak. This reduction at lower temperatures could be due to the help of molybdenum which facilitates the reduction. Since it is easier to reduce the molybdenum oxide compared to the tungsten oxide; on the surface the number of low valent molybdenum atom is high, which facilitates the hydrogen dissociation and subsequently the reduction. Based on the TG-MS data the final carburization temperature of 650 °C is enough to synthesize the single phase metal carbides. The

XRD data show that all samples are single phase with the hexagonal structure of W_2C as reported in Figure 3.9. Although the EDS data in Table 3.1 show these materials are homogenous at the micron scale, and the metal ratios are very close to the loaded metallic ratios in the solution, the cell volume sizes do not follow Vegard's law (Figure 3.12). This could be due to the different carbon contents in the lattice of these materials (since results show these materials are slightly carbon-deficient) or due to the presence of residual oxygen in the lattice of the final carbides. Carburization at higher temperatures did not help to get sharper diffractograms, and the final weight did not change with increasing the final carburization temperature.

Direct reduction of freeze-dried materials is a good method for synthesis of (mixed) metals for application in catalysis, due to their small particle sizes it is easy to reduce them to the metallic form. Since, it is easier to carburize the oxides compared to the metals, the freeze-dried precursors were calcined to form oxides, and then the oxides were carburized.

Freeze-dried precursors containing only molybdenum only tungsten and MoW-0.5 were calcined to a final temperature of 600 °C. The final products after calcinations are MoO_3, WO_3 and a mixture of MoO_3-WO_3.The theoretical weight losses to go from the freeze-dried precursors to their corresponding oxides are 18.47, 11.18 and 22.34% which are in good agreement with 17.57, 11.81 and 21.5% values observed from TG data in Figure 3.4.

MS data in Figures 3.5 and 3.6 show that during calcination of precursors water and NO are the main products from oxidation of hydrogen and nitrogen in the precursors. Thermal decomposition of ammonium heptamolybdate to MoO_3 [25] and

ammonium paratungsates to WO_3 has been reported elsewhere [26, 27]. However, the difference between the decomposition of commercial precursors and the freeze-dried counterparts is in the slope of weight loss. The decomposition of commercial salts happens in distinct steps with sharp slope of weight loss whereas the decomposition of freeze-dried salts has a mild slope of weight loss.

MS data for calcination of MoW-0.5 and W-FD follows the same pattern, two peaks of water and a broad NO peak. However, the last peak of water and the peak of NO start to form at lower temperatures for calcination of MoW-0.5 compared to the calcination of pure tungsten. This shows that calcination of mixed metal precursors is easier than calcination of precursors containing only one metal.

Carburizations of the oxide forms of freeze-dried precursors are reported in Figure 3.7. The experimental weight losses for transformation of MoO_3, WO_3 and MoO_3-WO_3 to Mo_2C, W_2C and MoWC are 29.6%, 18.64% and 21.5% which are very close to their corresponding theoretical weight losses of 29.18%, 18.12% and 22.35%. An interesting observation is that WO_3 is still going through a dip in weight ($WO_{0.22}$) and after that dip, gains 1.28% weight to W_2C. Such a behavior has not been observed before during carburization of the commercial WO_3 [22, 28]. However, going through a metallic phase during reduction of a metal oxide was reported before [23, 29]. Reduction of WO_3 to a near-metallic phase ($WO_{0.22}$) could be because of small particle sizes of calcined W-FD compared to the commercial WO_3. The surface area of the calcined freeze-dried tungsten sample used in this work is 7.6 m^2/g and thus five times higher than that of commercial WO_3 which is 1.5 m^2/g.

The MS data in Figure 3.8 show the standard behavior of carburization of molybdenum and tungsten oxide to their carbidic form, two water peaks and a CO peak that forms with the last peak of water. However, it is worth to mention that MoW-0.5 oxide starts to reduce at lower temperatures compared to both MoO_3 and WO_3, as it can be seen both in the TG data and the first water peak in the MS. This behavior is due to the increase of oxygen mobility in the lattice of mixed metal oxides compared to their mono metal oxide form. This is caused by the distortion of the metal oxide lattice by incorporation of another metal [30, 31].

The first peak of water is observed when enough sites for dissociation of hydrogen are created on the surface of metal oxide (low oxidation states of oxide or metallic sites, as indicated by stoichiometries of $MoO_{2.3}$, $WO_{1.74}$ and $MoWO_{5.23}$). When atomic hydrogen is produced it can participate in the reduction of metal oxide. At higher temperatures, when the surface is more reduced by hydrogen (as indicated by stoichiometries $MoO_{0.79}$, $WO_{1.15}$ and $MoWO_{2.85}$) methane can be activated by adsorbing on the surface and can participate in the reduction by forming CO.

The weight loss behavior of mixed metal carbides of molybdenum and tungsten in the direct carburization of freeze-dried precursors or carburization of calcined Mo-W materials that observed during carburization of the precursor containing only tungsten. The XRD data of WO_3 and MoW-0.5 oxide are also similar to each other, as it is shown in Figure 3.10. Carburization of the two precursors containing only molybdenum leads to the formation of hexagonal structures, no matter the final temperature. However, in the case sample containing only tungsten, carburization of the calcined freeze-dried precursors or direct carburization of freeze-dried precursors results in different

structures. Tungsten carbide can go through different structures upon increasing the temperature: W_2C, W_2C+WC and WC [28]. The results in this work show that carburization of the W-FD precursor leads to the same phase transformations as it is shown in Figure 3.9 and 3.11.m. However, the phase transformation is different for carburization of the calcined freeze-dried tungsten sample. At 750 °C it forms the hexagonal structure of W_2C (Figure 3.11.d), but at 900 °C it forms two phases of W_2C and WC (Figure 3.11.f). The pure WC phase could not be prepared in this work by carburization of the calcined precursor.

The carbide phase transformations during carburization of calcined MoW-0.5 and the calcined precursor containing only tungsten are also different. The single phase mixed metal carbide from carburization of calcined MoW-0.5 could not be prepared. Both at 700 and 800 °C, it forms two phases of cubic WC and hexagonal W_2C. This structure of mixed metal carbide was also reported when the precursor was prepared from physical mixing of MoO_3 and WO_3 and was carburized using a low heating rate [32].

Formation of a metal carbide with the cubic structure of tungsten carbide is interesting. Molybdenum and tungsten carbides with cubic structure can be prepared by different routes such as first preparation of molybdenum and tungsten nitrides which have cubic structure and then the topotactic transformation of the metal nitrides to the cubic metal carbides [33] or adding some metals such as nickel or platinum to the oxide precursor and then performing the carburization [34]. In the latter case, the metal carbide will have the cubic structure because addition of active metals will cause reduction to occur at lower temperatures. In this work, adding the second metal

facilitates the reduction and creation of oxygen vacancies, as a result the lattice of the metal oxide will rearrange in a way to remove these vacancies, either by collapse of the lattice or by inserting hydrogen or carbon into the lattice. This oxyhydride (bronze) has cubic structure, and the rest is again a topotactic transformation of this cubic structure to the cubic carbide structure [35]. The formation of both the cubic and hexagonal structures of metal carbides could be due to the carburization of metal oxyhydride that results in formation of the cubic structure with an impurity of hexagonal structure. Formation of each phase depends on the number of oxygen vacancies, and whether these vacancies are filled with hydrogen or carbon, or not [36].

The synthesis of single phase MoW-0.5 carbide (from the oxide precursor) by changing the temperature ramps to 2 or 10 K/min to the final carburization temperature was tried. However, changing the temperature ramp did not result in the formation of single phase mixed metal carbide. One solution to obtain the single phase cubic structure of mixed metal carbide from an oxide precursor is first to prepare mixed metal nitrides with cubic structure [17], and then carburize the nitrides to the carbides. Another way could be baking the oxide in hydrogen for a long time to form oxyhydride and then performing the carburization with high concentration of ethane to get single phase carbide with cubic structure [37].

Since the goal of this work is synthesis of single phase mixed metal carbides the route of direct carburization of FD precursors was used to test the catalytic activities of mixed metal carbides.

3.4.2 Passivation and reduction of samples

Metal carbides are pyrophoric and need to be passivated before coming in contact with the ambient. The “stepwise” passivation method was used to be able to recover more metallic sites during regeneration [22]. The major weight gain to reach the “knee shape” (as it was shown in Chapter 2) of weight gain happens during passivation with 0.1% O_2 in Ar. Samples that were prepared by carburization of calcined freeze-dried MoW-0.5 gained more weight during passivation than the sample that was prepared by direct carburization of MoW-0.5. Also, the near-metallic MoW-0.5 could dissociate oxygen at room temperature, resulting in oxygen chemisorption and the uptake of 2.8%.

Reduction of samples with hydrogen produced water from removal of oxygen and methane from removal of carbon as reported in Figure 3.13. In the case of molybdenum carbide, there is only one water peak, which indicates that oxygen is removed from one type of sites. However, in the case of tungsten-containing samples, two peaks of water can be observed, which are due to the presence of two different sites or removal of oxygen from surface or subsurface [38].

Methane formation is interesting to notice. The size of the methane peak for molybdenum carbide is the smallest; this indicates that the surface of molybdenum carbide can be preserved better in the presence of hydrogen than those of the rest of the samples even at high temperatures. Creation of (sub) surface carbon vacancies will become easier and happens at lower temperatures with adding the second metal into the structure of pure molybdenum carbide. This is due to the distortion of the structure, as it was shown by XRD data, which eases the removal of carbon. The shape of the methane

peak for MoWC-0.75 is similar to that for molybdenum carbide but the size of the peak is larger. For MoWC-0.5, there are two peaks of methane, which could again be interpreted as removal of two different types of carbon. With increasing tungsten concentration, the amount of carbon removed increases. This is due to two reasons; one, distortion of the structure by adding another metal into it, and two, the presence of oxygen on the surface of tungsten-containing materials. As shown before [22], oxygen adsorbs strongly on the surface of tungsten carbide, and pulls the electrons of tungsten to the oxygen-tungsten bond, which weakens the tungsten-carbon bond. The reduction data in Figure 3.13 are at atmospheric pressure; at this condition, carbon starts to be removed from the carbide surface at about 400 °C. When the reduction was performed at 20 bar pressure (reaction pressure), it was observed that in the case of MoWC-0.5 methane starts to form at about 100 K lower temperatures than during reduction at atmospheric pressure. As a result, one should note that at high hydrogen pressure carbon can be removed at lower temperatures, and this can change the catalytic activities of metal carbides [22].

3.4.3 Toluene hydrogenation to methylcyclohexane on mixed Mo-W carbides

The hydrogenation activity of the mixed Mo-W carbide series was tested by hydrogenation of toluene. Adsorption of hydrogen on the surface of Mo_2C can be both atomic (with low energy barrier) or molecular depending on the plane [39] and is stronger than on noble metals [40]. For aromatic molecule such as benzene, some reported they adsorb very strongly and are converted according to an Eley-Rideal mechanism [41, 42], while others reported hydrogenation follows a Langmuir-Hinshelwood mechanism [36, 43]. Benzene TPD from Mo_2C is similar to that of Ru

(benzene desorption temperature around 384 K) [44] and the adsorption energy is comparable with that on noble metals. Heats of adsorption of carbon on the surface of Mo_2C are reported to be similar to the heat on noble metals like Ru [40]. Since metal carbides are reported to have similar behavior to the noble metals during TPD or adsorption, the apparent activation energies for hydrogenation of toluene on metal carbides and noble metals will be compared.

The apparent activation energies for hydrogenation of toluene to MCH on the Mo-W carbide series were calculated by plotting the logarithm of rate versus 1000/T in Figure 3.14 and their values were reported in Table 3.2. The reaction rate was assumed to be zero order with respect to toluene [45]. The values for the activation energies are comparable with activation energies for hydrogenation of toluene with noble metals: 40-50 kJ/mol on Pt/ZSM-22 [46] and 29-55 kJ/mol on supported Pd [47]. An activation energy of 58.1 kJ/mol is reported for molybdenum carbide; this value is different from the value in this research because of the presence of an oxide phase impurity and the cubic structure of the molybdenum carbide in the study [45]. Activation energies for dehydrogenation of cyclohexane on Mo-W carbide show the same trend: similar activation energies for pure molybdenum and tungsten carbide, and higher activation energies for mixed metal carbide because of modification of the active sites [21].

CO chemisorption was used to titrate the active sites of metal carbides [48]. The turnover frequencies (TOF) of toluene conversion to MCH for the Mo-W carbide series are reported in Figure 3.15 and show, molybdenum carbide has the highest activity, and with increasing the molybdenum content in the Mo-W carbide series the TOF increases.

It is worth to mention that for some samples the initial activity at 193 °C was high and did not fall on the straight line in the activation energy plot. However, remeasuring this data on the next day showed that the activity was consistent with the rest of the data points. This behavior could be due to the saturation of the surface or even storage of hydrogen in the bulk of metal carbides [41, 49]. The initial high hydrogenation activity could be due to the consumption of a high number of hydrogen atoms on the surface. All samples showed no deactivation after about 24 hours time on stream under reaction conditions.

3.4.4 Reaction of toluene at 400 °C on mixed Mo-W carbides

The catalytic behavior of the samples was also tested at 400 °C; at this temperature, a wide range of products was observed: C_1 to C_6 compounds, methylcyclohexane (MCH), ethylcyclopenatane (ECP), benzene and xylene. All samples showed deactivation over 24 hours time on stream as reported in Figure 3.16. Mo_2C showed the highest deactivation of about 52% (56 μmoles of toluene converted/mg catalyst), while the MoWC-0.25 showed the lowest deactivation about of 17% (9 μmoles of toluene converted/mg catalyst) loss of its initial activity.

Over time on stream a change in product distribution with deactivation was observed as it is shown in Figure 3.17. Initially, light products (C_1-C_6) dominate but with declining activity MCH, benzene, xylene and ECP start to form. This is due to the change in the active sites. The presence of different sites such as metallic, acidic or dual sites has been reported for oxycarbides and nitrides [48]. The metallic characteristic of metal carbides is responsible for (de)hydrogenation and hydrogenolysis. Formation of MCH (hydrogenation) and light gases (hydrogenolysis) are due to the metallic behavior

of these materials. However, the oxidation state of the metal sites determines hydrogenation versus hydrogenolysis. Strong and weak hydrogenolysis sites have been reported on the surface of metal carbides [50]. Strong sites (low oxidation state) can break single carbon-carbon bonds while weaker sites (higher oxidation state) can break double bonds. Over the time on stream strong hydrogenolysis sites will be deactivated, and that is why the formation of light gases decreases. It was reported that the presence of excess carbon on the surface of molybdenum carbide will change the selectivity in favor of dehydrogenation compared to hydrogenolysis [21]. The surface of Mo_2C can be reduced more easily compared to the tungsten-containing samples; as a result it has the highest hydrogenolysis activity. Also, the hydrogenolysis behavior of molybdenum carbide is more like that of Ru, Ni or Co, while the hydrogenolysis behavior of tungsten carbide is more like that of Pt or Pd [21].

After deactivation of the strong hydrogenolysis sites other products (MCH, benzene, xylene and ethylcyclopentane (ECP)) can be observed. Formation of xylenes and ethylcylcopentane occurs because of the acid functionality of metal (oxy) carbides. There are numerous papers about bifunctional behavior of metal (oxy) carbides. The origin of acidity has been attributed to the charge transfer from metal to carbon and formation of Lewis acid sites [51] but mainly to the presence of oxygen on the surface of metal carbides (oxycarbide) and formation of Brønsted acid sites. Tungsten oxycarbide can catalyze alkane isomerization [52-56], also molybdenum oxycarbide [57, 58] and molybdenum-tungsten oxycarbide [32, 59, 60] can catalyze alkane isomerization with high selectivity to isomers at high conversion.

However, no ring opening of naphthalene has been observed on molybdenum oxycarbide, due to the low acidity and caused by low acidity for ring contraction before ring opening [61]. In this research a small amount of ring contraction and formation of ECP was observed. Ring contraction of six-membered rings to five-membered rings needs strong Brønsted acid sites [62]. In all of our samples little ECP is formed, which can be due to the suppressing of acid functionality necessary for ring contraction over hydrogenation. The balance between acidic and metallic sites determines the fractions of hydrogenation and acid-catalyzed products. As reported elsewhere, a low amount of metallic sites and a high amount of Brønsted sites will favor ring contraction products [63].

It is worth mentioning that ECP and MCH both are primary products, since they start to form linearly with change in conversion (Figure 3.17). However, much more hydrogenation products (MCH) are formed than acid-catalyzed products (ECP) due to the higher amounts of hydrogenation sites. Toluene can adsorb on acid sites and be hydrogenated by spill over of hydrogen from nearby metallic sites [64], but when the amount of spill over hydrogen is too much, the intermediate products of hydrogenation are fully hydrogenated before ring contraction of carbenium ions can occur. Even at low toluene conversions (16%) still the hydrogenation and hydrogenolysis products are predominant, as shown in Table 3.3.

Formation of xylene on Mo_2C and molybdenum-rich samples is more than on tungsten-rich samples. A significant variation in benzene selectivity can be observed among the samples. Since both benzene and xylene are formed; one can attribute the formation of some benzene to disproportionation of toluene. But, more benzene than

xylene is formed. Benzene can also form by dealkylation of toluene. The role of dealkylation is more pronounced, since two moles of toluene can form one mole of benzene and one mole of xylene. The amount of benzene formed is two times and four times higher than the amount of xylene formed for molybdenum carbide and tungsten-containing samples, as reported in Table 3.3.

As shown by TPR data, in the case of tungsten-containing samples, creation of carbon vacancies is easier than in the case of molybdenum carbide. It was also demonstrated that the presence of oxygen on the surface of tungsten carbide facilitates the removal of carbon from tungsten carbide compared to the pristine surface of W_2C [22]. These carbon vacancies serve as sites for dealkylation due to their affinity to carbon. A similar phenomenon has been reported for direct desulfurization by sulfur vacancies in sulfides [65] or deoxygenation by oxygen vacancies in oxide catalysts [66].

The change of catalytic activities of tungsten carbide with going up and down in temperature was investigated as it is reported in Figure 3.18. After heating up to 400 °C over 24 hours, some deactivation has been observed. When the reactor was cooled down under reaction conditions to 250 °C, the conversion was the same as at 400 °C after 24 hours.

Hydrogenation of toluene at 400 °C produces hydrogenation and hydrogenolysis products. It was shown that under high pressure of hydrogen at 400 °C carbon is removed from the surface [22]. In fact, the carbon on the surface of metal carbides is very dynamic, which can change their catalytic activities. If carbidic carbon is removed, the hydrogenation activity decreases, and if the amount of carbidic carbon increases, the hydrogenation activity increases. The loss in activity can be explained by the adsorption

of carbonaceous compounds on the surface or removing carbidic carbon from the surface. The gain in the activity could be due to an increase of carbidic carbon, which happens when more carbidic carbons are replaced compared to the initial situations. When carbide is heated up to 400 °C carbidic carbon is removed from the surface and when it is cooled down some carbonaceous compounds (reaction products or carbonaceous intermediates) fill the carbon vacancies which changes the hydrogenation activity of metals carbides, as explained before [22].

Surface decarburization and recarburization under reaction conditions has been reported before [67]. However, surface reconstruction under changing operating conditions and the importance of the carbon chemical potential (μ_c) on the surface Gibbs free energy of Mo_2C has been reported elsewhere [68]. Changing μ_c will change the surface termination of different planes from metallic to mixed metallic/carbon which indeed changes the catalytic activity of metal carbides, as different plane terminations show different adsorption/dissociation activities toward CO [69]. The surface reconstruction will cause a change in carbon coverage on the surface [70] and a change in the amount of carbon on the (sub)surface will change the heat of adsorption of reactants on the surface [40] that leads to a change in catalytic activity.

3.5 Conclusions

A series of single phase Mo-W carbides was synthesized by direct carburization of freeze-dried precursors. All samples were active for hydrogenation of toluene, and their activation energies were comparable with the activation energies of toluene hydrogenation on noble metals. Pure molybdenum carbide was the most active and pure tungsten carbide was the least active catalysts for hydrogenation of toluene.

All samples showed deactivation at 400 °C and 20 bar hydrogen pressure over 24 hours time on stream, molybdenum carbide lost 53% and MoWC-0.25 lost 17% of their initial activities. Initially, formation of light gases (C_1-C_6) dominates the product selectivities of all the samples, however with deactivation of the catalysts the product selectivities changed and MCH, benzene, ECP and xylene also formed. Pure molybdenum carbide showed high activity for hydrogenolysis, since it can be reduced more easily compared to the tungsten-containing samples. Formation of ECP and xylene are due to the presence of acid sites on the surface of oxycarbides. The active sites for formation of benzene were carbon vacancies, which were created at 400 °C under 20 bar hydrogen pressure. Tungsten carbide had lower hydrogenolysis activity and also produces more benzene compared to molybdenum carbide; however its rate of reaction was low. By adding molybdenum to the tungsten carbide, the rate of reaction increased while the product selectivities are similar to the tungsten carbide. Increasing the temperature to 400 °C and cooling down to 250 °C under reaction condition will cause activity enhancement due to surface reconstruction.

References

[1] R. B. Levy, M. Boudart, Platinum-Like Behavior of Tungsten Carbide in Surface Catalysis, Science, 181 (1973) 547-549.

[2] J. R. Kitchin, J. K. Nørskov, M. A. Barteau, J. G. Chen, Trends in the chemical properties of early transition metal carbide surfaces: A density functional study, Catalysis Today, 105 (2005) 66-73.

[3] H. A. Al-Megren, S. L. González-Cortés, T. Xiao, M. L. H. Green, A comparative study of the catalytic performance of Co-Mo and Co(Ni)-W carbide catalysts in the hydrodenitrogenation (HDN) reaction of pyridine, Applied Catalysis A: General, 329 (2007) 36-45.

[4] J. B. Claridge, A. P. E. York, A. J. Brungs, M. L. H. Green, Study of the Temperature-Programmed Reaction Synthesis of Early Transition Metal Carbide and

Nitride Catalyst Materials from Oxide Precursors, Chemistry of Materials, 12 (1999) 132-142.

[5] T. Xiao, H. Wang, A. P. E. York, V. C. Williams, M. L. H. Green, Preparation of Nickel-Tungsten Bimetallic Carbide Catalysts, Journal of Catalysis, 209 (2002) 318-330.

[6] T. C. Xiao, A. P. E. York, H. Al-Megren, C. V. Williams, H. T. Wang, M. L. H. Green, Preparation and Characterisation of Bimetallic Cobalt and Molybdenum Carbides, Journal of Catalysis, 202 (2001) 100-109.

[7] S. T. Oyama, C. Charles Yu, S. Ramanathan, Transition Metal Bimetallic Oxycarbides: Synthesis, Characterization, and Activity Studies, Journal of Catalysis, 184 (1999) 535-549.

[8] X. H. Wang, M. H. Zhang, W. Li, K. Y. Tao, A simple synthesis route and characterisation of Co_3Mo_3C, Dalton Transactions, (2007) 5165-5170.

[9] S. Chouzier, P. Afanasiev, M. Vrinat, T. Cseri, M. Roy-Auberger, One-step synthesis of dispersed bimetallic carbides and nitrides from transition metals hexamethylenetetramine complexes, Journal of Solid State Chemistry, 179 (2006) 3314-3323.

[10] M. Patel, J. Subrahmanyam, Synthesis of nanocrystalline molybdenum carbide (Mo_2C) by solution route, Materials Research Bulletin, 43 (2008) 2036-2041.

[11] C. Giordano, C. Erpen, W. Yao, B. Milke, M. Antonietti, Metal Nitride and Metal Carbide Nanoparticles by a Soft Urea Pathway, Chemistry of Materials, 21 (2009) 5136-5144.

[12] C. Giordano, C. Erpen, W. Yao, M. Antonietti, Synthesis of Mo and W Carbide and Nitride Nanoparticles via a Simple "Urea Glass" Route, Nano Letters, 8 (2008) 4659-4663.

[13] L. A. Bastos, W. R. Monteiro, M. A. Zacharias, G. M. da Cruz, J. A. J. Rodrigues, Preparation and Characterization of Mo/W Bimetallic Carbides by Using Different Synthesis Methods, Catalysis Letters, 120 (2008) 48-55.

[14] M. Arbib, E. Silberberg, F. Reniers, C. Buess-Herman, On the synthesis and characterization of mixed (Mo,W) carbides, Journal of the European Ceramic Society, 18 (1998) 1503-1511.

[15] L. Leclercq, M. Provost, H. Pastor, J. Grimblot, A. M. Hardy, L. Gengembre, G. Leclercq, Catalytic properties of transition metal carbides: I. Preparation and physical characterization of bulk mixed carbides of molybdenum and tungsten, Journal of Catalysis, 117 (1989) 371-383.

[16] T. H. Nguyen, T. V. Nguyen, Y. J. Lee, T. Safinski, A. A. Adesina, Structural evolution of alumina supported Mo–W carbide nanoparticles synthesized by precipitation from homogeneous solution, Materials Research Bulletin, 40 (2005) 149-157.

[17] A. El-Himri, P. Núñez, F. Sapiña, R. Ibanez, A. Beltran, J. M. A. Martí nez-Agudoc, Synthesis of new molybdenum-tungsten, vanadium-tungsten and vanadium-molybdenum-tungsten oxynitrides from freeze-dried precursors, Journal of Solid State Chemistry, 177 (2004) 2423-2431.

[18] A. El-Himri, F. Sapina, R. Ibanez, A. Beltran, Synthesis of new vanadium-chromium and chromium-molybdenum oxynitrides by direct ammonolysis of freeze-dried precursors, Journal of Materials Chemistry, 10 (2000) 2537-2541.

[19] A. El-Himri, M. Cairols, S. Alconchel, F. Sapina, R. Ibanez, D. Beltran, A. Beltran, Freeze-dried precursor-based synthesis of new vanadium-molybdenum oxynitrides, Journal of Materials Chemistry, 9 (1999) 3167-3171.

[20] C. C. Yu, S. Ramanathan, B. Dhandapani, J. G. Chen, S. T. Oyama, Bimetallic Nb-Mo Carbide Hydroprocessing Catalysts:Synthesis, Characterization, and Activity Studies, The Journal of Physical Chemistry B, 101 (1997) 512-518.

[21] L. Leclercq, M. Provost, H. Pastor, G. Leclercq, Catalytic properties of transition metal carbides: II. Activity of bulk mixed carbides of molybdenum and tungsten in hydrocarbon conversion, Journal of Catalysis, 117 (1989) 384-395.

[22] A. Mehdad, Mixed Metal Carbides: Understanding the Synthesis, Surface Properties and Catlytic Activities, PhD Dissertation, The University of Oklahoma (2015).

[23] P. Arnoldy, J. C. M. De Jonge, J. A. Moulijn, Temperature-programed reduction of molybdenum(VI) oxide and molybdenum(IV) oxide, The Journal of Physical Chemistry, 89 (1985) 4517-4526.

[24] G. Leclercq, M. Kamal, J. M. Giraudon, P. Devassine, L. Feigenbaum, L. Leclercq, A. Frennet, J. M. Bastin, A. Löfberg, S. Decker, M. Dufour, Study of the Preparation of Bulk Powder Tungsten Carbides by Temperature Programmed Reaction with CH_4+ H_2 Mixtures, Journal of Catalysis, 158 (1996) 142-169.

[25] Z. M. Hanafi, M. A. Khilla, M. H. Askar, The thermal decomposition of ammonium heptamolybdate, Thermochimica Acta, 45 (1981) 221-232.

[26] M. J. G. Fait, H. J. Lunk, M. Feist, M. Schneider, J. N. Dann, T. A. Frisk, Thermal decomposition of ammonium paratungstate tetrahydrate under non-reducing conditions: Characterization by thermal analysis, X-ray diffraction and spectroscopic methods, Thermochimica Acta, 469 (2008) 12-22.

[27] A. O. Kalpakli, A. Arabaci, C. Kahruman, I. Yusufoglu, Thermal decomposition of ammonium paratungstate hydrate in air and inert gas atmospheres, International Journal of Refractory Metals and Hard Materials, 37 (2013) 106-116.

[28] T. Xiao, A. Hanif, A. P. E. York, J. Sloan, M. L. H. Green, Study on preparation of high surface area tungsten carbides and phase transition during the carburisation, Physical Chemistry Chemical Physics, 4 (2002) 3522-3529.

[29] J. M. Giraudon, P. Devassine, J. F. Lamonier, L. Delannoy, L. Leclercq, G. Leclercq, Synthesis of Tungsten Carbides by Temperature-Programmed Reaction with CH_4–H_2 Mixtures. Influence of the CH_4 and Hydrogen Content in the Carburizing Mixture, Journal of Solid State Chemistry, 154 (2000) 412-426.

[30] A. B. Kehoe, D. O. Scanlon, G.W. Watson, Role of Lattice Distortions in the Oxygen Storage Capacity of Divalently Doped CeO_2, Chemistry of Materials, 23 (2011) 4464-4468.

[31] D. O. Scanlon, B. J. Morgan, G. W. Watson, The origin of the enhanced oxygen storage capacity of $Ce_{1-x}(Pd/Pt)_xO_2$, Physical Chemistry Chemical Physics, 13 (2011) 4279-4284.

[32] A. F. Lamic, C. H. Shin, G. Djéga-Mariadassou, C. Potvin, Characterization of New Bimetallic Oxycarbide ($MoWC_{0.5}O_{0.6}$) for Bifunctional Isomerization of n-Heptane, Catalysis Letters, 107 (2006) 89-94.

[33] L. Volpe, M. Boudart, Compounds of molybdenum and tungsten with high specific surface area: II. Carbides, Journal of Solid State Chemistry, 59 (1985) 348-356.

[34] K. T. Jung, W. B. Kim, C. H. Rhee, J. S. Lee, Effects of Transition Metal Addition on the Solid-State Transformation of Molybdenum Trioxide to Molybdenum Carbides, Chemistry of Materials, 16 (2003) 307-314.

[35] C. Bouchy, S. B. Derouane-Abd Hamid, E. G. Derouane, A new route to the metastable FCC molybdenum carbide α-MoC_{1-x}, Chemical Communications, (2000) 125-126.

[36] P. Delporte, F. D. R. Meunier, C. Pham-Huu, P. Vennegues, M. J. Ledoux, J. Guille, Physical characterization of molybdenum oxycarbide catalyst; TEM, XRD and XPS, Catalysis Today, 23 (1995) 251-267.

[37] W. Xu, P. Ramirez, D. Stacchiola, J. Rodriguez, Synthesis of α-MoC_{1-x} and β-MoC_y Catalysts for CO_2 Hydrogenation by Thermal Carburization of Mo-oxide in Hydrocarbon and Hydrogen Mixtures, Catalysis Letters, 144 (2014) 1418-1424.

[38] K. J. Leary, J. N. Michaels, A. M. Stacy, The use of TPD and TPR to study subsurface mobility: Diffusion of oxygen in Mo_2C, Journal of Catalysis, 107 (1987) 393-406.

[39] T. Wang, Y. W. Li, J. Wang, M. Beller, H. Jiao, Dissociative Hydrogen Adsorption on the Hexagonal Mo_2C Phase at High Coverage, The Journal of Physical Chemistry C, 118 (2014) 8079-8089.

[40] A. J. Medford, A. Vojvodic, F. Studt, F. Abild-Pedersen, J. K. Nørskov, Elementary steps of syngas reactions on $Mo_2C(001)$: Adsorption thermochemistry and bond dissociation, Journal of Catalysis, 290 (2012) 108-117.

[41] A. S. Rocha, A. B. Rocha, V. T. da Silva, Benzene adsorption on Mo_2C: A theoretical and experimental study, Applied Catalysis A: General, 379 (2010) 54-60.

[42] B. Zhou, X. Liu, J. Cuervo, D. Salahub, Density functional study of benzene adsorption on the α-$Mo_2C(0001)$ surface, Structural Chemistry, 23 (2012) 1459-1466.

[43] X. Liu, A. Tkalych, B. Zhou, A.M. Köster, D.R. Salahub, Adsorption of Hexacyclic C_6H_6, C_6H_8, C_6H_{10}, and C_6H_{12} on a Mo-Terminated α-Mo_2C (0001) Surface, The Journal of Physical Chemistry C, 117 (2013) 7069-7080.

[44] J. S. Choi, J. M. Krafft, A. Krzton, G. Djéga-Mariadassou, Study of Residual Oxygen Species over Molybdenum Carbide Prepared During In Situ DRIFTS Experiments, Catalysis Letters, 81 (2002) 175-180.

[45] M. L. Frauwallner, F. López-Linares, J. Lara-Romero, C. E. Scott, V. Ali, E. Hernández, P. Pereira-Almao, Toluene hydrogenation at low temperature using a molybdenum carbide catalyst, Applied Catalysis A: General, 394 (2011) 62-70.

[46] J. W. Thybaut, M. Saeys, G. B. Marin, Hydrogenation kinetics of toluene on Pt/ZSM-22, Chemical Engineering Journal, 90 (2002) 117-129.

[47] M. Vasiur Bahaman, M. Albert Vannice, The hydrogenation of toluene and o-, m-, and pxylene over palladium: I. Kinetic behavior and o-xylene isornerization, Journal of Catalysis, 127 (1991) 251-266.

[48] J. S. Choi, G. Bugli, G. Djéga-Mariadassou, Influence of the Degree of Carburization on the Density of Sites and Hydrogenating Activity of Molybdenum Carbides, Journal of Catalysis, 193 (2000) 238-247.

[49] R. R. Oliveira Jr, A. S. Rocha, V. Teixeira da Silva, A. B. Rocha, Investigation of hydrogen occlusion by molybdenum carbide, Applied Catalysis A: General, 469 (2014) 139-145.

[50] B. Frank, T. P. Cotter, M. E. Schuster, R. Schlögl, A. Trunschke, Carbon Dynamics on the Molybdenum Carbide Surface during Catalytic Propane Dehydrogenation, Chemistry – A European Journal, 19 (2013) 16938-16945.

[51] S. K. Bej, C. A. Bennett, L. T. Thompson, Acid and base characteristics of molybdenum carbide catalysts, Applied Catalysis A: General, 250 (2003) 197-208.

[52] F. H. Ribeiro, M. Boudart, R. A. Dalla Betta, E. Iglesia, Catalytic reactions of n-Alkanes on β-W_2C and WC: The effect of surface oxygen on reaction pathways, Journal of Catalysis, 130 (1991) 498-513.

[53] E. Iglesia, F. H. Ribeiro, M. Boudart, J. E. Baumgartner, Synthesis, characterization, and catalytic properties of clean and oxygen-modified tungsten carbides, Catalysis Today, 15 (1992) 307-337.

[54] A. Muller, V. Keller, R. Ducros, G. Maire, Catalytic activity and XPS surface determination of tungsten carbide for hydrocarbon reforming. Influence of the oxygen, Catalysis Letters, 35 (1995) 65-74.

[55] F. H. Ribeiro, R. A. Dalla Betta, M. Boudart, J. Baumgartner, E. Iglesia, Reactions of neopentane, methylcyclohexane, and 3,3-dimethylpentane on tungsten carbides: The effect of surface oxygen on reaction pathways, Journal of Catalysis, 130 (1991) 86-105.

[56] E. Iglesia, J. E. Baumgartner, F. H. Ribeiro, M. Boudart, Bifunctional reactions of alkanes on tungsten carbides modified by chemisorbed oxygen, Journal of Catalysis, 131 (1991) 523-544.

[57] G. Boskovic, P. Putanov, K. Foettinger, H. Vinek, Activation of Mo-based catalyst for paraffins isomerization, Applied Catalysis A: General, 317 (2007) 175-182.

[58] M. J. Ledoux, P. Del Gallo, C. Pham-Huu, A. P. E. York, Molybdenum oxycarbide isomerization catalysts for cleaner fuel production, Catalysis Today, 27 (1996) 145-150.

[59] A. F. Lamic, T. L. H. Pham, C. Potvin, J. M. Manoli, G. Djéga-Mariadassou, Kinetics of bifunctional isomerization over carbides (Mo, W), Journal of Molecular Catalysis A: Chemical, 237 (2005) 109-114.

[60] A. F. Lamic, C. H. Shin, G. Djéga-Mariadassou, C. Potvin, Characterization of Mo_2C–WO_2 composite catalysts for bifunctional isomerization: A new pulse method to quantify acid sites, Applied Catalysis A: General, 302 (2006) 5-13.

[61] S. J. Ardakani, X. Liu, K. J. Smith, Hydrogenation and ring opening of naphthalene on bulk and supported Mo_2C catalysts, Applied Catalysis A: General, 324 (2007) 9-19.

[62] K. Shimizu, T. Sunagawa, C. R. Vera, K. Ukegawa, Catalytic activity for synthesis of isomerized products from benzene over platinum-supported sulfated zirconia, Applied Catalysis A: General, 206 (2001) 79-86.

[63] J. Wang, Q. Li, J. Yao, The effect of metal–acid balance in Pt-loading dealuminated Y zeolite catalysts on the hydrogenation of benzene, Applied Catalysis A: General, 184 (1999) 181-188.

[64] S. D. Lin, M.A. Vannice, Hydrogenation of Aromatic Hydrocarbons over Supported Pt Catalysts .II. Toluene Hydrogenation, Journal of Catalysis, 143 (1993) 554-562.

[65] M. Egorova, R. Prins, Hydrodesulfurization of dibenzothiophene and 4,6-dimethyldibenzothiophene over sulfided NiMo/γ-Al_2O_3, CoMo/γ-Al_2O_3, and Mo/γ-Al_2O_3 catalysts, Journal of Catalysis, 225 (2004) 417-427.

[66] T. Pham, D. Shi, D. Resasco, Kinetics and Mechanism of Ketonization of Acetic Acid on Ru/TiO_2 Catalyst, Topics in Catalysis, 57 (2014) 706-714.

[67] L. Delannoy, J. M. Giraudon, P. Granger, L. Leclercq, G. Leclercq, Chloropentafluoroethane Hydrodechlorination over Tungsten Carbides: Influence of Surface Stoichiometry, Journal of Catalysis, 206 (2002) 358-362.

[68] T. Wang, X. Liu, S. Wang, C. Huo, Y. W. Li, J. Wang, H. Jiao, Stability of β-Mo_2C Facets from ab Initio Atomistic Thermodynamics, The Journal of Physical Chemistry C, 115 (2011) 22360-22368.

[69] T. Wang, Q. Luo, Y. W. Li, J. Wang, M. Beller, H. Jiao, Stable surface terminations of orthorhombic Mo_2C catalysts and their CO activation mechanisms, Applied Catalysis A: General, 478 (2014) 146-156.

[70] G. G. Asara, A. Roldan, J.M. Ricart, J.A. Rodriguez, F. Illas, N.H. de Leeuw, New Insights into the Structure of the C-Terminated β-Mo_2C (001) Surface from First-Principles Calculations, The Journal of Physical Chemistry C, 118 (2014) 19224-19231.

4. Mixed molybdenum-niobium carbides catalyst: synthesis, characterization and catalytic activity

4.1 Introduction

The catalytic behavior of early transition metals will change when carbon is inserted into their lattice, and metal carbides are formed. The catalytic activity of metal carbides can be further tuned by adding nonmetals (more carbon/oxygen) or another metal into their structures or on their surfaces.

It was already demonstrated that different methods of passivation and reduction of molybdenum and tungsten carbide can change their catalytic activities. This change in catalytic activities is due to the change in the amounts of carbon and oxygen (nonmetal) on the (sub) surface of metal carbides [1]. Molybdenum and tungsten carbide have strong metallic behavior. As a result, hydrogenation and hydrogenolysis products are the predominant products. On the other hand, very active monometallic carbides such as Mo_2C lose their activities over time on stream under high pressure and high temperature reaction conditions. One solution to tune this strong metallic behavior and increase the stability of metal carbides at high temperature and high pressure is to prepare mixed metal carbides.

Mixed metal carbides show a catalytic behavior that differs from that of their monometallic counterparts. Mo-W carbide is a better reforming catalyst [2], and alumina-supported Mo-Nb carbides have better HDS and HDN activities per active site compared to the commercial sulfided Ni-Mo/Al_2O_3 [3]. Mo-Ni and Mo-Co carbides are active for hydrotreating [4, 5]. The single phase mixed metal oxycarbides of Mo-Nb are

more active for HDS and HDN and show better activity compared to non-single-phase mixed metal carbides [6].

Single phase Mo-W carbides were synthesized and tested for hydrogenation of toluene [7]. Molybdenum carbide has stronger metallic behavior than tungsten carbide, and it is easier to reduce its surface than that of tungsten carbide. The combination of these two metals in mixed Mo-W carbides still results in good metallic activity (hydrogenation/hydrogenolysis) with not much acid-catalyzed (ring contraction) products. The reason for that is the metallic sites suppress the acid sites by fully hydrogenating the intermediate (methylcyclohexene).

Niobium (oxy)carbides have been tried for reactions such as hydrotreating [8-10], or hydrogenation and isomerization [11, 10].

The goal of this chapter is to synthesize series of mixed metal carbides, that have bifunctional activities. In fact, series of mixed metal carbides will be prepared that do not have much metallic behavior to surpass the acidity. Mo_2C and NbC have been chosen to fulfill this goal. Mo_2C has very strong metallic behavior while NbC is almost inactive for hydrogenation. Molybdenum and niobium oxides have different redox properties (niobium oxide needs a higher temperature to be reduced compared to the molybdenum oxide). Their different affinities toward oxygen will be important when they form oxycarbides for acid-catalyzed reactions.

4.2 Experimental section

4.2.1 Catalyst and materials

Ammonium heptamolybdate (ACS reagent, 81-83% MoO_3, Sigma Aldrich) was dissolved in 0.5 M oxalic acid (anhydrous, purity>0.99%, Sigma-Aldrich), and

ammonium niobate (V) oxalate hydrate (99.99%, Aldrich) was dissolved in water. The volume of the water was adjusted to a total volume of 100 ml. The amount of each salt was adjusted to have total salts weight of 4 g with molar ratios of Mo/Nb=0, 1, 2, 4, 6, 21 and pure molybdenum. The two solutions containing salts were mixed together and stirred for 15 minutes. The clear solution was transferred to a 250 ml Teflon liner of a stainless steel autoclave. The autoclave was heated to 175 ℃ for 3 days under static conditions. After 3 days, the solution was centrifuged to separate any solids from the solution. The solid was washed three times with water, and then dried over night at 80 ℃ in a chemical oven.

Another series of samples was prepared by the freeze-drying method. Different amounts of ammonium heptamolybdate and ammonium niobate oxalatehydrate were dissolved separately in water and mixed together to have various metal ratios with a final total metal concentration of 0.1 M. The amounts of salts were adjusted to have a final solid weight of 1 g in the solution. The solution was added dropwise to liquid nitrogen, and the solid was freeze-dried at a pressure of 110 µtorr in an ATR FD3.0 freeze drier. Freeze-dried samples (pure molybdenum, pure niobium and a mixed metal sample with Mo/Nb= 7) were calcined in 80% air (zero grade, Airgas) in argon (UHP, Airgas) with a total flow rate of 50 ml/min. The temperature was increased from 40 to 600 °C with a temperature ramp of 5 K/min, and was held at the final temperature for 30 minutes.

Precursors were carburized in and monitored by a thermogravimetry analyzer (TG) connected to an online MS (Netzsch STA 449 F1 and QMS 403 C). Carburization gases were 20 ml/min of methane (UHP, Airgas), 70 ml/min H_2 and 10 ml/min argon

(both ultra high purity from Airgas); all flow rates at STP. Synthesis of all metal carbides was carried out at atmospheric pressure by heating from 40 to 450 °C at 5 K/min and from 450 °C to the final temperature at 2 K/min. Temperature was held at the final temperature until no weight change was observed with the TG and formation of CO was terminated. All metal carbides were cooled down to room temperature under flow of Ar. Mass-charge ratios of 2-78 were scanned with online MS. Before exposure of carbides to the ambient, they were passivated isothermally at 40 °C with air (zero grade, Airgas) diluted in Ar (UHP, Airgas). The concentration of oxygen was increased from 0.1% (10 hours) to 1% (9 hours) and 16% (2 hours) in Ar, with the total flow rate between 60 and 402 ml/min. Air and hydrogen were purified by flowing them through a moisture trap (Agilent, MT400-2) and argon was purified by flowing through a dual trap for moisture and oxygen removal (Z-Pure Dual Purifier).

4.2.2 Temperature-programmed reduction (TPR)

The TPR experiments were carried out in the TG-MS on about 11 mg of passivated sample. The total flow rate was 100 ml/min with 80% hydrogen in argon. The temperature was set to 40 °C for 10 minutes and then increased from 40 to 700 °C with a temperature ramp of 10 K/min. The gas phase products were monitored by online MS.

4.2.3 Reaction

The reactor was a ¼ inch stainless steel flow reactor equipped with an Eldex liquid feed pump. The feed was 0.01 ml/min of liquid toluene (99.5%, Mallinckrodt Chemicals) and 75 ml/min STP H_2 (Ultra high purity, Airgas). The reactor total pressure was 20 bar, which was controlled by a back pressure valve. Samples were tested at

temperatures of 250 °C and 400 °C. The reactor was loaded with different amounts of passivated carbides mixed with SiC (Aldrich, 200-450 mesh) to avoid channeling and local heating. The temperature was controlled using a thermocouple inside the reactor at the bottom of the catalyst bed. All samples were reduced at atmospheric pressure in 150 ml/min of H_2 at 300 °C for one hour before the catalytic reaction. After reduction, the reactor was cooled to 250 °C and pressurized to 20 bar, then the feed was introduced to the reactor and samples of the effluent were collected.

Then the reactor was heated to 400 °C and was held at this temperature for 24 hours, during this time samples were taken. After that the reactor was cooled down to 250 °C and some data points were collected. Products were analyzed every 30 minutes using an online HP 5890 GC with a flame ionization detector (FID), equipped with a 30 m, 0.32 mm GASPRO column. The reaction was carried out in the gas phase, and transfer lines to the GC were heated to ensure that no condensation occurred before the GC. The GC temperature program was, 5 minutes isothermal at 60 °C, then with a temperature ramp of 10 K/min to the final temperature of 240 °C, which was held for 4 minutes. Conversion of toluene is defined as the difference between the moles of toluene in the feed and in the product divided by moles of toluene in the feed. Selectivity of compound *i* was calculated as number of moles of compound *i* times its carbon number divided by total moles of products times their carbon number.

4.2.4 Characterization

The bulk structure of the samples was characterized by X-ray diffraction (XRD) using a Bruker D8 instrument operating with Cu Kα radiation. The samples were measured in reflection geometry, and Ni metal powder (Matheson Coleman & Bell, 200

mesh) was used for a reference. Diffractograms were collected by scanning in steps of 0.05 in 2θ over the angular range of 20-90°. The lattice parameters of each product were obtained by fitting the diffractograms using Powdercell software. The carbon content of the samples was measured by combustion analysis in a CE-440 Elemental Analyzer. The ratios of Mo/Nb were determined by energy-dispersive X-ray spectroscopy (EDS) on a JEOL JSM-840A scanning electron microscope with a Kevex X-ray analyzer and IXRF software and digital imaging capability. The operating voltage was 15 kV, and the energy range of the analysis was 0-9 keV. BET surface areas were measured using a Micromeritics ASAP 2020 and N_2 at 77 K. Pore size distributions were determined by applying the BJH method to nitrogen desorption isotherms. Before measuring the surface area, the samples were degassed at 350 °C for four hours. The number of metal sites was measured by CO chemisorption; prior to CO chemisorption, samples were reduced in H_2 at 350 °C, then they were cooled down to 35 °C for CO chemisorption.

4.3 Results

4.3.1 Synthesis of metal carbides

Precursors for carburization were prepared by two methods: hydrothermal synthesis (HT) and freeze drying (FD). The yield of products (weight of final solid/ weight of solid loaded) for the HT method was between 20-30% while the FD method produced yields of about 95%. The precursors prepared by the HT method were directly carburized, whereas the precursors prepared by the FD method were first calcined and then carburized.

4.3.1.1 Carburization of precursors synthesized by hydrothermal synthesis

The weight losses and MS data during carburization are reported in Figures 4.1 and 4.2.

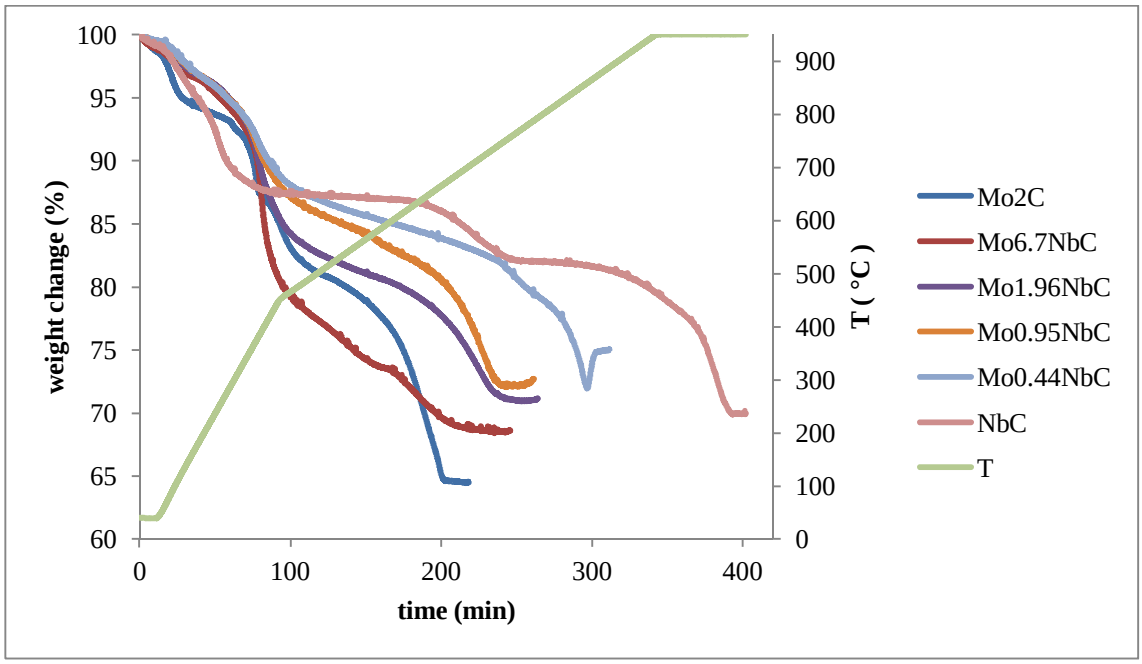

Figure 4.1: Direct carburization of HT precursors from bottom to top with Mo/Nb ratios of: pure molybdenum, 6.7, 1.96, 0.95, 0.44 and 0. Gas phase mixture 20% CH_4/70%H_2/10% Ar.

The pure molybdenum precursor has the highest weight loss and reaches its final weight at lower temperatures compared to the other samples. The pure niobium precursor needs a very high temperature (950 ℃) for carbide synthesis. However, addition of molybdenum significantly decreases the synthesis temperature of the niobium-containing carbides. For the samples rich in molybdenum, the formation of CO happens simultaneously with the formation of water, while for the samples rich in niobium, CO starts to form at high temperatures without any water formation.

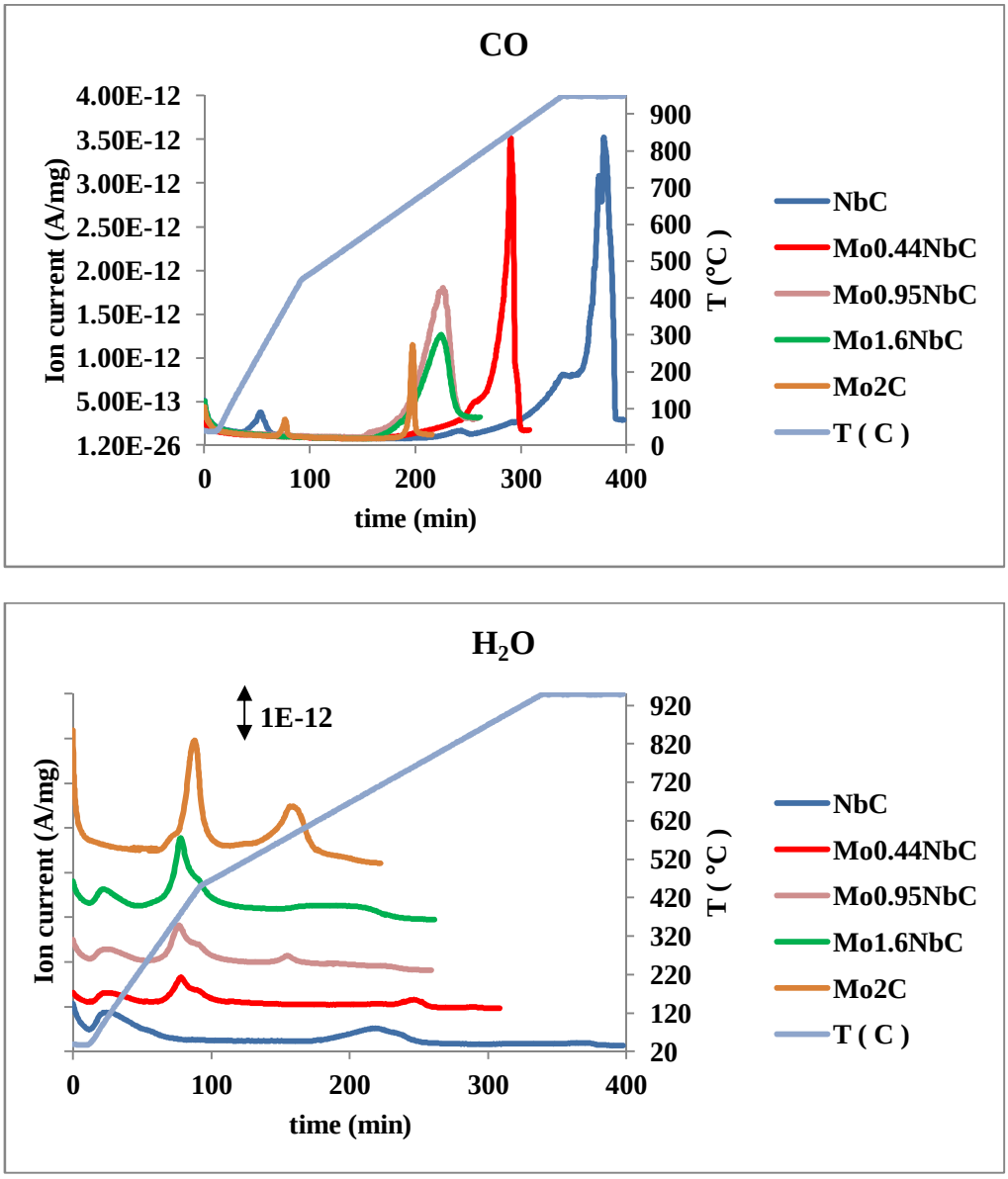

Figure 4.2: MS data for carburization of precursors from hydrothermal synthesis. Water formation (bottom) and CO formation (top). Gas phase mixture 20% CH_4/70%H_2/10% Ar.

Adding molybdenum to the niobium (at Mo/Nb=0.44) causes CO formation to happen at about 150 K lower temperature than during synthesis of NbC. Among all the samples, this is the only one that starts to quickly build up carbon on the surface when it

reaches its minimum weight. For the catalytic test and the characterization measurements the carburization was stopped before this sample started to build up coke, which happens when the CO peak reaches its maximum.

4.3.1.2 Carburization of calcined freeze-dried precursors

Freeze-dried molybdenum (Mo_FD), niobium (Nb_FD) and molybdenum-niobium (Mo_7Nb-FD) with a metal ratio of 6 (Mo/Nb=7 loaded, EDS shows Mo/Nb=5.9±0.6, we refer to it as Mo_6Nb) were calcined in the TG-MS apparatus to 500 and 600 °C, respectively with a temperature ramp of 5 K/min and were held at the final temperature for 30 minutes until the weight loss leveled off and no more gas phase products were observed with the online MS. The XRD data for the calcined samples are reported in Figure 4.3, and results indicate that the Mo_6Nb oxide has the same structure as MoO_3. The calcined samples were carburized in the TG-MS apparatus, as reported in Figures 4.4 and 4.5.

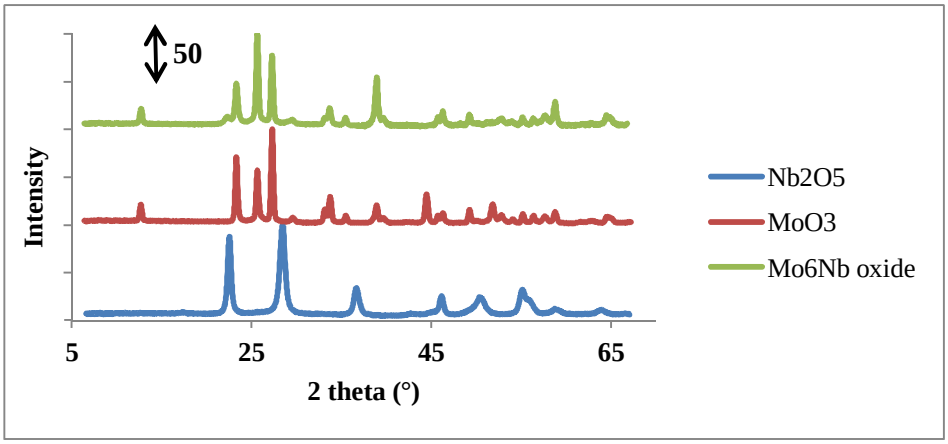

Figure 4.3: Calcination of Nb-FD (600 °C), Mo-FD (500 °C) and Mo_6Nb_FD (600 °C) in 80% air/Ar with temperature ramp of 5 K/min.

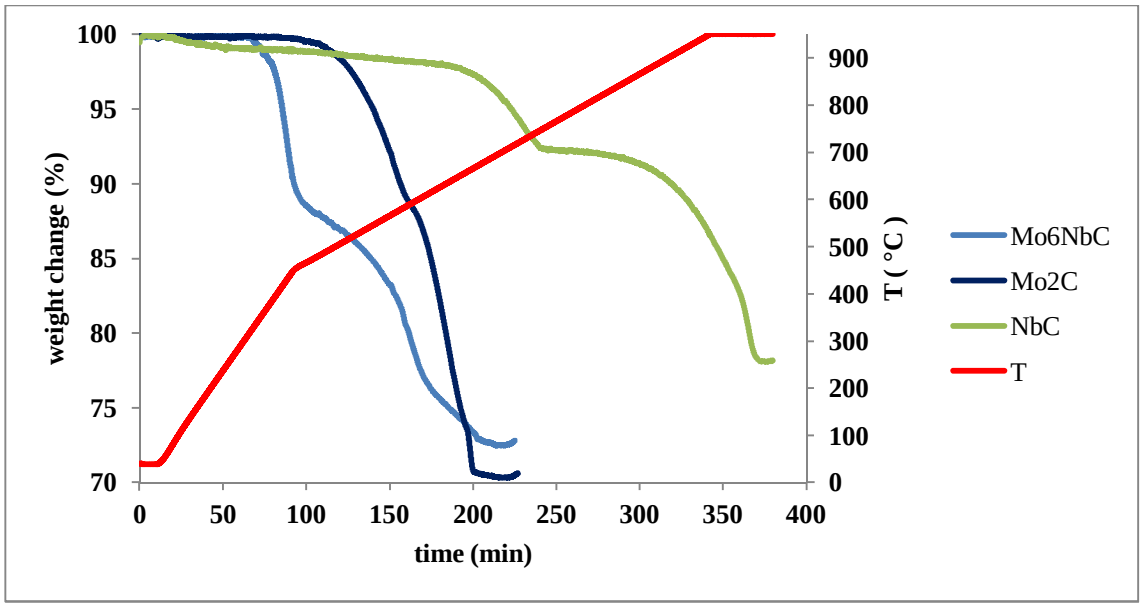

Figure 4.4: Carburization of calcined precursors, from left to right: oxides of Mo_6Nb, Mo and Nb. Gas phase mixture 20% CH_4/70%H_2/10% Ar.

The results show that the carburization of pure niobium oxide needs a very high temperature (950 °C), whereas carburization of the mixed metal oxide of Mo_6Nb stoichiometry needs the lowest temperature for synthesis. For carburization of all oxides, there are two water peaks, and Mo_6Nb oxide is reduced at lower temperatures compared to its mono-metallic counterparts.

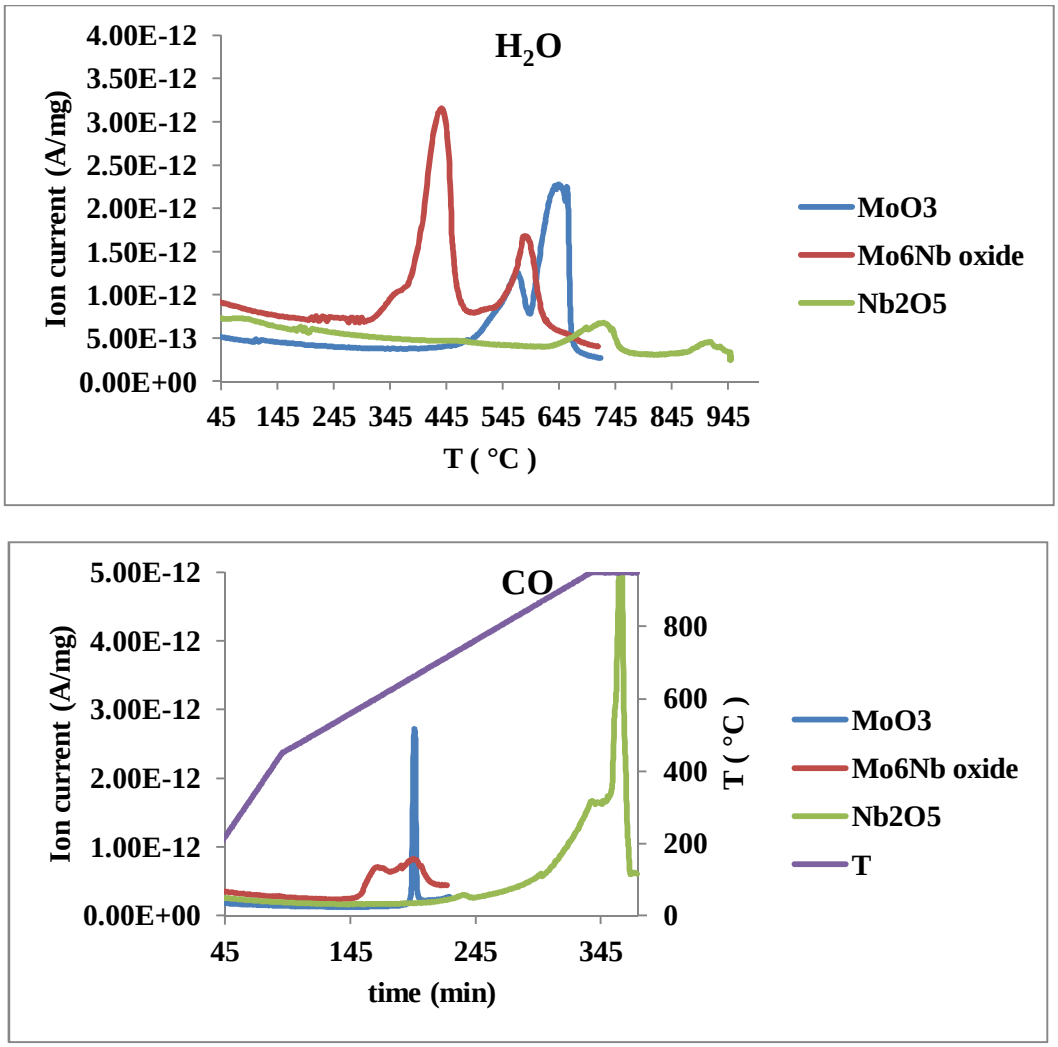

Figure 4.5: Carburization of calcined freeze-dried precursors. Gas phase mixture 20% CH_4/70%H_2/10% Ar.

The first water peaks are observed at 450, 550 and 750 °C for reduction to $Mo_6NbO_{11.1}$, $MoO_{2.3}$ and $NbO_{1.58}$ respectively. The second water peaks appear at higher temperatures, in the case of molybdenum-containing samples simultaneously with the evolution of CO, whereas for the pure niobium oxide CO forms without any water formation. During the carburization of the sample containing only molybdenum, there is a sharp CO peak at about 650 °C and CO forms when molybdenum oxide is reduced to

$MoO_{0.79}$. Carburization of Mo_6Nb oxide results in two broad peaks of CO at 550 and 650 °C and CO forms when the starting oxide is reduced to $Mo_6NbO_{6.01}$. In the carburization of pure niobium oxide, there are two CO peaks, a small CO peak is observed with the first peak of water at 750 °C and a large peak of CO is observed around 950 °C. During carburization of Nb_2O_5, at 800 °C ethylene starts to form after formation of the first water peak and its formation rate increases at higher temperatures.

For the molybdenum-containing samples, the water peaks are larger than the CO peak, whereas in the case of pure niobium the CO peak is larger than the water peaks, and its size is larger than that of the CO peak of the molybdenum-containing samples. Considering MoO_3, Nb_2O_5 and (MoO_3+Nb_2O_5) as starting materials and Mo_2C, NbC and $(Mo_6Nb)C_{3.5}$ as the final products, the experimental weight losses are 29.59, 20.77 and 27.51% which are very close to the theoretical values of 29.39, 21.06 and 26.58%.

4.3.2 Characterization of the materials

The structures of the samples were analyzed by XRD. The diffractograms are reported in Figure 4.6. All niobium-containing samples prepared by the HT method have the cubic structure of NbC (ICDD: 00-038-1364), Figure 4.6d-h. Pure molybdenum carbide (Fig.4.6k) and Mo_6Nb carbide prepared by carburization of the FD precursor (Fig.4.6j) have hexagonal structure as reported for Mo_2C (ICDD: 00-035-0787). $Mo_{6.7}Nb$ carbide prepared by carburization of a HT precursor with an intended ratio of Mo/Nb=21 consists of two phases of NbC and Mo_2C as reported in Fig.4.6i. The diffractograms were fit using Powdercell software and a curve based on Vegard's law was generated by plotting the lattice parameter of the samples versus the niobium mole fraction, as shown in Figure 4.7.

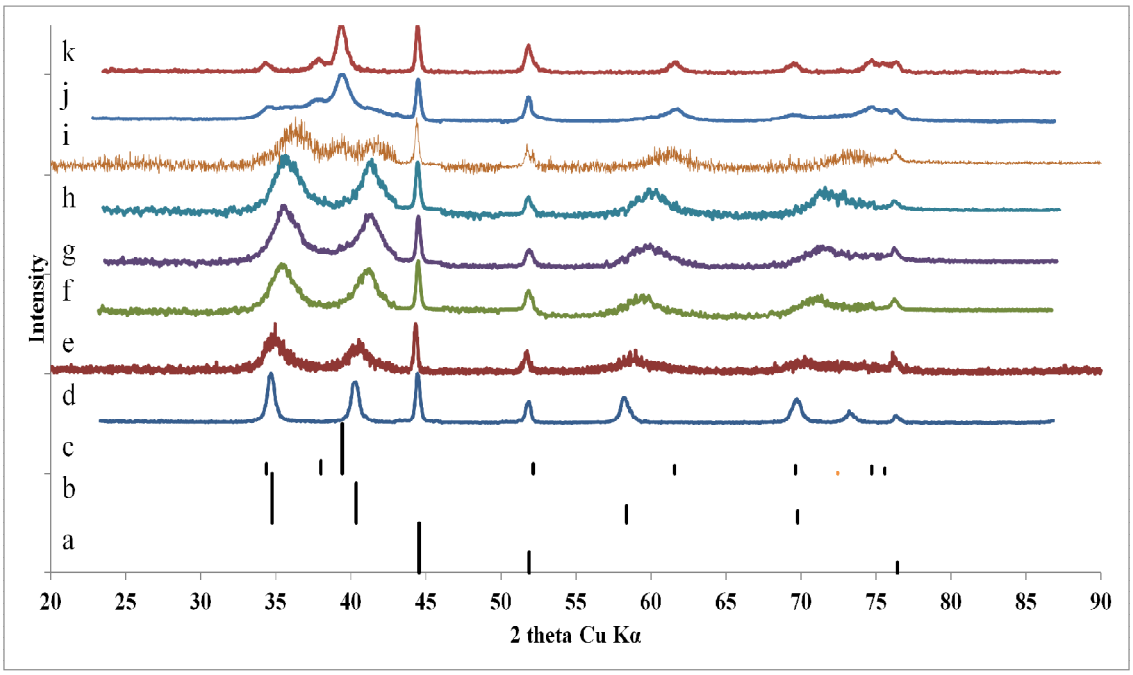

Figure 4.6: XRD data for Mo-Nb carbide series. (a) Ni (ICDD:00-004-0850) (b) NbC (ICDD:00-038-1364) (c) Mo_2C (ICDD: 00-035-0787) (d) NbC (e) $Mo_{0.44}NbC$ (f) $Mo_{0.95}NbC$ (g) $Mo_{1.96}NbC$ (h) $Mo_{1.6}NbC$ (i) $Mo_{6.7}NbC$ (j) Mo_6NbC (k) Mo_2C

Metal ratios, carbon content, surface areas, CO site densities, weight gains after passivation, amounts of oxygen left on the surface after reduction and pore size values are reported in Table 4.1. The N_2 physisorption isotherms were type IV with a pore size distribution in the mesoporosity range. The metal ratios of the samples are plotted versus the ratios in the synthesis solution in Figure 4.8.

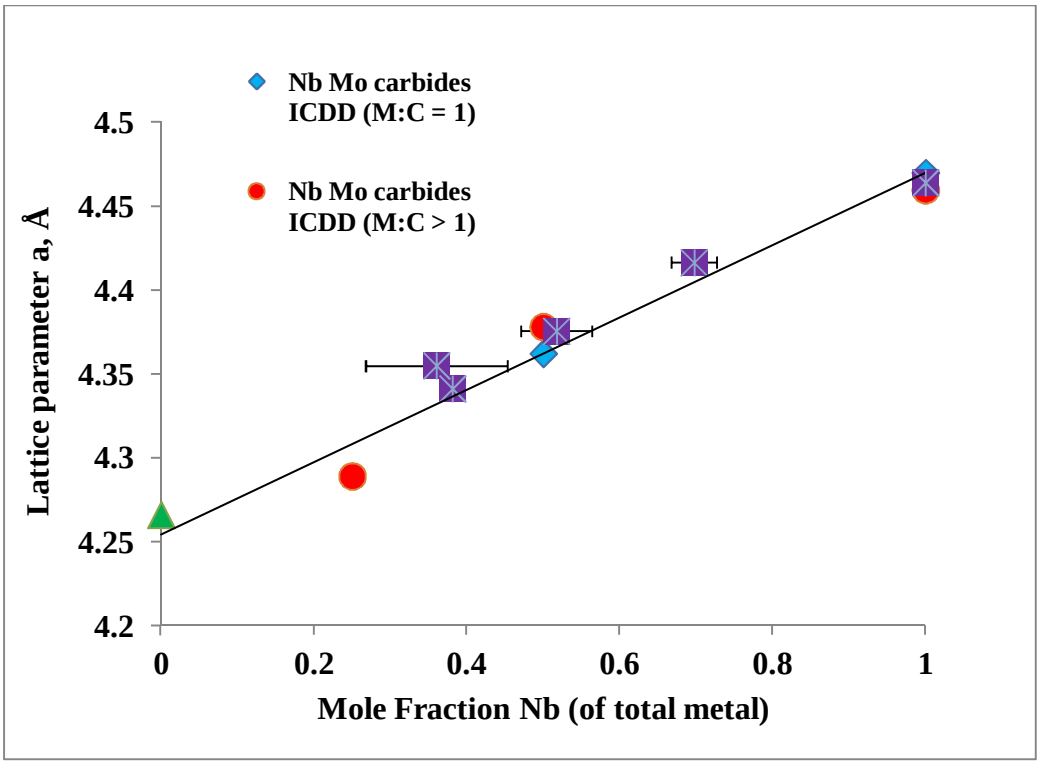

Figure 4.7: Lattice parameter of Mo-Nb carbides with NbC structure vs. mole fraction of niobium. Δ $MoC_{0.66}$, o (Nb/C >1), ◊ (Nb/C=1)

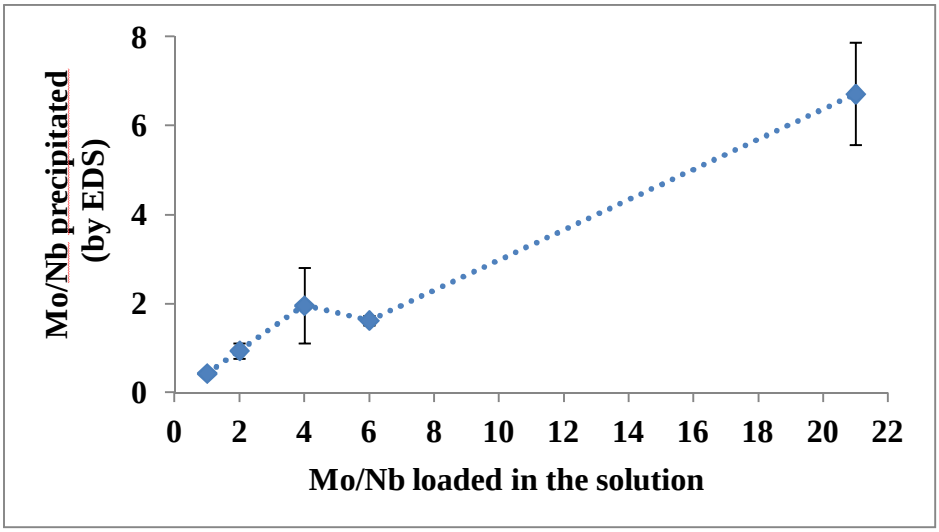

Figure 4.8: Mo/Nb precipitated during hydrothermal synthesis vs. Mo/Nb loaded in the solution

Table 4.1: Characterization data for Mo-Nb carbide samples

Sample	T_f (°C)	%Wt carbon content	%weight gain after passivation	%oxygen left on the surface after reduction	SA (m^2/g)	BJH volume (cm^3/g)	BJH pore diameter (Å)	CO site density ($\mu mol/m^2$)
Mo_2C	650	5.0±0.2	2.49	1.99	16.5	0.052	111.9	1.12
Mo_6NbC**	650	5.1±0.11	2.85	2.27	23.7	0.079	119.5	0.63
$Mo_{1.6}NbC$	700	5.4±0.2	5.67	4.24*	58.4	0.166	113.6	0.23
$Mo_{0.95}NbC$	700	5.8±0.1	5.80	4.43*	102.2	0.134	49.7	0.08
$Mo_{0.44}NbC$	840	8.2±0.1	1.70	1.42	57.5	0.18	99.5	0.04
NbC	950	12.0±0.2	0.00	0.00	16.7	0.088	165.2	0.00

* Amount of oxygen left on the surface (weight was measured after removal of the oxide layer and ethane desorption)

** Carburization of freeze dried precursor

4.3.3 Reduction of samples

Temperature-programmed reduction (TPR) in 80%H_2/Ar at atmospheric pressure was used to investigate the temperature range necessary to remove oxygen and carbon from the (sub) surface of the samples. The TPR results are shown in Figure 4.9.

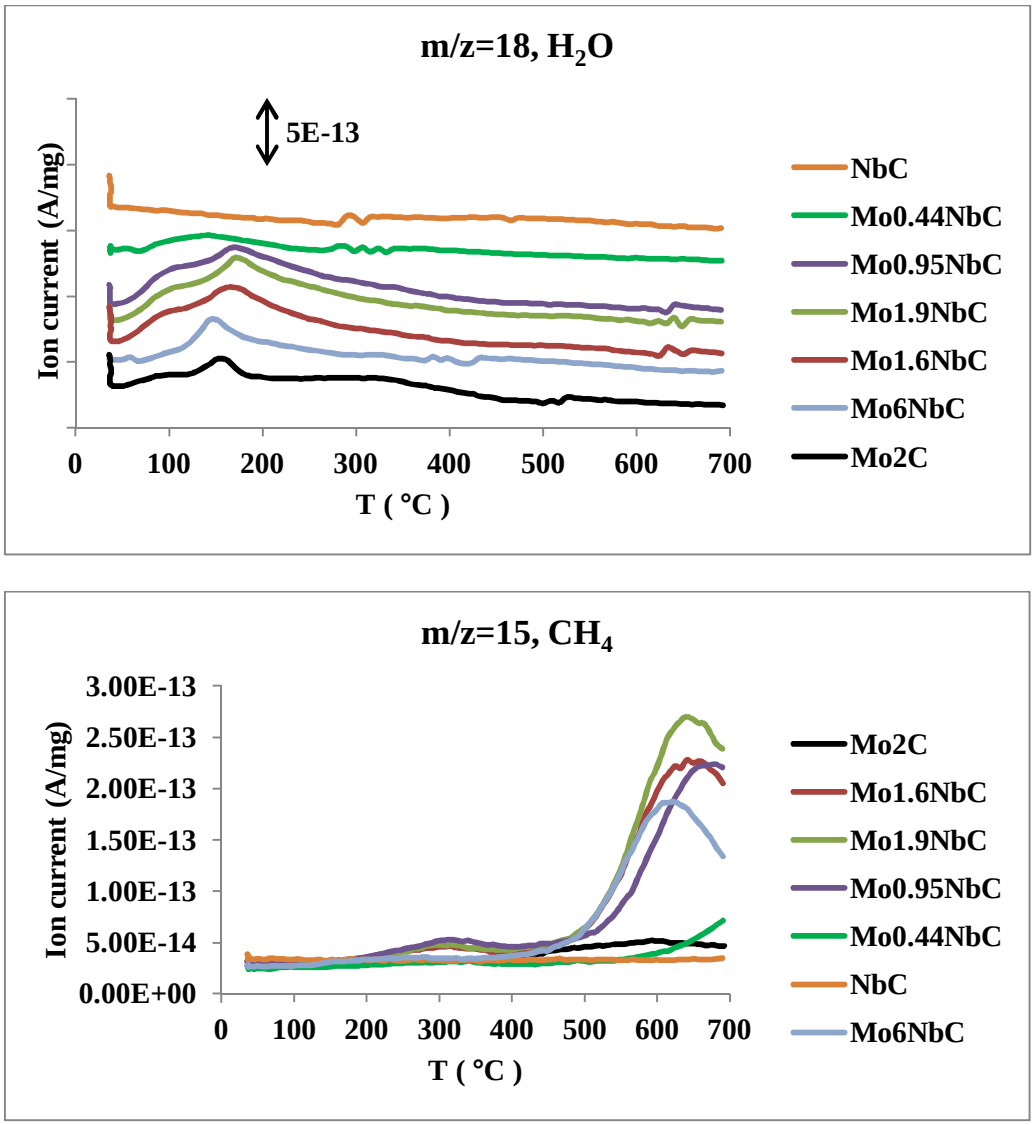

Figure 4.9: TPR data for mixed metal carbides. Formation of water (top) and methane (bottom).

The main gas phase products were water (m/z=18), methane (m/z=15) and ethane (m/z=30). TPR data for NbC shows no gas phase products but for the rest of the samples water starts to form in the temperature range from 100 to 300 °C. For mixed metal carbides, water starts to form at lower temperatures compared to the pure molybdenum carbide. For two of the mixed metal carbides that are rich in molybdenum and were prepared from HT precursors (Mo/Nb=0.95 and 1.6) ethane evolution was observed at about 300 °C. Pure molybdenum carbide forms a small amount of methane, while the mixed metal carbides rich in molybdenum form much more methane than pure molybdenum carbide, implying that more carbon vacancies are created. Methane starts to evolute from 400 °C for all samples except NbC. The maximum of the methane peaks in the mixed metal carbides shifts to lower temperatures with increasing molybdenum content; Mo_6Nb carbide has the methane peak at 600 °C whereas $Mo_{0.44}Nb$ starts to form methane at 600 °C.

4.3.4 Catalytic activity

Toluene hydrogenation was applied as the test reaction to check activity and stability of the samples. At 250 °C, product selectivity was 100% methylcyclohexane (MCH). Rates of reaction at 250 °C normalized to the weight of catalyst are reported in Figure 4.10. After cooling down to 250 °C from 400 °C all samples show some deactivation except Mo_6Nb carbide.

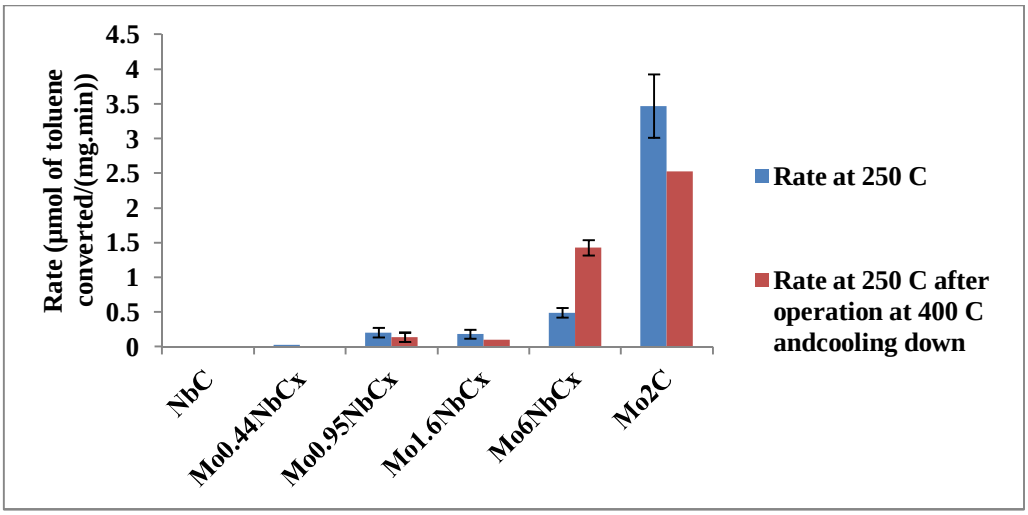

Figure 4.10: Rate of toluene hydrogenation at 250 °C and 20 bar H_2 pressure for Mo-Nb carbide samples. The blue bars show initial activity and the red bars show rate of toluene conversion at 250 °C after cooling down from 400 °C.

Turn over frequencies (TOF) for hydrogenation of toluene on different samples at 250 °C are reported in Figure 4.11. The numbers of sites were counted by CO chemisorption. Results revealed that the pure molybdenum carbide has the highest activity whereas niobium carbide showed no activity, with increasing amount of molybdenum, the activity increased.

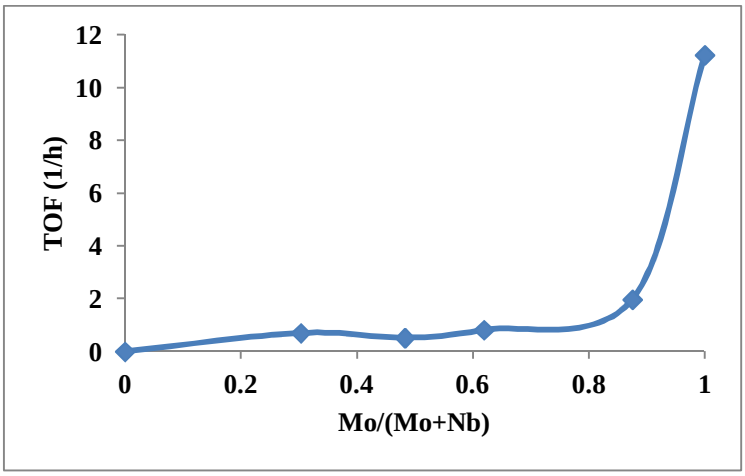

Figure 4.11: Turn over frequencies (TOF) for hydrogenation of toluene at 250 °C and 20 bar H_2 pressure on a series of Mo-Nb carbides.

At 400 °C, the activity of $Mo_{0.44}Nb$ carbide was very low (W/F=0.25 h, less than 2% conversion), however the other molybdenum-containing samples were active and formed light gases (C_1-C_6), MCH, ethylcyclopentane (ECP), dimethylcyclopentane (DMCP), benzene and xylene. The product selectivities are reported in Table 4.2.

Table 4.2: Product selectivities (in %) for Mo-Nb carbides at 400 °C and 20 bar H_2

Sample	Conv.	C_1-C_6	MCH	ECP	DMCP	Benz.	Xylene
Mo_2C	14.9	41.9	40.9	0.0	0.0	11.6	5.6
Mo_6NbC	14.6	40.1	40.7	2.1	0.0	11.5	5.6
$Mo_{1.6}NbC$	16.9	22.4	23.7	17.6	14.0	14.6	7.7
$Mo_{0.95}NbC$	16.6	34.6	20.2	16.9	11.8	10.7	5.8
MoWC-0.5*	16	34.7	40.4	1.6	0.0	15.7	7.6

* Synthesis and reduction explained in ref. [7].

At this temperature, Mo_2C was the most active catalyst and by increasing the amount of niobium, the activity decreases but the stability increases. As reported in Figure 4.12, over 24 hours time on stream all samples showed some deactivation: molybdenum carbide 36%, Mo_6Nb carbide 24%, $Mo_{1.6}Nb$ carbide 4% and $Mo_{0.99}Nb$ carbide 7%. The product selectivity did not change with deactivation. Samples rich in molybdenum show more hydrogenolysis products with not much ECP and DMCP products. However, adding the niobium decreases the amount of hydrogenolysis products and increases the amount of ECP and DMCP. All samples catalyze the

formation of benzene and xylene, however samples with a lower amount of niobium produce slightly more benzene and xylene than the other carbides.

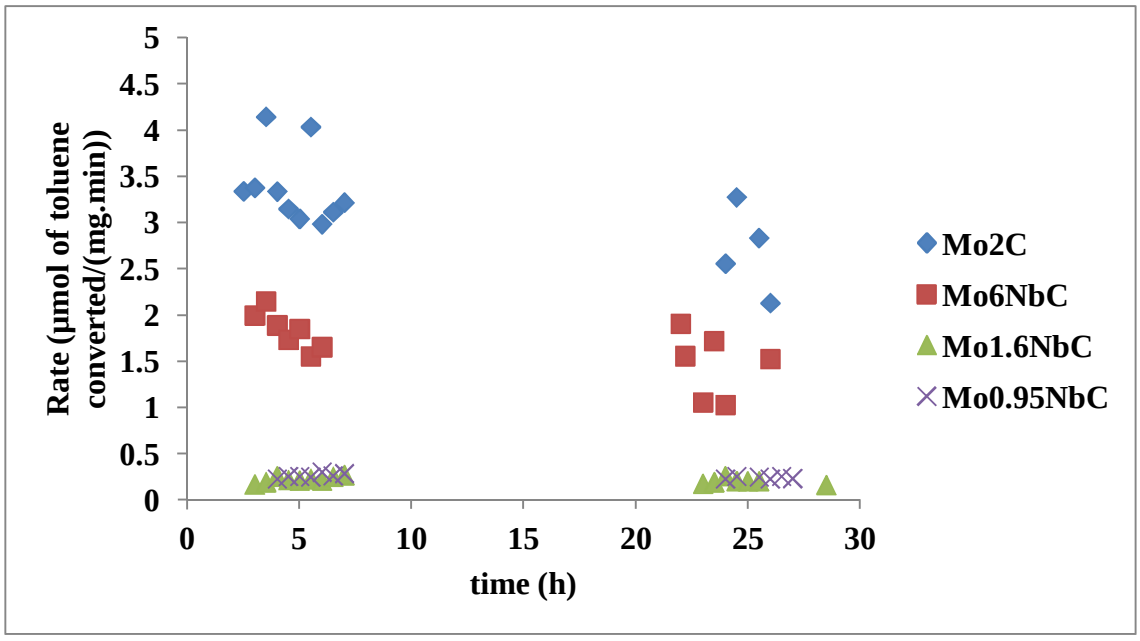

Figure 4.12: Hydrogenation of toluene on Mo-Nb carbide at 400 °C and 20 bar H_2 pressure.

4.4 Discussion

4.4.1 Carburization of samples

The precursors were synthesized by two different methods: freeze-drying and hydrothermal method. The FD method was used and explained in Chapter 3. The HT synthesis method for mixed metal oxides of Mo-Nb was reported elsewhere [12]. In this work, this method is modified by using two soluble salts and using acid. The molybdenum precursor was dissolved in oxalic acid to prevent precipitation. Also, adding the oxalic acid will cause formation of smaller particles (the final carburization temperature of a precursor prepared with oxalic acid is lower than the final

carburization temperature of a precursor prepared without using oxalic acid), which leads to a lower final carburization temperature.

Among all of the samples the pure niobium precursor needs the highest final carburization temperature, as reported in Figure 4.1. Adding the second metal (molybdenum) into the structure of niobium oxide will cause a significant decrease in the final carburization temperature. This could be due to the distortion of the lattice by adding the second metal which will facilitate oxygen mobility and consequently easier reduction and oxygen-metal bond cleavage or because of the role of molybdenum atoms on the surface that help dissociation of hydrogen.

The MS data in Figure 4.2 shows that in the case of niobium-rich samples, CO forms after formation of water while in the case of molybdenum-rich samples formation of CO happens simultaneously with formation water. Evolution of water with formation of CO indicates that during the last step of carburization both hydrogen and methane have a role for reduction. However, if only CO forms it shows that hydrogen does not have any role during reduction (since there is no water formation) and at high temperature the rate of methane dehydrogenation is higher than the rate of carbon hydrogenation which can cause surface contamination with carbon. There is also another interesting difference between carburization of niobium-containing materials and carburization of pure molybdenum or pure tungsten samples [7], which is the size of the CO peak. The size of the CO peak during carburization of niobium-containing materials is larger than the size of the CO peak during carburization of pure molybdenum or tungsten materials. To explain that, the stoichiometry of the final metal carbide should be noted. If they have niobium carbide structure, it will be cubic NbC

(carbon/metal=1) and if they have molybdenum carbide structure it will be hexagonal Mo_2C (carbon/metal=0.5). As a result, samples with NbC structure have a higher carbon to metal ratio compared to the samples with Mo_2C structure. Since the formation of CO is an indication of carburization (introduction of carbon into the lattice), samples with NbC structure are characterized by a larger CO peak.

The MS data for synthesis of NbC showed at 800 °C, ethylene starts to form. Formation of ethylene was observed with an empty crucible in the TG apparatus. However, the amount of ethylene formed is twice as large with the catalysts present.

Carburization of calcined precursors was reported in Figures 4.4 and 4.5. TG data show that niobium oxide needs high temperatures for reduction (about 700 °C) whereas molybdenum oxide needs 550 °C. However, Mo_6Nb oxide starts to reduce at lower temperatures (400 °C) compared to both molybdenum oxide and niobium oxide. This again could be due to the distortion of the lattice by adding the second metal. The first weight loss happens with formation of water which indicates reduction and removal of oxygen by hydrogen. The second water peak is observed at higher temperatures and in the case of molybdenum-containing samples simultaneously with formation of CO. Once again in the case of pure niobium oxide initially the second peak of water forms and then the CO peak starts to form, which indicates at that temperature only methane has an active role for reduction/carburization. The size of the CO peak during carburization of niobium oxide is the largest compared to the size of the CO peak during carburization of MoO_3 or Mo_6Nb oxide. This is because of the final products stoichiometry, the samples with NbC structure have a carbon/metal ratio of one whereas the samples with Mo_2C structure have a carbon/metal ratio of 0.5.

The solid state transformation of molybdenum oxide to molybdenum carbide is reported as follows: MoO_3 to MoO_2 to MoO_xC_y to Mo_2C [13]. A similar phase transformation happens during synthesis of niobium carbide: Nb_2O_5 to NbO_2 to NbO_xC_y to NbC [14]. However, there is a significant difference between the required temperature (activation energy) for each step during phase transformation of molybdenum oxide and niobium oxide.

As MS data show, the first step happens with formation of water for both oxides; however the transformation of MeO_2 (Me means metal) to the final carbide is the difference. In the case of molybdenum carbide, it happens with simultaneous water (reduction) and CO (carburization) formation whereas in the case of niobium carbide, formation of water and CO is not simultaneous. The slope of weight loss in the TG curve indicates how fast reduction or carburization occurs. In the case of molybdenum oxide, the slopes of reduction and carburization are steep with the slope of carburization being slightly steeper, which shows that the rate-limiting step is reduction, and incorporation of carbon into the lattice is easy. For transformation of niobium oxide it is the opposite, reduction is fast compared to the carburization as it can be seen from the weight loss curve in the TG data. This conclusion is in agreement with literature that suggests the carburization is the rate-limiting step for phase transformation of niobium oxide [14]. The first reduction (Nb_2O_5 to NbO_2) [14] and also the second step (NbO_2 to NbC) [15] follows nucleation kinetics. Since carburization is the rate-limiting step and needs high temperatures to proceed, the surface of the final NbC product is likely to be contaminated with carbon, and that is the major problem with synthesis of niobium carbide, which ultimately leads to the poor catalytic activity.

Incorporation of another metal into the structure of niobium oxide makes the kinetics of the synthesis very different; the reduction during the first step is very fast and happens at low temperatures (faster than reduction of both pure molybdenum oxide and pure niobium oxide); however, still carburization is the rate-limiting step and the slope of weight change in the TG curve is lower than the slope of weight change during the reduction, but carburization needs much lower temperature compared to the synthesis of niobium carbide. In fact, incorporation of the second metal decreases the induction period of reduction compared to both molybdenum oxide and niobium oxide and the induction period of carburization compared to the niobium oxide. One should also not forget the role of the structure; NbC has cubic structure whereas molybdenum and Mo_6Nb carbide have hexagonal structure.

In the case of carburization of samples rich in niobium the final temperature of carburization is very high, because as mentioned above, the rate-limiting step for carburization of niobium-containing samples is incorporating the carbon into the lattice of the oxide. To overcome this problem, different precursors (with a different oxidation state of niobium or a different particle size) for carburization have been tried to make reduction or the process of mass transport (diffusion of oxygen out and diffusion of carbon in) easier [14, 16, 17]. However, the change in the precursors did not significantly lower the final synthesis temperature of NbC, and surface contamination with carbon remained a major problem.

However, synthesis of niobium nitride can happen at lower temperatures and in one step from Nb_2O_5 to niobium oxynitride [18] and does not have the surface contamination problem. Using niobium nitride as the precursor for the carburization has

been tried, and results indicate that carburization of niobium nitride at elevated temperatures will lead to the formation of niobium carbonitride and not mono-carbides [19].

With the decomposition method it is possible, depending on the source of carbon, to initially go through a nitride phase and then to the carbide phase, but obtaining carbide phase from the nitride phase needs high temperatures to remove nitrogen from the sample [8].

Using metal additives such as nickel on niobium oxide will activate methane at lower temperatures but eventually will cause surface contamination with carbon. NbC was prepared at temperatures as low as 550 °C by the decomposition method [20, 21], but the drawback of the decomposition method is surface contamination by the carbon source.

One might suggest using others sources of carbon with longer carbon chains, which are reported to perform the carburization at lower temperatures for synthesis of molybdenum carbide [22]. In this work carburization of niobium oxide with ethane was tried and it was not successful, since high temperatures are needed for removal of oxygen by the carbon source; before that step, ethane was cracked and deposited on the surface. This deposited layer will serve as a barrier for oxygen to diffuse out, and as a result the final product will be mixed phases of carbide with a predominate fraction of oxide phase [17].

For synthesis of mixed metal carbide two different methods have been used: freeze-drying and hydrothermal method. The advantage of using FD method is to have control over the stoichiometry of the final products, which can be a wide range of

stoichiometries. However, using the HT method will result in high surface areas of the final products without having control over the metal ratios of the precipitated solids.

The analysis of samples containing niobium prepared by the HT method, as reported in Figure 4.6 shows that they have the cubic structure of NbC. They are solid solutions because they follow Vegard's law as it is shown in Figure 4.7. The equilibrium Gibbs free energy will determine whether the structure of the carbide is cubic or hexagonal. Cubic NbC is more stable than hexagonal Mo_2C [23]. The synthesis of mixed metal carbides of Mo-Nb with molybdenum carbide structure was tried by increasing the concentration of Mo/Nb to 21 in the solution. XRD results (Figure 4.6-i) show that the final product consisted of two phases with the structures of Mo_2C and NbC. To synthesize a mixed metal carbide of Mo-Nb with the hexagonal Mo_2C structure, mixed metal precursors containing both molybdenum and niobium were prepared by the freeze-drying method, which already showed promising results [7]. Carburization of precursors with ratios of Mo/Nb less than seven resulted in NbC structures but carburization of a sample with the ratio of Mo/Nb=7 resulted in the Mo_2C structure. Direct carburization of Mo_6Nb_FD leads to a broad peak assigned to the (002) plane in the Mo_2C structure; to overcome this problem the FD precursor was calcined and then it was carburized. However, it is worth to mention that in the XRD data of Mo_6Nb carbide; not all the peaks of Mo_2C could be perfectly fit with the Powdercell.

Unlike the FD method in which the final sample has a metal ratio close to that initially combined in the solution, the HT method produces materials with a metal ratio different from that in the solution as shown in Figure 4.8. Also, with the HT method it was not possible to prepare materials with a metal ratio of Mo/Nb larger than 2 that

were single phase Mo-Nb carbide. However, the samples that were prepared by the HT method have higher surface areas compared to samples that were prepared by the FD method, as shown in Table 4.1.

Amounts of weight gain during passivation and CO site densities as produced by CO chemisorption are reported in Table 4.1. The samples rich in niobium have lower amounts of oxygen chemisorption during passivation because of their lower surface areas that were caused by high synthesis temperatures. The surface areas of mixed metal carbides of Mo-Nb are higher than those of monometallic materials. The surface area of pure niobium carbide is also good although it was synthesized at 950 °C; this could be due to the deposited carbon on the crystallites which inhibits sintering by decreasing the atom motilities. Addition of niobium to the molybdenum materials leads to an increase in surface area although the final carburization temperatures are higher; this high surface area is because of the increase in pore volume by adding niobium to molybdenum. However, the active sites titrated by CO chemisorptions increase by increasing the amounts of molybdenum, which is an opposite trend to the oxygen chemisorptions. This behavior can be explained by the differences between the sites on which oxygen and CO chemisorb. Oxygen chemisorbs on all the metallic sites but CO chemisorbs selectively on noble metal-like sites [24].

All samples were passivated in an initially low concentration of oxygen to be able to regenerate more sites after reduction [1]. The time of each step was adjusted to have the minimum time for passivation. The most important step during passivation is the initial step of oxygen introduction to the surface. The major weight gains happen during this step and a low concentration of oxygen should be used until the weight gain

curve in TGA passes the “knee shape” (most of the weight gains happens during this time, the weight gain curve increases until it reaches a plateau). This time depends on the surface area and the ability of metal carbides to dissociate oxygen. Since carburization of HT prepared precursors leads to high surface area carbides it takes about 10 hours to reach the “knee shape” of weight gain. It is worth to mention that the passivation time also depends on the amount of sample and mass transfer issues.

4.4.2 Reduction

TPR data in Figure 4.9 shows that depending on the temperature, oxygen or carbon can be removed from the (sub) surface of carbides. It is interesting to notice that in the case of mixed metal carbides of Mo-Nb, oxygen can be removed more easily and at lower temperatures compared to the pure molybdenum carbide. This can be due to the electronic effects that weaken chemisorption of oxygen on the surface or it could be due to the higher amounts of chemisorbed oxygen (higher surface area). Another observation is that after reduction of Mo-Nb mixed metal carbides, they were pyrophoric and burned in the air upon removal from the inert atmosphere. None of the passivated and reduced carbides reported in Chapters 2 and 3 burned in the air upon removal from the inert atmosphere. This shows that Mo-Nb carbide can be good candidates for HDO reactions since oxygen adsorbs more weakly to their surfaces compared to the pure molybdenum carbide. The electron density of Mo-Nb carbide compared to the pure molybdenum shows that in the case of the mixed metal carbide electron density is removed from both molybdenum and the molybdenum-carbon covalent bond [25]. This could be the reason for weaker oxygen adsorption on the

surface of Mo-Nb carbide and the weaker metal-carbon bond as shown by methane formation in TPR.

Carbon is removed at higher temperatures during TPR. For samples rich in molybdenum and prepared by the HT method, at 300 °C ethane evolved. Ethane (or C_xH_y fragments) can be formed during synthesis, and desorbs during TPR. Molybdenum carbide produces a small amount of methane, whereas pure niobium carbide does not produce any methane. It seems that there is a layer of deposited carbon on the surface of NbC which cannot be removed by hydrogen treatment at 700 °C. It was reported that this layer can be burnt in oxygen at 350 °C, and this treatment will cause an increase in CO chemisorption [26]. It was attempted to oxidize the NbC surface and then recarburize the niobium oxycarbide, but it needed high temperature (950 °C) for carburization (to see formation of a CO peak). This behavior demonstrates that oxygen can adsorb very strongly on the surface of niobium. Surface cleaning to remove deposited carbon can be done at high temperatures (950 °C) with hydrogen and not with oxidation [19]. However, adding molybdenum to the niobium carbide and increasing the amounts of molybdenum will ease creation of carbon vacancies. Among all the samples, Mo_6Nb carbide starts to release methane at the lowest temperature. In general, adding the second metal into the structure of monometallic carbides will facilitate creation of carbon vacancies. This behavior was shown for Mo-W carbide [7] and in this paper for Mo-Nb carbide. This phenomenon is important for reactions that need creation of vacancies as active sites such as direct desulfurization (DDS) [27].

4.4.3 Catalytic performance

Hydrogenation of toluene at 250 °C and 20 bar pressure was used to test the activity of these materials. The rate normalized by mass of catalyst is reported in Figure 4.10. NbC did not show any activity, which could be due to the contamination of the surface with carbon because the surface did not chemisorb any oxygen or CO, and also evolution of methane or water during TPR was not observed. However, it is reported that oxygen dissociatively adsorbs on the clean surfaces of NbC (100) and NbC(111) [28-31]. This indicates that NbC with a clean surface can be catalytically active.

The electronic structures of molybdenum carbide and niobium carbide are different. The Fermi level is shifted to higher values from niobium carbide to molybdenum carbide, also molybdenum carbide has a higher DOS at the Fermi level compared to niobium carbide [23].

Adding molybdenum into the structure of niobium carbide increases the number of active sites (judged from the values of adsorbed CO), which leads to an increase of the hydrogenation activity, which is associated with the metallic behavior of metal carbides. Increasing the temperature to 400 °C under reaction conditions and then cooling down to 250 °C resulted in an increased activity only for Mo_6Nb carbide and some deactivation for the rest of the samples. It is worth to mention that Mo_6Nb carbide can lose carbon at lower temperatures compared to the rest of the samples. As a result, under reaction conditions (400 °C and 20 bar pressure) some carbon can be removed and during cooling down to 250 °C surface reconstruction can happen [1, 7] .

TOF results in Figure 4.11 show the same trend as the rate normalized by the weight. Adding molybdenum into the structure of NbC increases the hydrogenation activity. Mo-Nb carbides with the cubic structure of NbC have almost the same hydrogenation activity, whereas samples with the hexagonal structure of Mo_2C are more active. These differences can be from a higher concentration of molybdenum atoms on the surface or the role of structure. Molybdenum carbide itself can be prepared in the hexagonal or cubic structure, with different catalytic activity. Molybdenum carbide with cubic structure is reported to be more active than molybdenum carbide with hexagonal structure for hydrogenation of CO whereas the hexagonal structure is more active for hydrogenolysis of ethane due to the difference in the structure of the main exposed planes [32]. However, cubic phase molybdenum carbide has been reported to be more active than hexagonal phase molybdenum carbide for hydrogenation of toluene [33]. In this report [33] hexagonal molybdenum carbide was commercial and cubic molybdenum carbide was prepared in house.

The rate of reaction at 400 °C and 20 bar pressure is reported in Figure 4.12. Over Mo-Nb carbides the same as Mo-W carbides [7], the rate of reaction at 400 °C does not increase much compared to the lower temperatures. This behavior is due to the strong adsorption of reactant on the surface, which needs high temperatures to desorb. The decrease in the rate of hydrogenation of aromatics versus temperature has been reported before [34].

The same trend for activity versus composition during the rate of reaction at 250 °C can be observed here, samples rich in molybdenum with hexagonal structure of Mo_2C are more active. Over 24 hours time on stream, molybdenum carbide loses 36%

of its activity. While adding niobium to molybdenum carbide lowers its activity it makes it more stable. Mo_6Nb carbide loses 24%, $Mo_{1.6}Nb$ carbide and $Mo_{0.95}Nb$ carbide which have the cubic structure of NbC lose only 4 and 7% of their activities. The product selectivities did not change with deactivation under operating conditions and the selectivities at the final conversions are reported in Table 4.2. The product selectivities of hydrogenation of toluene on Mo-W carbide were explained before [7], which is similar to this study. One major difference concerns the metallic behavior of molybdenum carbide or the mixed metal carbides with hexagonal structure of Mo_2C compared to that of the Mo-Nb carbides with NbC structure. Molybdenum carbide has a pronounced metallic behavior, which can be seen in its hydrogenolysis/hydrogenation behavior. Even mixing molybdenum carbide with niobium or tungsten cannot tame its hydrogenolysis activity [7]. At 15% conversion light gases and MCH are dominant products, adding niobium or tungsten will lead to some acid-catalyzed products (ECP) by formation of strong Brønsted acid sites. However, adding more niobium changes product selectivities significantly by taming the metallic behavior of molybdenum carbide. As a result, the amount of light gases and MCH formation decrease by half as a consequence of the decreasing metallic behavior. For ring contraction of six-membered rings to five-membered rings strong Brønsted acid sites are needed [35]. Formation of ECP and DMCP requires bifunctional catalysts. Since niobium is very oxophilic, a good solid acid catalyst can be obtained through formation of Brønsted acid sites. Niobium nitride can adsorb more oxygen over time than molybdenum or tungsten nitride, because of the affinity of niobium to oxygen [36], which is another indication that niobium can adsorb more oxygen compared to molybdenum or tungsten. In the case of

mixed Mo-Nb carbides, oxygen tends to adsorb more on niobium [6]. The reduction data in Table 4.1 shows that after reduction, still some oxygen is left on the surface of the samples.

The difference in the amounts of acid-catalyzed products on Mo-W carbide [7] compared to Mo-Nb carbide can be attributed to the balance between metallic and acidic sites. In fact, toluene will be partially hydrogenated to methylcyclohexene, then depending on the number of metallic sites versus number of acid sites hydrogenation/hydrogenolysis or ring contraction can happen. Molybdenum oxynitride has been compared with niobium oxynitride for metal-catalyzed reactions (hydrogenation of toluene) and acid-catalyzed reactions (isomerization of cyclohexane) and results revealed that molybdenum oxynitride has more pronounced metallic behavior whereas niobium oxynitride has more pronounced acid behavior [10].

4.5 Conclusions

Mixed metal carbides of molybdenum and niobium with different metal ratios have been prepared. The mixed metal carbides are single phase solid solutions, and based on the metal ratios or precursors synthesis they have cubic NbC structure or hexagonal Mo_2C structure. Samples prepared from hydrothermally precipitated precursors have high surface areas and high oxygen uptakes. Addition of molybdenum into the structure of niobium causes reduction and carburization to happen at lower temperatures compared to the synthesis of NbC. TPR data show that creation of carbon vacancies or surface reduction is easier for mixed metal carbides compared to their monometallic counterparts. NbC was not active at all for hydrogenation due to the surface contamination with carbon. Results show that the samples with Mo_2C structure

yield more metal-catalyzed products (hydrogenation and hydrogenolysis) whereas metal (oxy) carbides with NbC structure are less active and produce more acid-catalyzed products. This difference in product selectivities is due to balance between metal and acid sites. All the samples are (oxy) carbides and oxygen attaches more to niobium due to its high oxophilicity. It is more difficult to reduce niobium (oxy) carbide compared to the molybdenum (oxy) carbide. This causes the niobium (oxy) carbide to be a better solid acid catalyst and to produce more acid-catalyzed products whitin the Mo-Nb (oxy) carbide series. Also, at 400 °C samples with NbC structure are more stable than the samples with Mo_2C structures.

References

[1] A. Mehdad, Mixed Metal Carbides: Understanding the Synthesis, Surface Properties and Catlytic Activities, PhD Dissertation, The University of Oklahoma, Chapter 2, (2015).

[2] L. Leclercq, M. Provost, H. Pastor, G. Leclercq, Catalytic properties of transition metal carbides: II. Activity of bulk mixed carbides of molybdenum and tungsten in hydrocarbon conversion, Journal of Catalysis, 117 (1989) 384-395.

[3] V. Schwartz, S. T. Oyama, J. G. Chen, Supported Bimetallic Nb−Mo Carbide: Synthesis, Characterization, and Reactivity, The Journal of Physical Chemistry B, 104 (2000) 8800-8806.

[4] H. A. Al-Megren, S. L. González-Cortés, T. Xiao, M. L. H. Green, A comparative study of the catalytic performance of Co-Mo and Co(Ni)-W carbide catalysts in the hydrodenitrogenation (HDN) reaction of pyridine, Applied Catalysis A: General, 329 (2007) 36-45.

[5] H. A. Al-Megren, T. Xiao, S. L. Gonzalez-Cortes, S. H. Al-Khowaiter, M. L. H. Green, Comparison of bulk CoMo bimetallic carbide, oxide, nitride and sulfide catalysts for pyridine hydrodenitrogenation, Journal of Molecular Catalysis A: Chemical, 225 (2005) 143-148.

[6] C. C. Yu, S. Ramanathan, B. Dhandapani, J. G. Chen, S. T. Oyama, Bimetallic Nb−Mo Carbide Hydroprocessing Catalysts: Synthesis, Characterization, and Activity Studies, The Journal of Physical Chemistry B, 101 (1997) 512-518.

[7] A. Mehdad, Mixed Metal Carbides: Understanding the Synthesis, Surface Properties and Catlytic Activities, PhD Dissertation, The University of Oklahoma, Chapter 3, (2015).

[8] C. Chagas, R. Pfeifer, A. Rocha, V. Teixeira da Silva, Synthesis of Niobium Carbonitride by Thermal Decomposition of Guanidine Oxaloniobate and Its Application to the Hydrodesulfurization of Dibenzothiophene, Topics in Catalysis, 55 (2012) 910-921.

[9] S. Ramanathan, S. T. Oyama, New Catalysts for Hydroprocessing: Transition Metal Carbides and Nitrides, The Journal of Physical Chemistry, 99 (1995) 16365-16372.

[10] H. S. Kim, C. Sayag, G. Bugli, G. Djega-Mariadassou, M. Boudart, Preparation, Characterization and Catalytic Activity of Niobium Oxynitride and Oxycarbide in Hydrotreatment, MRS Online Proceedings Library, 368 (1994) 3-14.

[11] M. K. Neylon, S. Choi, H. Kwon, K. E. Curry, L. T. Thompson, Catalytic properties of early transition metal nitrides and carbides: n-butane hydrogenolysis, dehydrogenation and isomerization, Applied Catalysis A: General, 183 (1999) 253-263.

[12] T. Murayama, N. Kuramata, S. Takatama, K. Nakatani, S. Izumi, X. Yi, W. Ueda, Synthesis of porous and acidic complex metal oxide catalyst based on group 5 and 6 elements, Catalysis Today, 185 (2012) 224-229.

[13] A. Hanif, T. Xiao, A. P. E. York, J. Sloan, M. L. H. Green, Study on the Structure and Formation Mechanism of Molybdenum Carbides, Chemistry of Materials, 14 (2002) 1009-1015.

[14] V. L. S. Teixeira da Silva, M. Schmal, S. T. Oyama, Niobium Carbide Synthesis from Niobium Oxide: Study of the Synthesis Conditions, Kinetics, and Solid-State Transformation Mechanism, Journal of Solid State Chemistry, 123 (1996) 168-182.

[15] F. A. O. Fontes, J. F. de Sousa, C. P. Souza, M. B. D. Bezerra, M. Benachour, Production Of Nbc from Nb_2O_5 in a rotating cylinder reactor: Kinetic study of reduction/carburization reactions, Chemical Engineering Journal, 175 (2011) 534-538.

[16] V. L. S. Teixeira da Silva, E. I. Ko, M. Schmal, S. T. Oyama, Synthesis of Niobium Carbide from Niobium Oxide Aerogels, Chemistry of Materials, 7 (1995) 179-184.

[17] S. Witkowski, M. Ruszak, C. Sayag, J. Pielaszek, G. Djéga-Mariadassou, Nanocrystalline NbC formation from mesostructured niobium oxide studied by HRTEM, SAED and in situ XRD, Applied Catalysis A: General, 307 (2006) 205-211.

[18] V. Schwartz, S. T. Oyama, Study of Niobium Oxynitride: Synthesis, Characterization, and Reactivity, Chemistry of Materials, 9 (1997) 3052-3059.

[19] H. S. Kim, G. Bugli, G. Djéga-Mariadassou, Preparation and Characterization of Niobium Carbide and Carbonitride, Journal of Solid State Chemistry, 142 (1999) 100-107.

[20] J. Ma, M. Wu, Y. Du, S. Chen, W. Jin, L. Fu, Q. Yang, A. Wen, Formation of nanocrystalline niobium carbide (NbC) with a convenient route at low temperature, Journal of Alloys and Compounds, 475 (2009) 415-417.

[21] L. Shi, Y. Gu, L. Chen, Z. Yang, J. Ma, Y. Qian, Synthesis and oxidation behavior of nanocrystalline niobium carbide, Solid State Ionics, 176 (2005) 841-843.

[22] T. Xiao, A. P. E. York, K. S. Coleman, J. B. Claridge, J. Sloan, J. Charnock, M. L. H. Green, Effect of carburising agent on the structure of molybdenum carbides, Journal of Materials Chemistry, 11 (2001) 3094-3098.

[23] H. W. Hugosson, O. Eriksson, U. Jansson, B. Johansson, Phase stabilities and homogeneity ranges in 4d-transition-metal carbides: A theoretical study, Physical Review B, 63 (2001) 134108.

[24] J. S. Choi, G. Bugli, G. Djéga-Mariadassou, Influence of the Degree of Carburization on the Density of Sites and Hydrogenating Activity of Molybdenum Carbides, Journal of Catalysis, 193 (2000) 238-247.

[25] H. W. Hugosson, L. Nordström, U. Jansson, B. Johansson, O. Eriksson, Theoretical studies of substitutional impurities in molybdenum carbide, Physical Review B, 60 (1999) 15123-15130.

[26] V. L. S. Teixeira da Silva, M. Schmal, V. Schwartz, S. T. Oyama, Synthesis of a Mo/Nb mixed carbide, Journal of Materials Research, 13 (1998) 1977-1988.

[27] M. Egorova, R. Prins, Hydrodesulfurization of dibenzothiophene and 4,6-dimethyldibenzothiophene over sulfided NiMo/γ-Al_2O_3, CoMo/γ-Al_2O_3, and Mo/γ-Al_2O_3 catalysts, Journal of Catalysis, 225 (2004) 417-427.

[28] K. Edamoto, T. Anazawa, E. Shiobara, M. Hatta, E. Miyazaki, H. Kato, S. Otani, Oxygen adsorption on a $NbC_{0.9}$ (111) surface: Angle-resolved photoemission study, Physical Review B, 43 (1991) 3871-3875.

[29] I. Kojima, M. Orita, E. Miyazaki, S. Otani, Adsorption of O_2, Co and CH_3OH on NbC (100) and (111) single crystal surfaces by ultraviolet photoelectron spectroscopy, Surface Science, 160 (1985) 153-163.

[30] W. Hayami, R. Souda, T. Aizawa, S. Otani, Y. Ishizawa, Structural analysis of NbC(111)-O and NbC(111)-D surfaces, Surface Science, 346 (1996) 158-164.

[31] T. Aizawa, W. Hayami, R. Souda, S. Otani, T. Tanaka, Y. Ishizawa, Molecular adsorption of oxygen on transition-metal carbide, Surface Science, 357–358 (1996) 645-650.

[32] G. S. Ranhotra, A. T. Bell, J. A. Reimer, Catalysis over molybdenum carbides and nitrides: II. Studies of CO hydrogenation and C_2H_6 hydrogenolysis, Journal of Catalysis, 108 (1987) 40-49.

[33] M. L. Frauwallner, F. López-Linares, J. Lara-Romero, C. E. Scott, V. Ali, E. Hernández, P. Pereira-Almao, Toluene hydrogenation at low temperature using a molybdenum carbide catalyst, Applied Catalysis A: General, 394 (2011) 62-70.

[34] M. Saeys, M. F. Reyniers, J. W. Thybaut, M. Neurock, G. B. Marin, First-principles based kinetic model for the hydrogenation of toluene, Journal of Catalysis, 236 (2005) 129-138.

[35] K. Shimizu, T. Sunagawa, C. R. Vera, K. Ukegawa, Catalytic activity for synthesis of isomerized products from benzene over platinum-supported sulfated zirconia, Applied Catalysis A: General, 206 (2001) 79-86.

[36] R. Brayner, J. A. J. Rodrigues, G. M. Cruz, Synthesis and molding of niobium oxynitrides with macropores generation: Reactivity and stability in cyclohexane dehydrogenation, Catalysis Today, 57 (2000) 219-223.

5. Recommendations

The results in Chapter 2 show that there is a carbon dynamics on the surface of metal carbides which can affect the catalytic activity of metal carbides. It would be interesting to apply some surface sensitive techniques to study the surface of metal carbides before and after surface reconstruction.

The results in Chapter 3 and 4 revealed that the mixed metal carbide have better stabilities for hydrogenation at high temperatures compared to their corresponding mono-metal carbides. It would be interesting to use mixed metal carbides for reactions that need high temperature such as dehydrogenation, and study their stabilities for dehydrogenation.

In Chapters 3 and 4, methods to synthesize single phase mixed metal carbides were developed and these catalysts were used for acid- and metal-catalyzed reactions. One also could try these materials for hydrotreating reactions such as HDS and HDO. One interesting point to notice will be the role of carbon vacancies as an active site for hydrotreating.

The results also show that the oxycarbides are bifunctional catalysts and can perform acid-catalyzed reactions. It would be interesting to perform a detailed study about the strength and the distribution of these acid sites.

Metal carbides such as Mo_2C can be prepared with different structures such as cubic or hexagonal. It would be interesting to investigate and to compare the catalytic activity of different structures of metal carbides.

In this thesis, synthesis of mixed metal (oxy) carbides was investigated. One can try synthesis of mixed metal (oxy) nitrides and investigate their catalytic activities.

Synthesis of metal carbonitride would also be interesting to study. Metal (oxy) carbides have good metallic behavior and metal (oxy) nitrides have good acidic behavior. As a result, by synthesis of metal (oxy) carbonitrides, it might be possible to synthesize a catalyst with both good acidic and metallic behavior.

6. Appendix A: GC calibration

The GC HP5890 equipped with a GS-GASPRO column (30m, 0.320 mm i.d.) with the following temperature program was used to analyze the reactor effluent:

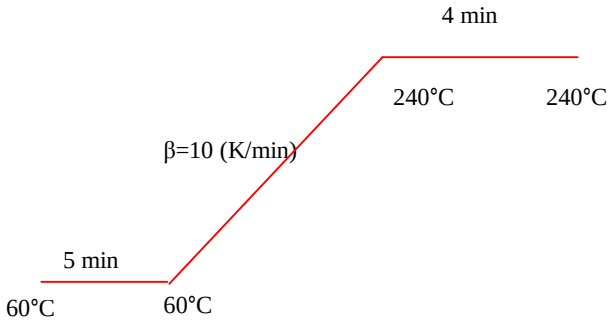

Figure 6.1: Temperature program of the GC

Calibration gases were bought from the Matheson Tri-Gas Inc. The cylinder contains C_1-C_6 light paraffins as below:

Table 6.1: Calibration gas content

Component	**Concentration (ppm)**
Methane	1000
Ethane	1000
Propane	1000
n-butane	1000
n-Pentane	1000
Hexane	1000
Helium	Balance

Samples were injected four times from the calibration gas cylinder, while the loop was heated (the same condition in the experiment), the retention times and the peak areas are as following:

Table 6.2: Retention time (RT) for the gases in the calibration gas cylinder

Compound	Retention time (min)
CH_4	1.25
C_2H_6	1.60
C_3H_6	3.06
C_4H_{10}	7.91
C_5H_{12}	12.26
C_6H_{14}	15.60

Table 6.3: Peak areas for injection of calibration gases

Compound	Peak Area						
	#1	#2	#3	#4	Average	Concentration%	Area/%mol
CH_4	29572.3	30124.1	30133.1	30389.5	30054.8	0.1	300,547.8
C_2H_6	93401.6	93681.0	93175.1	94122.5	93595.0	0.1	935,950.4
C_3H_6	121233.4	121956.8	121943.0	122738.9	121968.0	0.1	1,219,680.2
C_4H_{10}	163435.4	164550.0	164545.2	165567.6	164524.6	0.1	1,645,245.7
C_5H_{12}	202711.8	205145.7	205374.0	206425.7	204914.3	0.1	2,049,143.1
C_6H_{14}	239634.6	246781.6	247026.4	248423.1	245466.4	0.1	2,454,664.3

Mole percentages of different compounds were calculated as following:

$$\%_CH_4 = \frac{PeakArea \times 0.1}{30054.78} \qquad \%_C_2H_6 = \frac{PeakArea \times 0.1}{93595.04}$$

$$\%_C_3H_8 = \frac{PeakArea \times 0.1}{121968} \qquad \%_C_4 = \frac{PeakArea \times 0.1}{164524.6}$$

$$\%_C_5 = \frac{PeakArea \times 0.1}{204914.3} \qquad \%_C_6 = \frac{PeakArea \times 0.1}{245466.4}$$

Toluene (tol) was pumped into the reactor with a flow rate of 0.02 (ml/min), and H_2 was sent into the reactor with a flow rate of 150 (ml/min). The pressure of the reactor was 20 bar. At these conditions, mole percentage of toluene was 2.99%, as reported in Table 6.4.

The average peak area under these conditions (0.02 ml/min and 20 bar), was 8763120. Pumping was started with 0.02 ml/min from the beginning and was kept constant throughout the experiment.

Table 6.4: Toluene partial pressure at different flow rates and pressures

Flow (ml/min)	mol toluene	% mol_toluene	Total Pressure (bar)	P_toluene (bar)
0.05	0.000472	0.071476	30	2.144278
0.03	0.000283	0.044148	30	1.324433
0.02	0.000189	0.029871	30	0.896143
0.01	9.44E-05	0.015162	30	0.454865
0.05	0.000472	0.071476	20	1.429519
0.03	0.000283	0.044148	20	0.882955
0.02	0.000189	0.029871	20	0.597428
0.01	9.44E-05	0.015162	20	0.303243

Moles of toluene= $\frac{0.02(ml/\min) \times 0.87(g/ml)}{92.14(g/mol)} = 1.89 \times 10^{-4}(mol/\min)$

Moles of H_2=

$$moles_Hydrogen = \frac{150(ml/\min) \times 101.3(kpa) \times 0.001(l/ml)}{8.314(kpa.l/K.mol) \times 298(K)} = 6.13 \times 10^{-3}(mol/\min)$$

Mole fraction of toluene= 2.99×10^{-2}

The Peak area/%mol of the compounds vs. carbon number for different compounds are plotted in Figure 6.2.

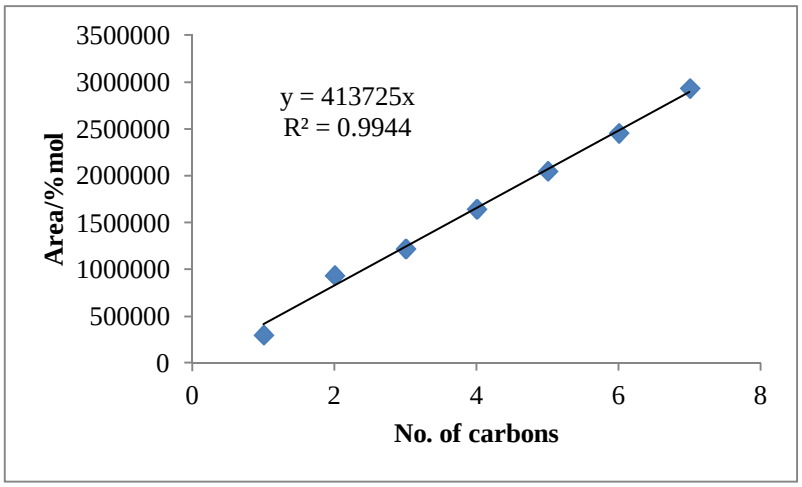

Figure 6.2: Peak area/%mol of the compounds vs. carbon number

For measuring the response factor (RF) of methylcyclohexane (MCH), mixtures of toluene, MCH and octane (as internal standard) with different ratios were dissolved in dichloromethane. The volumes of all samples were 10 ml. They were injected with a syringe to the GC. The peak areas and response factors are reported in Table 6.5 and Figure 6.3.

Table 6.5: Response factor (RF) for toluene (tol) and methylcyclohexane (MCH) with octane as internal standard

Liquid Injection							RF		[Ax/(Ais/Cis)]	
MCH (mg)	Octane (mg)	Tol. (mg)	Area (MCH)	Area (Tol)	Area (Octane)	Area/Mass (Octane)	MCH	Tol	MCH	Tol
26.5	31.5	93.5	9728623	33475850	10111274	320992.8	1.1437	1.1154	30.3079	104.2885
63.5	27.4	74.7	22227170	27143614	9712255	354461.9	0.9875	1.0251	62.7068	76.5770
85.8	35.2	42	34494672	16612056	13308837	378092	1.0633	1.0461	91.2336	43.9365
104.3	28.7	35.5	39892088	15201327	11010481	383640.5	0.9970	1.1162	103.9830	39.6239

$$\frac{RF_Toluene}{RF_MCH} = 1.129$$

$$\%_MCH = \frac{1.129 \times (Area_MCH)}{\frac{Area_Toluene}{2.99}}$$

The molar percentage of ethylcyclopentane (ECP) was calculated in the same manner as that of MCH.

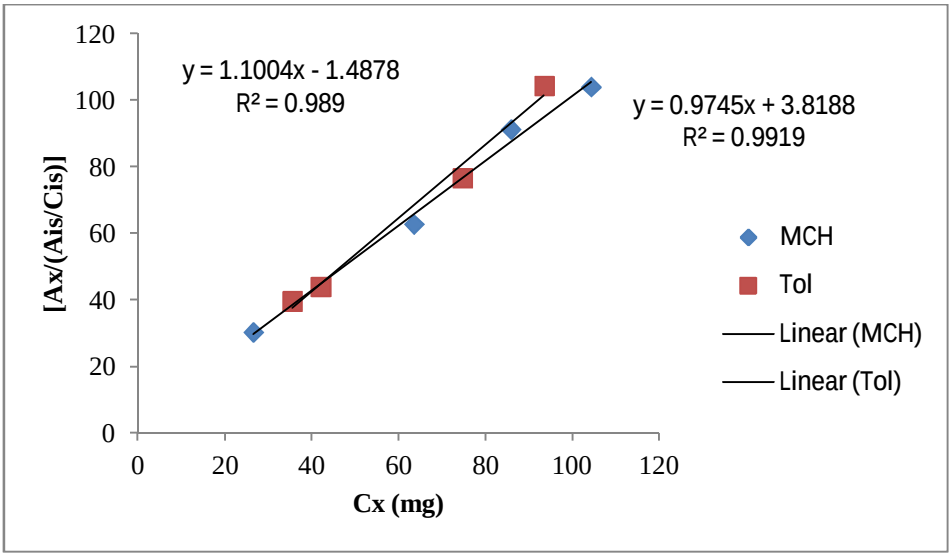

Figure 6.3: Response factor (RF) of toluene and methylcyclohexane with octane as internal standard